The Dissertation Committee for Cyril L.C. Bussiere Certifies that this is the approved version of the following dissertation:

Late cytoplasmic maturation of the large ribosomal subunit

Committee:

Arlen W. Johnson, Supervisor

Scott Stevens

Jon Huibregtse

Tanya T. Paull

Karen S. Browning

Late cytoplasmic maturation of the large ribosomal subunit

by

Cyril L.C. Bussiere, B.S.

Dissertation

Presented to the Faculty of the Graduate School of

The University of Texas at Austin

in Partial Fulfillment

of the Requirements

for the Degree of

Doctor of Philosophy

The University of Texas at Austin

May, 2011

Dedication

This dissertation is dedicated to my parents and family for their love and support throughout my graduate study and to my fiancée for making it all worthwhile.

Acknowledgements

I thank my advisor, Dr. Arlen Johnson, for his support and patience throughout the years. I also appreciate the guidance from my committee members**,** Dr. Jon huibregst, Dr. Tanya Paull, Dr. Karen Browning, and especially Dr. Scott Stevens for his repeated input during joint group meetings. I appreciate all my lab members, past and present, Dr. Matthew West, Dr. Lingna Wang, Dr. Nai-Jung Hung, Dr. Peggy Huang, Dr. Simrit Dhaliwal, Dr Kai-yin Lo, Richa Sardana, Joshua White, Kara Helmke, Reed Pfifer, Stafan Bresson, Collin Bates, Monica Noori, and Michael Goldsmith for discussions of all kind and for making my years in grad school enjoyable during work hours. I thank the members of the Stevens Lab for reagents.

I appreciate the unyielding support from my parents and siblings throughout my graduate career and my life at large. I am grateful for companionship and friendship from my friends in Austin and away. I thank my fiancée for her love and her presence in my life. She gives me the will to complete my PhD study and to look brightly to the future.

I thank Dr Joachim Frank and lab members of the Frank lab, especially Dr Jayati Sengupta and Dr Jesper Pallesen for their collaboration on the Nmd3-60S structural work, and Dr Yaser Hashem for his modeling of Efl1. I also thank Sucheta Arora for her contribution in generating Rpl10 P-site loop mutants. This work was supported by NIH GM53655 to A.W. Johnson. Additional support was provided by the Program of Microbiology, the School of Biological Sciences, and the University of Texas at Austin.

Late cytoplasmic maturation of the large ribosomal subunit

Publication No._____

Cyril L.C. Bussiere, PhD

The University of Texas at Austin, 2011

Supervisor: Arlen W. Johnson

In all life ribosomes are the ribonucloprotein machines in charge of decoding the genetic code and synthesizing proteins. In eukaryotes, ribosomes are pre-assembled in the nucleus and exported to the cytoplasm where the final maturation steps occur prior to their partaking in translation. My dissertation work focused on aspects of the last two known steps of the pre-60S subunit cytoplasmic maturation. In the penultimate step, the anti-association factor Tif6 is released from 60S by the concerted action of the translocase-like GTPase Efl1 and Sdo1. The release of Tif6 is

necessary for the ultimate maturation step, which involves release of the export adaptor Nmd3 by the ribosomal protein Rpl10 and the putative GTPase Lsg1.

Nmd3 is an essential export adaptor of the 60S subunit. Nmd3 binds to the ribosome in the nucleolus and is the last known trans-acting factor to be released from the subunit in the cytoplasm. In order to gain a better understanding of the molecular events leading to the release of Nmd3 from the 60S subunit I set out to identify the binding site of Nmd3 on 60S. In a collaboration with Dr Joachim Frank's laboratory, we obtained a cryo-EM model of Nmd3 in a complex with 60S showing Nmd3 binding to the subunit joining face of the ribosome. This work provided the first visualization of an export factor on a ribosomal subunit.

The release of the anti-association factor Tif6 requires the translocase-like GTPase Efl1. Mutations in a loop of Rpl10 which embraces the P site tRNA trapped Tif6 on the subunit. These Rpl10 mutants could be suppressed by Tif6 mutants which have weakened affinity for the subunit. Mutations in Efl1 which suppress these Rpl10 mutants were also obtained. These suppressing mutations in Efl1 mapped to regions on the translocases eEF2 and EF-G important for conformational changes during translation. These results highlight molecular signaling between the P site, involving a loop of Rpl10, and Tif6, 90Å away. I propose that Efl1 promotes a translocation-like event during biogenesis of the 60S subunit prior to its first round of *bona fide* translation.

Table of Contents

List of tables

List of Figures

List of Illustrations

Chapter I

Introduction

1.1 Overview

In all living organisms the pathway of decryption of the genetic code is conserved. DNA is transcribed into ribonucleic acid (RNA) which is subsequently translated into proteins. Translation of the genetic code from nucleic acid to amino acid is undertaken by the ribonucleoprotein (RNP) complex, the ribosome.

Ribosomes are composed of two subunits (40S and 60S in eukaryotes) that are separately preassembled in the nucleus prior to being exported to, and matured in, the cytoplasm. Upon completion of their maturation in the cytoplasm the 40S and 60S subunits come together on a messenger RNA (mRNA) to form 80S ribosomes that decode mRNA in the 40S and synthesize polypeptides in the 60S subunit.

Eukaryotic ribosome biogenesis is a complex, energy intensive process that involves more than 200 trans-acting factors, most acting in the nucleus. Upon reaching the cytoplasm a relatively small number of maturation steps yields translationally active subunits (Illustration 1.1). My dissertation work focused on specific aspects of cytoplasmic maturation of the large ribosomal subunit in the yeast *Saccharomyces cerevisiae.* Two critical factors that must be removed during cytoplasmic maturation are the nuclear export adaptor Nmd3 and the subunit anti-

association factor Tif6. In my thesis work I identified the binding site of Nmd3 on the large subunit. I also identified a molecular signaling pathway that triggers the release of Tif6. I propose that this molecular signaling represents a quality control step in 60S biogenesis. My work has deepened our understanding of the ways in which the cell assures that only translation-competent ribosomes are released in the pool of active ribosomes.

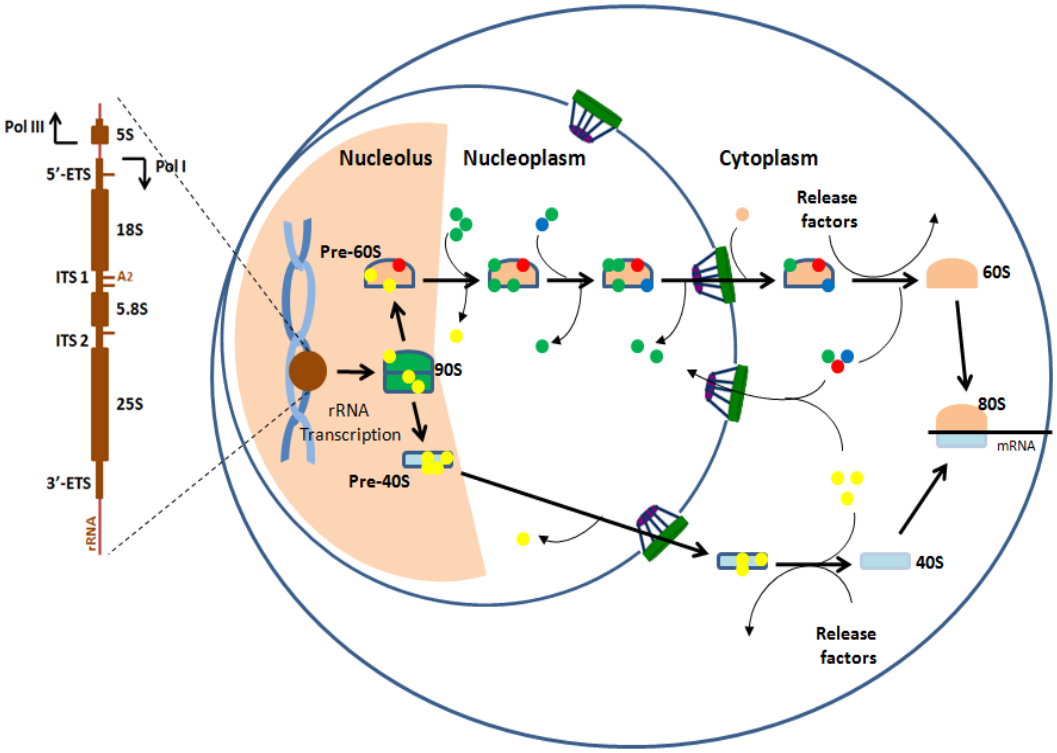

Illustration 1.1 Overview of ribosome biogenesis in eukaryotes
Ribosome synthesis initiates in the nucleolus. rDNA transcription yields a pre-rRNA 35S (not shown), which assembles with biogenesis factors to make up the 90S particle. rRNA cleavage yields pre-40S and pre-60S. Early binding factors are released as ribosome assembly progresses and need to be recycled to the initial site of binding (factors that bind in the nucleus and are released in the cytoplasm need to recycle back to the nucleus to support further rounds of biogenesis, for example Tif6 (solid red) and Nmd3 (solid blue)). Color code based on binding site of factor: yellow, nucleolar factor; green, nuclear factor, pink, cytoplasmic factor.

1.2 The ribosome

Ribosomes are the macromolecular complexes that translate messenger RNAs (mRNA) into proteins. Although ribosome function is conserved between the prokaryotic and eukaryotic ribosome, major differences exist both in composition and biogenesis of ribosomes.

1.2.1 Composition of the ribosome

In eukaryotes the ribosome is comprised of a small, 40S, and a large, 60S, subunit, defined by their behavior in velocity sedimentation. The small subunit carries out mRNA decoding and the large subunit catalyzes peptide synthesis via the peptidyl-transferase reaction. The 60S subunit is composed of three different ribosomal RNAs (rRNA): 5S, 5.8S and 25S (28S in higher eukaryotes), and 46 ribosomal proteins (r-proteins) (Planta and Mager, 1998). The 40S subunit is made up of a single rRNA, 18S, and 33 r-proteins (Planta and Mager, 1998; Sengupta et al., 2004). The two subunits come together for translation and form the 80S ribosome. In contrast, the prokaryotic ribosome (of bacteria and archaea) is made up of 30S and 50S subunits which together form the 70S. The 50S subunit is composed of 5S and 23S rRNA and some 30 proteins, while the 30S subunit is made up of a single rRNA, 16S, and about 21 proteins. The bacterial and archaeal ribosomes are similar in size, around 2.5MDa, in contrast eukaryotic ribosomes are larger. The yeast *Saccharomyces cerevisiae* ribosome is roughly 40% larger than *Escherichia*

coli ribosome, at about 3.2MDa. Higher eukaryote ribosomes are around 3.8MDa (Morgan et al., 2000).

1.2.2 Structure of the ribosome

1.2.2.1 Ribosome structures

In the past 10 years, an impressive amount of structural work has provided invaluable insights into the structure and function of prokaryotic and eukaryotic ribosomes. At the turn of the century, crystal structures of the prokaryotic ribosome provided a first glimpse at the atomic structure of the ribosome. These atomic structures confirmed that the ribosome is at its core a ribonucleic acid machine, or ribozyme, decorated with ribosomal proteins on its surface. The initial large subunit structure from the archaea *Haloarcula marismortui* (Ban et al., 2000) and small subunit structure from the bacteria *Thermus thermophilus* (Wimberly et al., 2000) were followed by a slew of structures of the bacterial 50S and 70S by crystallography or cryo-EM of increasing resolution (Gao et al., 2003; Harms et al., 2001; Schuwirth et al., 2005; Selmer et al., 2006; Yusupov et al., 2001). Flexible elements like the L7/L12 and the L1 stalk, which were not resolved in these structures, were solved separately (Diaconu et al., 2005; Nikulin et al., 2003). The eukaryotic ribosome proved to be more difficult to crystallize. Docking of prokaryotic atomic structures into eukaryotic cryo-EM provided the first structural models but lacked eukaryotic specific segments and r-proteins (Spahn et al., 2001; Spahn et al., 2004). Later cryo-EM structures of the eukaryotic ribosome revealed

the position of rRNA extension elements and additional eukaryotic-specific r-proteins (Becker et al., 2009). These were resolved in higher-resolution cryo-EM in which 74 out of the 80 eukaryotic r-proteins have been modeled (Armache et al., 2010a, b). Recently, the actual crystal structure of the *S. cerevisiae* 80S was obtained at 4.25Å (Ben-Shem et al., 2010).

Overall this large body of structural work confirmed numerous biochemical studies and highlights two striking features of ribosomes across the domains of life.

1.2.2.2. Ribosomes are highly conserved molecular machines at their functional core.

As mentioned above, across life the repartition of task between the large and small subunits is conserved. The small subunit carries out decoding of the mRNA, with the help of tRNAs, which each carry an amino acid (aa) specific to the anti-codon present on the tRNA (aminoacyl-tRNA (aa-tRNA)). In contrast, the large subunit is the place where peptides are synthesized via the rRNA dependent peptidyl-transferase reaction. The functional core of the ribosome is rRNA-based and the overall architecture of ribosomes is conserved. See Illustration 1.2 for a more detailed account of the conserved salient features of the large ribosomal subunit. The core of the small subunit, where aminoacylated-tRNAs are decoded, of the large subunit, where peptide bonds are formed, and, on both subunits, where tRNAs bind during translocation, are highly conserved from bacteria to higher eukaryotes (Gutell et al., 1985). Similarly, r-proteins crucial to the ribosome activity are

conserved. For example the P0/P1/P2 stalk (L10/L7/L12 in prokaryotes), which is essential for recruitment and activation of GTPases to the ribosome during biogenesis and translation is highly conserved

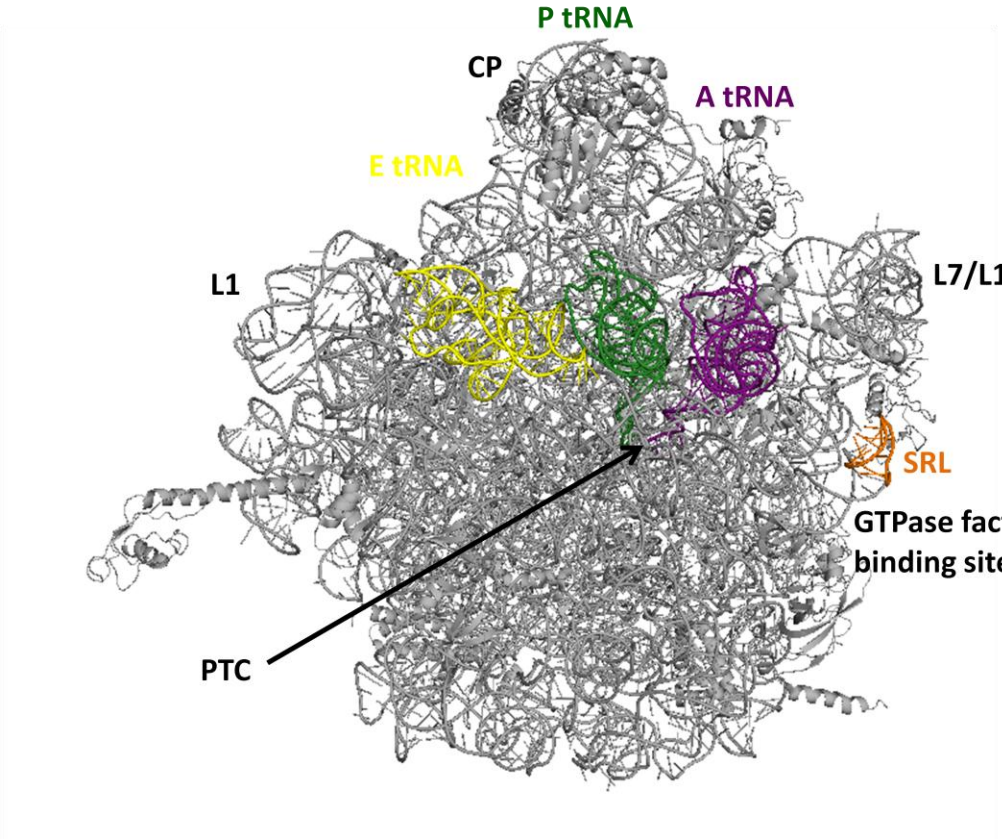

Illustration 1.2 Salient features of the large ribosomal subunit
The three tRNA binding sites on the ribosome: the A site, where the incoming aminoacyl-tRNA binds, the P site where the peptidyl-tRNA, containing the nascent peptide chain, binds and the E (exit) site where the deacylated P-site tRNA resides after peptide-bond formation but before being released from the ribosome. A tRNA (purple): aminoacyl-tRNA. P tRNA (green): peptidyl-tRNA. E tRNA (yellow): exit-tRNA. PTC: peptidyl transferase center (catalytic center of the large subunit where the peptidyl transferase reaction occurs - the rRNA catalyzed reaction whereby the nascent peptide on the P-site tRNA is transferred to the amino acylated tRNA in the A site). CP: Central protuberance. L1: L1 stalk (element that interacts with the newly deacetylated tRNA in the P site and facilitates its movement to the E site)
L7/L12: L7/L12 stalk (P1/P2 stalk in eukaryotes) (involved in recruitment and activation the GTPases). (L10/P0 forms the base of the stalk (not shown)).
GTPase factor binding site: also named GTPase activating center (GAC), region of the large subunit composed of rRNA elements where GTPase bind the ribosome. The sarcin ricin loop (SRL, orange), a conserved rRNA loop in the GAC which is essential for binding of translation factors to the ribosome (cleavage by the toxins sarcin and ricin prevent binding of GTPases, hence the name of the loop). (adapted from PDB 3I8F and 3I8G (Jenner et al., 2010b))

1.2.2.3 Ribosomes across the three domains of life are nonetheless different

Comparison of prokaryotic and eukaryotic ribosomes reveals, as expected, a larger eukaryotic ribosome with rRNA expansion segments inserted into the highly conserved rRNA core and extending primarily on the surface of the ribosome. Comparison also reveales the position of eukaryotic or prokaryotic specific r-proteins and of eukaryotic-specific extension segments in the conserved r-proteins. Eukaryotic ribosomes have more r-proteins per rRNA than their prokaryotic counterparts. An interesting example of differences in r-proteins are bacterial L16 and its eukaryotic ortholog Rpl10. Comparison of bacterial and eukaryotic structures reveals structural differences in the P site of the large subunit: in prokaryotes the P site is in part made of the N terminus of L27, a prokaryote-specific r-protein, and of a loop of the globular r-protein L16 which extends towards the P site (Gao et al., 2009). Eukaryotes lack L27, and cryo-EM reconstruction of the large subunit reveal an extended loop of Rpl10 (the L16 homolog) which replaces L27 (Illustration 1.8). The functional significance of L16/Rpl10 will be discussed in section 1.5.5.1 These observations, together with other available structures of the ribosome in complex with different GTPases, in the presence of tRNAs or locked in specific translation intermediates by the use of antibiotics, enabled us to frame the work presented in chapter IV.

1.2.3 Eukaryotic ribosome biogenesis: Why so many factors?

1.2.3.1 Eukaryotic ribosome assembly involves numerous factors

In addition to the size and composition differences between the bacterial and eukaryotic ribosome, the assembly of ribosomes is extremely different.

Bacteria contain a relatively small number of ribosome biogenesis factors (Iost and Dreyfus, 2006; Jiang et al., 2007; Karbstein, 2007; Maki et al., 2002). Of these assembly factors only the few rRNA modifying enzymes and nucleases, required for cleavage of the pre-rRNA transcript, are essential (Britton, 2009; Connolly and Culver, 2009; Kaczanowska and Ryden-Aulin, 2007). None of the nucleoside triphosphate (NTP) consuming enzymes involved in bacterial ribosome biogenesis are essential (Britton, 2009). Furthermore, the functional bacterial ribosome can be assembled *in vitro* without any factors (Rohl and Nierhaus, 1982; Sanchez et al., 1990).

In stark contrast to prokaryotic ribosome biogenesis, eukaryotic ribosome biogenesis involves numerous essential factors which coordinate what appears to be an intrinsically spontaneous process in prokaryotes. Ribosome assembly in eukaryotes is a complex process involving over 200 factors (Henras et al., 2008) alongside more than 70 small nucleolar RNAs (snoRNAs) (Decatur et al., 2007). These factors aid the assembly, transport and maturation of the eukaryotic ribosome and are involved in rRNA cleavage, modification and folding events, as well as r-protein binding and bridging interaction with the nuclear pore complex (NPC) during export to the cytoplasm. These numerous steps and their temporal and physical relationships were initially characterized to a limited extent by genetic screens in yeast (Kressler et al., 1999; Venema and Tollervey, 1999). It was not until the advent of advanced

purification methods (i.e. TAP) and drastic advances in mass spectrometry techniques that a clearer picture of how these factors come together to generate the ribosome emerged (Tschochner and Hurt, 2003; Zemp and Kutay, 2007).

One outstanding question that arises from these observations is why did such a complex process evolve? Most likely the main reason lays in the overall increased complexity of eukaryotic cellular processes. Increased complexity requires both quality control and increased coordination between various cellular processes. The need for quality control in ribosome biogenesis becomes evident when considering the fact that in *S. cerevisiae*, about 80% of the mRNAs are present in less than 2 copies per cell (Wang et al., 2002). Binding of a deficient ribosome to an mRNA, and therefore the sequestration of that mRNA, would have dramatic consequences on the proteome of a cell. Similarly, greater complexity of cellular processes requires coordination between these processes and thus factors that bridge different processes and coordinate their regulation. Given the central role ribosomes play in the life of a cell, extensive quality control and cross-talk with various other cellular processes seem to justify the increased number of factors and the accompanying increased energy requirement (in the form of NPTases) observed in eukaryotic ribosome biogenesis.

1.2.3.2 Quality control

Quality control can be envisioned to take place throughout ribosome biogenesis and be dependent on recruitment platforms which would be made up of any combination of the following elements: rRNA folds, trans-acting factors, snoRNAs and r-proteins

(Henras et al., 2008; Lafontaine et al., 1998). These elements would come together to form binding platforms which allow for the recruitment of subsequent elements. Sequentially, factors would bind the nascent ribosome, modify it in a specific fashion (for example by promoting a specific folding event, inducing rRNA cleavage or allowing for the recruitment of an r-protein or a scaffolding factor) and then be released from the ribosome either spontaneously (when the event induced by the factor reduces its affinity for the ribosome) or by recruitment of release factors. Thus, during its assembly and maturation the ribosome is an evolving binding platform which sequentially promotes events that move it towards translation competency. For example, it has been suggested that once the nuclear pre-60S is far enough along its assembly pathway it exhibits the proper binding surface that allows for binding of the export adapter Nmd3, thus ensuring that only export competent ribosomes are exported to the cytoplasm (Johnson et al., 2001; Johnson et al., 2002). Further exemplifying this recruitment platform concept is the release of the anti-association factor Tif6. The formation of the ribosomal stalk is required for the release of Tif6 (Kemmler et al., 2009; Lo et al., 2010). Tif6 release also requires the translocase-like factor Efl1 (Becam et al., 2001; Senger et al., 2001). During translation the ribosomal stalk recruits the Efl1 homolog translocase eEF2 which binds the GTPase activating center (GAC), in part composed of the sarcin-ricin loop (SRL) (Ballesta and Remacha, 1996; Berk and Cate, 2007; Gonzalo and Reboud, 2003; Uchiumi et al., 1999). Published data supports Efl1 and eEF2 sharing a binding site on the subunit (Senger et al., 2001). Thus, release of Tif6 appears to be

dependent on the ribosome reaching a state in its maturation which allows for recruitment and activation of Efl1. Such events enable monitoring of the structural and functional integrity of the ribosome prior to occurrence of subsequent steps. Binding surfaces could potentially monitor large part of the nascent ribosome by involving cooperation between multiple factors, r-proteins and rRNA helices. In a similar fashion, binding of factors can prevent premature downstream events such as folding of rRNA or assembly of r-protein or association of factors. For example place-holders are used during ribosome biogenesis to prevent the premature binding of trans-acting factors or r-proteins. This is the case with Mrt4 and Rlp24 which are place holders for P0 and Rpl24 respectively (Kemmler et al., 2009; Lo et al., 2010; Lo et al., 2009; Rodriguez-Mateos et al., 2009). This intensive interplay of factors and ribosome elements during biogenesis is thought to allow for proper folding of rRNA and addition of r-proteins and prevent the occurrence of dead-end assembly intermediates which might yield inactive or defective ribosome subunits (Mulder et al., 2010; Strunk and Karbstein, 2009).

1.2.3.3 Ribosome degradation

Eukaryotic cells have evolved means of structurally and functionally checking the nascent ribosome as it is assembled. What happens to pre-mature subunits which are defective and fail such a test? Cells have developed multiple mechanisms to dispose of nascent subunits not moving along the assembly pathway in a timely manner before accumulation of defective subunits reaches harmful levels (Lafontaine, 2010). In eukaryotic cells RNAs are degraded by the exosome (Schmid and Jensen, 2008), a

complex associated with the RNases, Rrp44 and Rrp6 and specificity factors which modulate its function and targets, whereas proteins are degraded by the proteasome following their targeting via ubiquitination .

Nuclear pre-ribosome monitoring: TRAMP is a nuclear complex consisting of either of two RNA poly(A) polymerases (Trf4 and Trf5), an RNA-binding protein and a helicase. The TRAMP complex adds a short poly(A) tail to RNAs (Houseley et al., 2006) , targeting them to and stimulating the activity of the exosome (Andersen et al., 2008). TRAMP monitors nascent pre-ribosomes during and following transcription of the rDNA, (Wery et al., 2009) and targets pre-ribosomes that are stalled in the assembly pathway (Dez et al., 2007; Wery et al., 2009).

Cytoplasmic pre-ribosome monitoring: Non functional rRNA Decay (NRD) degrades cytoplasmic nascent and mature subunits (LaRiviere et al., 2006). Small subunit NRD and large subunit NRD are mechanistically different. Small subunit NRD targets translating ribosomes and involves the translation termination factor-related proteins Dom34 and Hbs1 (Cole et al., 2009), in concert with the exoRNAse Xrn1 (Fujii et al., 2009) and the RNA exosome (Doma and Parker, 2006), both of which are also involved in No Go Decay (NGD) (mechanism by which mRNA harboring a stalled ribosome are degraded) (Doma and Parker, 2006). Large subunit NRD involves the ubiquitination of unidentified components of the defective large ribosomal subunits by Mms1 and Rtt101 (Fujii et al., 2009), components of an E3 ubiquitin ligase (Fujii et al., 2009), and the subsequent targeting of the subunit to the proteasome (Beau et al., 2008).

Numerous mutations in rRNA, r-proteins and ribosome biogenesis factors causing the production of defective subunits have been identified. The pathways by which these defective subunits are tagged for degradation and the complexes involved in their degradation are being elucidated. However, what initially flags a ribosome as defective is not yet known.

1.2.3.4 Cross-talk

Another probable reason why eukaryotic ribosome biogenesis involves such a staggering number of factors is the need to coordinate such an energy intensive and essential process with other cellular processes. This is accomplished via the sharing of components between pathways and through co-regulation with other pathways. Ribosome biogenesis shares components with replication, cell cycle control, rRNA transcription, tRNA export and stress response (Angermayr and Bandlow, 2002; Bernstein et al., 2007; Du and Stillman, 2002; Killian et al., 2004; Steiner-Mosonyi et al., 2003). As well, ribosome biogenesis is co-regulated with other pathways. This co-regulation can occur via modification of elements from both pathways by a single enzyme. For example, the kinase Gcn2 regulates translation initiation, in response to nutrient starvation via uncharged tRNAs, and cell cycle checkpoint control, in response to DNA damage (Hinnebusch and Natarajan, 2002; Menacho-Marquez et al., 2007). Gcn2 was shown to genetically and physically interact with numerous ribosome biogenesis factors (Collins et al., 2007; Gavin et al., 2006; Gavin et al., 2002; Schafer et al., 2003; Wilmes et al., 2008). Hence Gcn2 might phosphorylate and inactivate ribosome biogenesis factors in response to nutrient stress.

Furthermore, the use of numerous NTP-dependent factors allows the cell to coordinate ribosome biogenesis with other pathways depending on the energy content of the cell (Strunk and Karbstein, 2009).

In the next sections I will briefly describe eukaryotic ribosome biogenesis, focusing mostly on the large subunit assembly in the nucleus, its transport to the cytoplasm and the final maturation steps in the cytoplasm, which yield a translation-competent subunit. From this account, ways in which quality control occurs in ribosome biogenesis will become evident.

1.3 Ribosome biogenesis in the nucleus

In the yeast *Saccharomyces cerevisiae* ribosome biogenesis initiates in the nucleolus, a protein-dense sub-nuclear structure which contains 150-200 identical rDNA repeats located on chromosome XII (Petes, 1979, Venema, 1999 #277). The nucleolus is the site of both the synthesis of rRNA and where most of the assembly and processing events leading to mature ribosomes happen. As such, the nucleolus contains numerous factors involved in both transcription of rDNA and early ribosome biogenesis (Boisvert et al., 2007). Nuclear ribosome biogenesis represents a physical compartmentalization which provides an environment separated from translation, preventing cytoplasmic factors, such as those involved in translation, from interfering with ribosome assembly (Panse and Johnson, 2010).

The transcription of the rDNA repeats yields two primary products: a 5S transcript synthesized by RNA polymerase III and a 35S transcript synthesized by

RNA polymerase I. The 35S transcript is the precursor to 18S, 5.8S and 25S. Synthesis of both subunits from a single transcript ensures that they are synthesized in equal stoichiometry. The 35S pre-rRNA has at its 5'and 3' ends external transcribed spacers (ETS). The 5'ETS is followed, in sequence, by 18S, 5.8S and 25S, with each rRNA being separated from the others by an internal transcribed spacer (ITS) (Illustration 1.1). The 35S and associated factors form the 90S precursor which will undergo numerous cleavages, modifications and folding events to yield the mature (40S and 60S) subunits (Fromont-Racine et al., 2003; Kressler et al., 1999; Venema and Tollervey, 1999). More than 200 trans-acting factors (including helicases, GTPases, AAA-ATPases and chaperones) are involved in these processes, as well as around 70 small nucleolar RNAs (snoRNAs) aiding in the targeting of modification enzymes and early nucleases to their rRNA site of action. These events are thought to ensure the proper folding of critical core rRNA regions, such as the peptidyl-transferase center and the decoding center, and provide en route to maturity increased stability of the ribosome, also aided in this task by the timely addition of the various r-proteins (reviewed in (Henras et al., 2008; Staley and Woolford, 2009; Strunk and Karbstein, 2009)).

1.3.1 rRNA cleavages

Ribosome biogenesis involves rRNA cleavages. Each cleavage event is an irreversible step and commits the nascent ribosome forward on its path to maturation. These cleavage events could represent check-points if the ribosome needs to be correctly assembled and exhibit the right binding surface in order to recruit the

proper nucleases. Endonuclolytic cleavage of 90S at the A_2 site yields 43S and 66S precursors. 43S is a pre-40S particle containing 20S rRNA. This pre-40S species is export competent, that is it presents the correct binding platform for its export factors, and is transported to the cytoplasm where final cleavage by Nob1 yields the mature 18S rRNA (Lamanna and Karbstein, 2009; Pertschy et al., 2009). Upon A_2 cleavage, large subunit r-proteins and factors bind the remaining 27S rRNA to form the pre-60S particle, 66S. 27S processing steps, which yield mature 5.8S and 25S, are shortly described below (reviewed in (Henras et al., 2008; Staley and Woolford, 2009; Strunk and Karbstein, 2009)). The 27SA species is processed into two products which differ by the presence ($27SB_L$) or absence ($27SB_S$) of additional sequence at their 5' end. Further processing frees the 5.8S precursors ($7S_L$ and $7S_S$ respectively) and 25S. Exonucleolytic removal of the 3' end of $7S_{L/S}$ releases the $6S_{L/S}$ species. At this point the pre-60S subunit is exported to the cytoplasm were final processing by the exonuclease Ngl2 generates the mature $5.8_{L/S}$ (Thomson and Tollervey, 2010).

1.3.2 rRNA modifications

In addition to cleavages, the pre-rRNAs are extensively modified, mostly in the context of the nascent 90S. Numerous methylase and pseudouridine synthase containing snoRNPs, directed to their site of actions by snoRNAs, introduce 55 pseudouridilations and 44 methylations in the yeast rRNA (reviewed in (Tschochner and Hurt, 2003; Venema and Tollervey, 1999)). Members of the box H/ACA family

of snoRNPs and box C/D snoRNPs perform the pseudouridilations (Ganot et al., 1997; Ni et al., 1997) and methylations (Cavaille et al., 1996; Kiss-Laszlo et al., 1996; Tycowski et al., 1996) respectively. Nop1 is the methyltransferase of box C/D snoRNPs and Cbf5 is the pseudouridine synthase of box H/ACA snoRNPs. These modifications occur mostly at functionally relevant rRNA sites, especially the peptidyl-transferase center in the 25S rRNA and the decoding center in the 18S rRNA (Decatur et al., 2007). Individually these modifications are not essential (Lowe and Eddy, 1999; Samarsky and Fournier, 1999); however they are as a whole (Green and Noller, 1996; Raychaudhuri et al., 1984; Tollervey et al., 1993). It is thus thought that they are required for fine-tuning the ribosome's function (Tollervey et al., 1993; Zebarjadian et al., 1999).

1.3.3 r-proteins

R-proteins are mostly added to the nascent subunits in the nucleus and only a few r-proteins are added in the cytoplasm (see section 1.5). The elucidation of the timing of protein association with the nascent subunit along the assembly pathway has relied on stalled assembly complexes purification, mostly TAP purification, followed by mass spectrometry. Due to the fact that r-proteins are usual contaminants in TAP purification experiments it has been difficult to determine their order of incorporation in nascent subunits.

1.4 Export of the 60S ribosomal subunit from the nucleus to the cytoplasm

Once the ribosomal subunits attain export competency, that is exhibit the proper recruiting platforms for their export factors, they are transported from the nucleus to the cytoplasm where they will undergo final maturation. Ribosomes are exported from the nucleus in a functionally inactive state (Panse and Johnson, 2010). Large subunits are exported bound by trans-acting factors which would prevent their function, for example the anti-association factor Tif6 (Si and Maitra, 1999). Furthermore, they lack crucial elements essential for ribosome function in translation, such as the P0/P1/P2 stalk (Kemmler et al., 2009; Lo et al., 2009; Rodriguez-Mateos et al., 2009) and r-proteins such as Rpl10 (Hedges et al., 2005; West et al., 2005). Indirectly, this non-functional state of the ribosome –i.e. lacking the P0/P1/P2 stalk- might facilitate the export of the subunit by conferring a tighter packaging that allows it to pass more readily through nuclear pore complexes (NPCs).

1.4.1 The Nuclear Pore Complex

Transport through the nuclear membrane occurs via nuclear pore complexes (NPCs). NPCs are huge complexes of around 65MDa in yeast and are made up of proteins termed nucleoporins (Nups) (Rout et al., 2000). About a third of these NUPs contain FG-repeats (GLFG, FXFG, SXFG or PXFG motifs) which are essential for interaction with transport receptors. The FG-repeats interact with one another and form a dense meshwork in and around the center of the NPCs. This meshwork

prevents the passage of most macromolecules while allowing the movement of small molecules. The interaction of hydrophobic residues on the surface of export factors with the phenylalanine ring of the FG-repeats allows for the disruption of the FG-repeats interactions and the partitioning of the transport complexes into the meshwork and the passage of these factors and associated cargos through the NPC (reviewed in (Wente and Rout, 2010)).

1.4.2 Large subunit export factors

Karyopherins are one such group of FG-repeats-interacting transport receptors which selectively bind to transport signals on cargo molecules and allow for controlled transport of cargos in and out of the nucleus (Gorlich and Kutay, 1999). Importins bind to nuclear localization signals (NLSs) and direct import of cargos while exportins bind to nuclear export signals (NESs) and orchestrate export of cargos. Thirteen karyopherins exist in yeast: 9 importins and 4 exportins (Pemberton and Paschal, 2005). Of particular importance is the export receptor Crm1, that is essential for export of ribosomes (Gadal et al., 2001; Ho et al., 2000b). The leucine-rich NES that Crm1 recognizes is well characterized ((Fornerod and Ohno, 2002; Guttler et al., 2010; Kutay and Guttinger, 2005; la Cour et al., 2004). Of particular technical interest is Crm1 sensitivity to the fungal metabolite Leptomycin-B (LMB). In humans, LMB alkylates a residue (Cys528) located in Crm1 NES binding groove (Dong et al., 2009), inhibiting its export function by blocking access to NESs (Kudo et al., 1999). Wild-type yeast is not sensitive to LMB. However, mutating residue

T539, corresponding to Cys528 in human Crm1, to Cys renders yeast Crm1 sensitive to LMB (Neville and Rosbash, 1999), which allows us to specifically inactive Crm1.

The directionality of active movement across the nuclear membrane is directed by a molecular gradient (reviewed in (Gorlich and Kutay, 1999). Ran, a GTPase, modulates karyopherin binding to transport signals. A RanGTP gradient is created across the nuclear membrane by a nuclear restricted nucleotide exchange factor (RanGEF) and a cytoplasmic GTPase activating protein (RanGAP). Export karyopherins such as Crm1 bind NES cargos cooperatively with RanGTP in the nucleus, and promote export of the ternary complex. Once in the cytoplasm, RanGAP activates the GTPase activity of Ran, inducing release of the cargo. Importins bind and transport NLS-containing cargos independently of Ran. Once in the nucleus, binding of RanGTP to the importin releases the cargo. RanGTP has been shown to be required for ribosome export (Hurt et al., 1999; Moy and Silver, 1999) due to its interaction with Crm1 (Ho et al., 2000b).

The surface of the large subunit is hydrophilic while the lumen of the NPC is hydrophobic, thus passage through the NPC requires export factors to facilitate its interaction with nucleoporins. Furthermore, the 60S subunit is one of the bulkiest cargos to be transported across the nuclear membrane and, accordingly, requires multiple export receptors for efficient transport through the NPC (Ribbeck and Gorlich, 2001). In yeast, multiple such factors have been identified to date: Nmd3/Crm1 (Gadal et al., 2001; Ho et al., 2000b), Mex67/Mtr2 (Bassler et al., 2001;

Yao et al., 2007), Arx1 (Bradatsch et al., 2007; Hung et al., 2008) and Ecm1 (Yao et al., 2010). These will be discussed independently below.

1.4.2.1 Nmd3

Nmd3, is an essential 59KDa protein in yeast (Ho and Johnson, 1999). Nmd3 is required for export of the large ribosomal subunit (Ho et al., 2000a) and provides the 60S ribosome an NES in trans (Gadal et al., 2001; Ho et al., 2000b). Nmd3 export of the subunit is Crm1-dependent since it contains a canonical leucine-rich NES. Accordingly, LMB treated cells trapped both Nmd3 and 60S in the nucleus (Ho et al., 2000b). Nmd3 binds the pre-60S in the nucleolus (as some Nmd3 mutants trap 60S in the nucleolus (Kallstrom et al., 2003)), and transports the subunit to the cytoplasm were it is released by the concerted action of the r-protein Rpl10 and the putative GTPase Lsg1 (Hedges et al., 2005; West et al., 2005). Extensive mutational analysis of Nmd3 has revealed multiple domains (Hedges et al., 2006). The N terminal region of yeast Nmd3 contains domains involved in subunit binding whereas its C terminus contains the transport signals required for import and export to and from the nucleus. Yeast Nmd3 is thought to contain at least two 60S-binding domains, one organized by two putative zinc binding motifs (Cys-X2-Cys) and a second in a region N-terminal to the C-terminal shuttling domain (Hedges et al., 2006). These two domains were identified by random mutagenesis of Ndm3 seeking to find loss of function mutants (Hedges et al., 2006). Mutations in these 60S binding domains weaken Nmd3 affinity for the ribosome (Hedges et al., 2006). At its utmost

C-terminal end, Nmd3 exhibits a canonical leucine-rich NES which provides the 60S subunit an export signal in trans. Deletion of the NES as well as mutations of several of the conserved leucines trap both Nmd3 and 60S in the nucleus and severely affects the growth of cells (Gadal et al., 2001; Hedges et al., 2006; Ho et al., 2000b). Disparate export capabilities of some of the NES mutants, depending on their context (full length Nmd3 or on an exogenous reporter), suggests that Nmd3 contains additional NES sequences. One such region is a coiled-coil present N-terminaly to the NES. Deletion of this element sensitizes NES mutants, increasing their export defect (Hedges et al., 2006). Studies in both Xenopus oocytes (Trotta et al., 2003) and Hela cells (Thomas and Kutay, 2003) support a similar role for Nmd3 in higher eukaryotes. While the C terminal shuttling domain is unique to eukarya, the N terminus portion of the protein is conserved in eukarya and archaea, suggesting additional function of Nmd3, probably in biogenesis.

1.4.2.2 Mex67/Mtr2

The second large ribosomal subunit export receptor is the Mex67/Mtr2 heterodimer. Mex67 and Mtr2 were first identified as the export receptor for mRNAs (Katahira et al., 1999). But multiple lines of evidence support a role for Mex67 and Mtr2 in ribosome export. First, a mutation in Mtr2 was shown to impair 60S export specifically without affecting mRNA export (Bassler et al., 2001). This allele was synthetic lethal and synthetic sick with an *nmd3* mutant and 60S biogenesis factors respectively (Bassler et al., 2001). Mutations or deletions of insertions in both

Mex67 and Mtr2 not present in metazoan orthologs exhibit 60S export defects and lethality (Yao et al., 2007), while overexpression of Mex67 suppresses the lethal phenotype of an *nmd3* NES deletion (Hung et al., 2008). Additionally, Mtr2 can be detected in pre-60S complexes (Bradatsch et al., 2007). In contrast to Nmd3, Mex67/Mtr2 mediated export is Crm1/Ran-independent and bridges the interaction between 60S and the FG repeats of nucleoporins directly (Santos-Rosa et al., 1998). In higher eukaryotes, Mex67 is not involved in ribosome export.

1.4.2.3 Arx1.

The third known 60S ribosome export receptor is Arx1 (Bradatsch et al., 2007; Hung et al., 2008). Unlike Nmd3/Crm1 and Mex67/Mtr2, Arx1 is not essential. Several lines of evidence support a role for Arx1 as a noncannonical 60S export receptor. First, deletion of *arx1* disrupts 60S export and sequesters both Nmd3 and 60S in the nucleus (Bradatsch et al., 2007; Hung et al., 2008). Synthetic lethality was observed between arx1 and both *nmd3* NES and *nup* mutants, while deletion of *arx1* shows genetic interaction with both Mex67 and Mtr2. Arx1 also physically interacts with Nups as shown by yeast 2-hybrid assay and *in vitro* binding experiments. Furthermore, deletion of *arx1* leads to enrichment of Nmd3, Crm1, Mex67 and Mtr2 in pre-60S particles (Bradatsch et al., 2007; Hung et al., 2008) due to the fact that these subunits are impaired in export and cannot reach the cytoplasm where the release factors for these export adaptors are found.

1.4.2.4 Ecm1.

The fourth and most recently identified 60S ribosome export receptor is Ecm1 (Yao et al., 2010). Ecm1 is a non essential, noncannonical export receptor which aids with export of the large ribosomal subunit. *ecm1* mutants exhibit synthetic lethality or sickness phenotypes with *arx1, mtr2, mex67, nmd3* and *nup* mutants (Bassler et al., 2001; Bradatsch et al., 2007; Yao et al., 2010). Ecm1 depletion in an a*rx1Δ* strain completely traps 60S in the nucleus. Furthermore, Ecm1 was shown to interact physically with both pre-60S factors (by TAP pull-down) and nuclear pore components (by yeast 2-hybrid). Finally, similarly to Arx1, an *ecm1Δ* is partially suppressed by overexpression of Mex67 (Yao et al., 2010).

Together these factors facilitate the transport of the large ribosomal subunit through the hydrophobic core of the nuclear pore complex by providing interactions with nucleoporins either directly (Arx1, Ecm1 and Mex67/Mtr2) or indirectly (Nmd3, which requires Crm1 to bridge such interaction). Although all these export factors bind the large subunit, the actual binding sites of these factors are unknown. Some genetic and biochemical data hint at the binding site of some of these factors. For example, it is thought that Arx1 binds near the exit tunnel since GFP-tagging of r-protein near the exit tunnel reduces its binding to the ribosome (Hung and Johnson, 2006). Similarly, biochemical studies have provided evidence that Mex67/Mtr2 bind to a platform formed by 5S on the large subunit (Yao et al., 2007). In chapter III, in collaboration with Dr Frank's laboratory, I uncovered the binding site of Nmd3. A cryo-EM model of an MBP-Nmd3 fusion protein in complex with the large ribosomal subunit revealed the Nmd3 fusion bound to the subunit joining face of the

large subunit and provided the first visualization of an export factor bound to the ribosome. The binding site of the anti-association factor Tif6 on the large subunit has been elucidated in a similar fashion (Gartmann et al., 2010).

Furthermore, it is not clear if all the export adaptors of 60S are found on the subunit at the same time. The fact that overexpression of Mex67 suppresses *arx1Δ*, *ecm1Δ* and *nmd3ΔNES* mutants and restores export of 60S argues that Mex67 is under-loaded on the subunit and that Mex67 is a limiting factor in the export pathway. Export factor fusions to *nmd3ΔNES* restore export of 60S, also arguing for a lack of direct requirement of Crm1 in export (Lo and Johnson, 2009). Additionally, the NES of Nmd3 fused in Cis to r-proteins supported ribosome export to some extent in an *arx1Δ nmd3ΔNES* strain, indicating an incredible level of flexibility in the 60S export pathway (Lo and Johnson, 2009).

In yeast the large ribosomal subunit has four separate export factors. Intriguingly, only Nmd3 has a conserved role in ribosome export in higher eukaryotes.

1.5 Cytoplasmic maturation of the 60S ribosome

Once exported to the cytoplasm the 60S subunits undergo the final maturation steps that will render them translationally competent. Cytoplasmic maturation of the pre-60S subunit involves the recycling of export factors, the removal of placeholder proteins and the assembly of several critical ribosomal proteins. These maturation events consist of 5 major steps which have been recently ordered in a maturation pathway where each step is dependent on the completion of previous ones

(Illustration 1.3) (Lo et al., 2010). Most of these steps are dependent on NTP-consuming enzymes (2 ATPases and 2 GTPases) and thus could be prone to regulation via cellular levels of NTPs. These steps could represent check-points that probe the ribosome for correct state along the maturation pathway. For example the assembly of the stalk, a crucial element for recruitment and activation of GTPases during translation (Ballesta and Remacha, 1996; Berk and Cate, 2007; Gonzalo and Reboud, 2003), is a prerequisite for release of Tif6 (Lo et al., 2010), an anti-association factor, via the translocase-like GTPase Efl1 (Becam et al., 2001; Senger et al., 2001). This step ensures that only ribosomes able to recruit GTPases correctly are allowed to release Tif6 from the ribosome, thus ensuring that only functional ribosomes enter the translational pool.

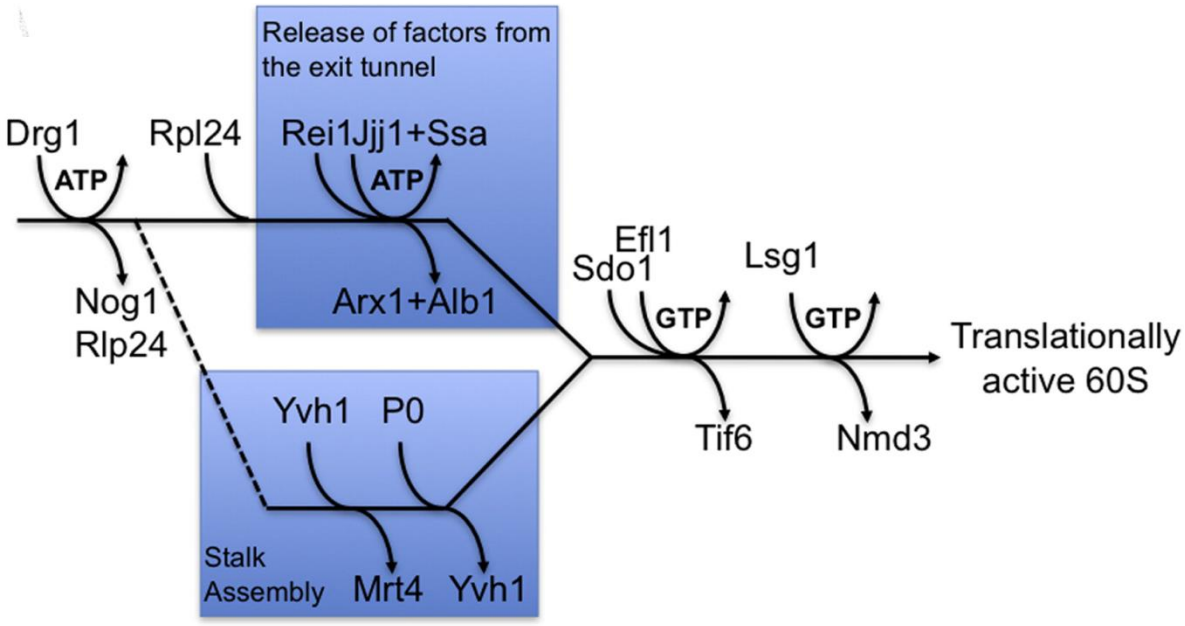

Illustration 1.3 The cytoplasmic maturation pathway of the large ribosomal subunit.

Drg1 facilitates the replacement of Rlp24 by Rpl24, which then recruits Rei1. The latter, together with Jjj1 and Ssa1/Ssa2, enables the release of the export receptor Arx1, located near the polypeptide exit tunnel. In parallel, Yvh1 enables replacement of Mrt4 with P0 to construct the ribosome stalk. In turn, the stalk recruits the GTPase Efl1 to the GTPase-associated center to release Tif6 from the subunit joining face of the particle. The release of Tif6 leads to activation of Lsg1 to release export adaptor Nmd3, also from the joining face. It is important to note that the events indicated represent the order of action of these factors but not necessarily their order of association with the pre-60S particle. From (Lo et al., 2010).

1.5.1 Drg1 step.

Upon pre-60S export to the cytoplasm the AAA-ATPase Drg1 (Zakalskiy et al., 2002) induces release of the placeholder Rlp24 (the nuclear paralogue of the r-protein Rpl24) and of the nuclear GTPase Nog1 (Pertschy et al., 2007). After release of Rlp24, Rpl24 binds to the subunit, probably at the same site. *drg1* mutants block recycling of Rlp24 and Nog1 as well as Arx1, Tif6 and Mrt4 (Lo et al., 2010; Pertschy et al., 2007). Persistence of Arx1 and Tif6 on the subunit is due to lack of release of Rlp24 or lack of loading of Rpl24 and not the lack of Drg1 activity since an *rlp24ΔC* mutant that fails to recruit Drg1 (Lo et al., 2010), traps *rlp24ΔC* on 60S and prevents the recruitment of Rei1, thus preventing the release of Arx1 and consequently the release of Tif6.

1.5.2 Arx1 release.

Next the export receptor Arx1 is released by the concerted action of the C_2H_2-zinc finger protein Rei1, the J domain-containing chaperone Jjj1 of the Hsp40 family and Ssa1, an Hsp70 family ATPase (Demoinet et al., 2007; Hung and Johnson, 2006; Lebreton et al., 2006b; Meyer et al., 2007). *rei1Δ* and *jjj1Δ* both trap Arx1 on the subunit and indirectly prevent release of Tif6. The persistence of Arx1 on 60S is the cause of the block inTif6 release since in a *rei1Δarx1Δ* strain Tif6 is released properly (Lo et al., 2010).

1.5.3 Stalk assembly.

The assembly of the ribosomal stalk takes place in parallel with the release of Arx1, and is also dependent on the Drg1 step (Lo et al., 2010). The ribosomal stalk is a crucial element for recruitment and activation of factors during translation (Ballesta and Remacha, 1996; Berk and Cate, 2007; Gonzalo and Reboud, 2003). The ribosome stalk is formed by a pentamer: P0 (L10 in prokaryotes) and two dimmers of the acidic proteins P1 and P2 (L7/L12 in prokaryotes) (Ballesta and Remacha, 1996; Krokowski et al., 2006). P0 binds to the 25S rRNA and with the r-protein Rpl12 (L11 in prokaryotes) forms the base of the stalk. The P1/P2 dimers interact with P0 (Briceno et al., 2009; Krokowski et al., 2006). The pre-60S subunit reaches the cytoplasm with a P0 nuclear paralogue, Mrt4, bound to the P0 binding site. Mrt4 needs to be released from 60S to allow P0 binding. The dual-specificity phosphatase Yvh1 is required for the release of Mrt4 since *yvh1Δ* traps Mrt4 in the cytoplasm on the 60S subunit (Kemmler et al., 2009; Lo et al., 2009). The Yvh1-containing subunit then requires loading of P0 to release Yvh1 and assemble the mature stalk (Lo et al., 2009).

1.5.4 Tif6 release.

The release of Arx1 and the ribosomal stalk assembly are prerequisites for the release of the anti-association factor Tif6 by the GTPase Efl1 and Sdo1 (Lo et al., 2010).

1.5.4.1 Tif6

The essential protein Tif6 (eIF6 in higher eukaryotes) is an anti-association factor which binds the pre-60S subunit in the nucleolus and prevents premature joining of

60S subunit with the 40S subunit. Tif6 anti-association activity has been shown by *in vitro* experiments both in yeast (Si and Maitra, 1999) and in higher eukaryotes (Raychaudhuri et al., 1984; Russell and Spremulli, 1979; Valenzuela et al., 1982). Recently the binding site of Tif6 on the 60S ribosome has been elucidated by cryo-EM reconstruction (Illustration 1.4 A and B)(Gartmann et al., 2010). Tif6 binds to the SRL and Rpl23 and its binding site coincides with the inter-subunit bridge B6. Binding of Tif6 at this site affects formation of surrounding bridges as well and explains its anti-association activity.

In yeast, depletion of Tif6 leads to rRNA processing defects and accumulation of 35S and 27S pre-rRNA precursors, while reducing the formation of mature 25S and 5.8S rRNA compared to 18S formation. Correspondingly, Tif6 depleted strains exhibit low levels of 60S subunits and consequently halfmer polyribosomes can be observed. (Basu et al., 2001; Si and Maitra, 1999). Halfmers are mRNAs that contain a 48S initiation complex that has not yet joined with 60S, indicative of a defect in biogenesis and/or subunit joining. The release of Tif6 involves two proteins: the translocase-like GTPase Efl1 (Illustration 1.4 C and D) and the Shwachman-Bodian Diamond Syndrome (SBDS) homolog Sdo1.

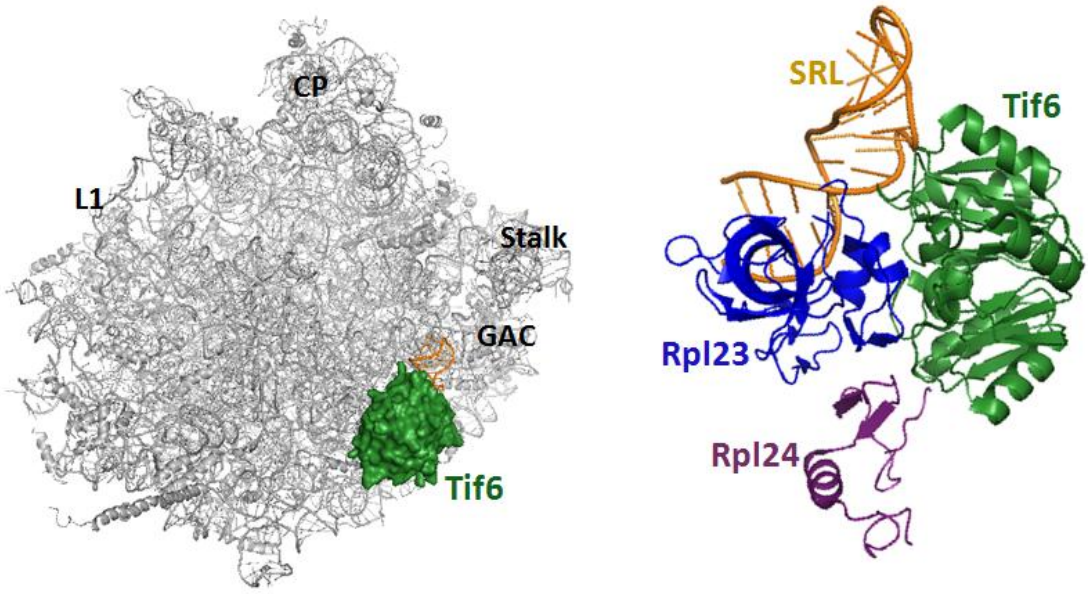

Illustration 1.4 Yeast Tif6 binding site on the large ribosomal subunit
Left panel: Tif6-60S complex, Grey, 60S ribosomal subunit; Green, Tif6; Orange, SRL (Sarcin Ricin Loop). L1: L1 stalk, Stalk: P-protein Stalk GAC: GTPase Activating Center, CP: central protuberance.
Right panel: Close up of Tif6-60S interaction. Tif6 binding platform consists of Rpl23, the SRL and to a lesser extent Rpl24 (Green, Tif6; Orange, SRL; Blue, RpL23; Purple, RpL24). Adapted from PDB 2XZN (Gartmann et al., 2010) and 3O58 (Ben-Shem et al., 2010).

1.5.4.2 Efl1.

Efl1 is a cytoplasmic GTPase, homologous in sequence to the translocase elongation factor 2 (eEF-2) (EF-G in prokaryote) (Becam et al., 2001; Senger et al., 2001). Several lines of evidence indicate that Efl1 is involved in ribosome biogenesis. GTPase activity of Efl1 requires the presence of 60S subunits (Senger et al., 2001). Deletion of *efl1* results in (i) decrease 60S subunit levels, (ii) the presence of halfmer polyribosomes (Becam et al., 2001) and (iii) prevents export of 60S subunit to the cytoplasm (Senger et al., 2001). Spontaneous suppressors of an *efl1Δ* were identified as mutations in Tif6 which have weakened affinity for the subunit (Becam et al., 2001; Senger et al., 2001). Further analysis revealed that *efl1Δ* traps Tif6 in the cytoplasm and *in vitro* reconstitution assays showed that Efl1 removes Tif6 from the subunit (Senger et al., 2001). These data provided strong evidence that Efl1 is required for release of Tif6.

Efl1 is homologous to the translocases eEF2 and EF-G. Sequence comparison of Efl1 and eEF2/EF-G highlights a conserved sequence except for insertions in Efl1 not present in eEF2/EF-G. Most notably, Efl1 has a 160aa insertion following the GTPase domain of eEF2/EF-G. However deletion of this domain in Efl1 does not affect growth (Johnson, unpublished). A wealth of structural data is available for both eEF2 and EF-G, both on and off the subunit. eEF2 and EF-G crystal structures have been solved and both structures are remarkably similar (Agrawal et al., 1998; Gao et al., 2009; Jorgensen et al., 2002; Jorgensen et al., 2003). They both exhibit six domains, organized in three blocks: domain I (the GTP-binding site or G-domain),

domain II and domain G' -a domain that interacts with the stalk and is involved in activation of GTP hydrolysis (Nechifor et al., 2007)- form a block at the N-terminus of the protein, domain III stands alone, and domain IV and V form a second block at the C-terminus of the translocase (A et al., 1994; Czworkowski et al., 1994; Jorgensen et al., 2003). Cryo-electron microscopy reconstructions of eEF2 (Gabashvili et al., 2000; Taylor et al., 2007) and EF-G (Agrawal et al., 1998; Stark et al., 2000) and X-ray structure of EF-G (Gao et al., 2009) on the ribosome revealed that the translocases bind to the same site on the ribosome. eEF2/EF-G, similarly to other GTPases involved in translation (EF-Tu for example (Schmeing et al., 2009)), bind at the base of the ribosomal stalk and interact with the sarcin-ricin loop (SRL) (Illustration 1.5). The G-domain, and domains III and V contact the SRL on the large subunit and domain V also contacts rRNA in the Rpl12 (L11 in bacteria) -binding region at the base of the stalk. Domain G' makes contact with P1/P2 (L12 in bacteria) of the stalk. Domain III also makes contact with the small subunit via both rRNA and r-proteins. Important for translocation, the tip of domain IV is seen entering the decoding center on the small subunit where it disrupts ribosome contact with the mRNA and tRNA (See section 1.6). cryo-EM reconstruction of EF-G on the 70S ribosome with a P-site tRNA clearly shows domain IV of EF-G in close proximity of the P-site tRNA (Gao et al., 2009). It has been suggested that Efl1 shares a binding site with eEF2 based on *in vitro* competition binding assays (Graindorge et al., 2005).

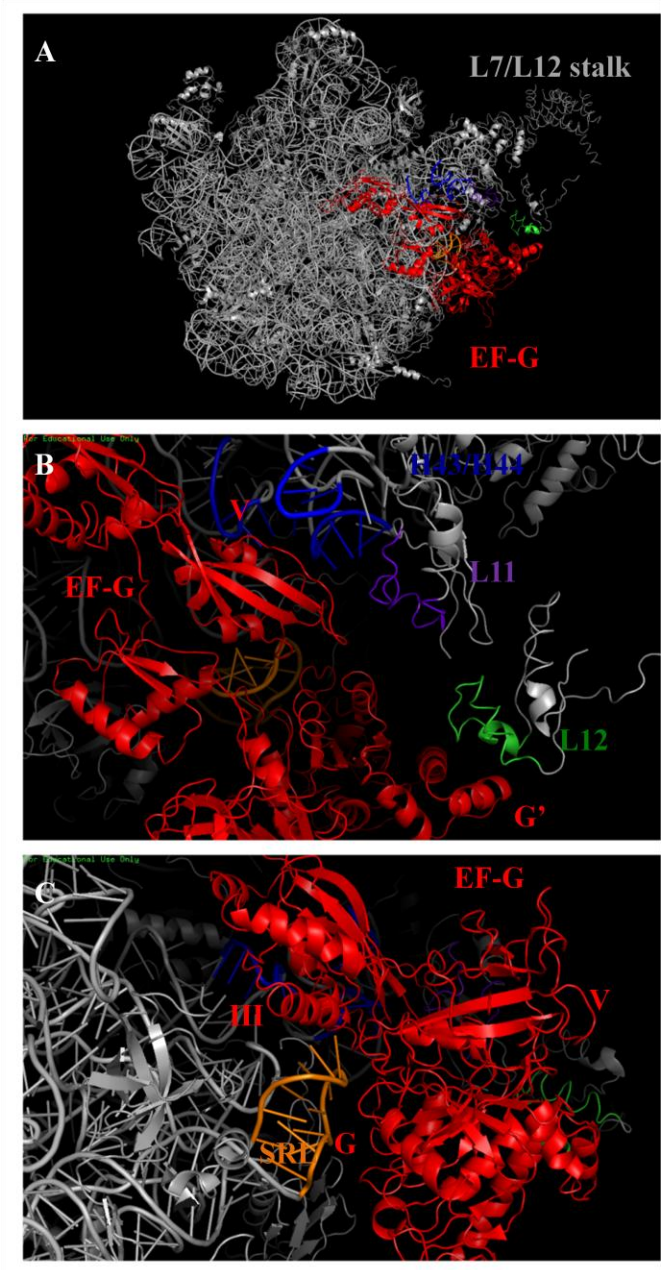

Illustration 1.5 EF-G interactions with the large ribosomal subunit
(A) EF-G (red) binding to the 50S subunit (grey). EF-G interacts with the SRL (orange) at the GTPase activating center and H43/H44 (blue) and L11 (Rpl12 in eukaryotes) (purple) at the base of the L7/L12 (P1/P2) stalk. L12 (green) makes contact with the G'domain. (B and C) close up of (A) Domains of EF-G contacting ribosomal elements are indicated in red. Adapted from PBD 2WRI and 2WRJ (Gao et al., 2009).

Docking of yeast Tif6 on the 50S-EF-G structure reveals Tif6 and the translocase in close proximity on the ribosome. Thus Efl1 probably makes physical contact with Tif6 on the large subunit during 60S biogenesis. How activation of Efl1 might induce release of Tif6 is not known. However, much is known about eEF2/EF-G conformational changes during translocation. Comparison of the structures of eEF2/EF-G in solution (A et al., 1994; al-Karadaghi et al., 1996; Czworkowski et al., 1994; Hansson et al., 2005; Jorgensen et al., 2003) with the ribosome-bound structures (Agrawal et al., 1998; Gomez-Lorenzo et al., 2000; Spahn et al., 2004; Stark et al., 2000; Valle et al., 2003) reveals major changes in the overall organization of the domains of the translocase. This conformation change upon binding to the ribosome is usually described as a joint hinge-like motion of domain III, IV and V relative to domain I, II and G' (Agrawal et al., 1998; Valle et al., 2003). Furthermore, structures of eEF2 and EF-G in complex with antibiotics which trap the translocase on the ribosome in a post-translocation state are available (Gao et al., 2009; Jorgensen et al., 2003). Sordarin binds to eEF2 domain III/V interface while fusidic acid binds to EF-G domain III/II interface. The state of fusidic acid-bound EF-G is similar to the state of sordarin-bound eEF2 and reveals major domain rearrangements as well, presumably trapping the translocases in a conformation representing an intermediate of translocation (Illustration 1.6). Most noticeable is the loss of interaction between domain III and domain II and V (Agrawal et al., 1998; Jorgensen et al., 2003; Stark et al., 2000). As will be shown in Chapter IV, in *rpl10* mutant strains which are deficient for release of Tif6, mutations in Efl1 that map to

domain III/ II and domain III/V interfaces allow for release of Tif6 from the large subunit. These mutations appear to promote for a conformational change in Efl1, similarly to structural changes in eEF2 or EF-G during translation, thus releasing Tif6.

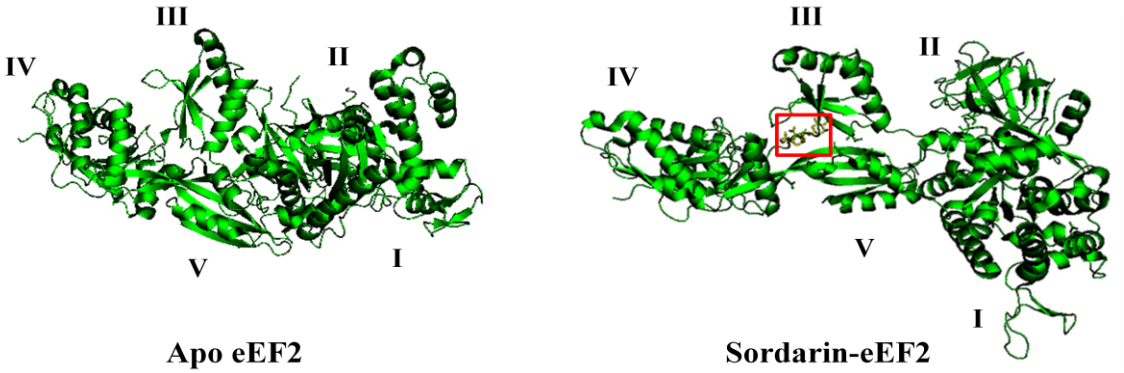

Illustration 1.6 Sordarin induces a large conformational change in the translocase eEF2

Crystal structures of eEF2 (right panel) and sordarin-bound eEF2 (left panel). eEF2: green. Sordarin:yellow, in the red box in the left panel. Sordarin binds at the interface of domain III and V and disrupts domain III/II and domain III/V interactions. Adapted from PDB 1NOU and 1NOV (Jorgensen et al., 2002; Jorgensen et al., 2003).

1.5.4.3 Sdo1.

Additionally to Efl1, Sdo1 is required for efficient release of Tif6. Sdo1 is orthologous to the human SBDS protein, mutations in which cause the Shwachman-Bodian-Diamond syndrome, an autosomal recessive bone marrow failure disease (Luz et al., 2009; Menne et al., 2007; Moore et al., 2010; Shammas et al., 2005). Similarly to Efl1, *sdo1Δ* causes subunit imbalance, traps Tif6 in the cytoplasm and impairs export of 60S subunits (Menne et al., 2007). Tif6 mutants that suppress *efl1Δ* also suppress *sdo1Δ* (Menne et al., 2007).

The data presented in Chapter IV, suggests that a molecular connection exists between Efl1 and Rpl10 via the P-site. A question that arises from my work is what bridges that connection? During translation, a P-site tRNA occupies the space between these proteins. A tRNA would be the ideal substrate for testing the function of the ribosome and could facilitate assembly of the P-site. Another possibility is that a tran-acting factor is found in the P-site in lieu of a tRNA during biogenesis. The structure of human and archaeal Sdo1 has been solved (de Oliveira et al., 2010; Savchenko et al., 2005; Shammas et al., 2005) and has been compared to the structure of a tRNA (Ng et al., 2009). Thus, Sdo1 could act as a tRNA mimic, bridging Rpl10 and Efl1 and conveying information about the P-site to Efl1.

1.5.5 Nmd3 release.

The last known step in the cytoplasmic maturation pathway of the 60S ribosomal subunit is the release of the export adaptor Nmd3. Release of Nmd3 requires the putative GPTase Lsg1, the r-protein Rpl10 and previous release of Tif6 (Hedges et

al., 2005; Lo et al., 2010; West et al., 2005). Lsg1 belongs to the circular permutated GTPase family. Its GTPase activity has not been shown but targeted mutations of conserved residues in the GTPase domain are lethal (West et al., 2005). Inactivation of *lsg1* traps Nmd3 on the 60S subunit, preventing its recycling to the nucleus and thus secondarily causes accumulation of nascent 60S in the nucleus (Hedges et al., 2005). Mutations in Nmd3 that weaken its affinity for the ribosome bypass *lsg1* mutants (Hedges et al., 2005). Similarly to Tif6 mutations bypassing *efl1* and *sdo1* mutants, these *NMD3* mutants allow for recycling independently of proper action of release factors and subsequently for the restoration of subunit export (Hedges et al., 2006; Hedges et al., 2005).

1.5.5.1 Rpl10.

Release of Nmd3 requires the essential r-protein Rpl10. Depletion or mutation of *rpl10* prevents Nmd3 shuttling (Hedges et al., 2005) and inhibits 60S export (Gadal et al., 2001). Some *rpl10* mutants, similarly to *lsg1* mutants, can be suppressed by expression of Nmd3 alleles which have weakened affinity for the ribosome (Hedges et al., 2006; Hedges et al., 2005; Hofer et al., 2007; Karl et al., 1999)} or by overexpression of Nmd3 (Zuk et al., 1999). Rpl10 binds the large subunit in a cleft between the central protuberance (CP) and the ribosomal stalk (Illustration 1.7). Bacterial L16, Rpl10 ortholog, induces a large conformational change upon binding to the subunit (Teraoka and Nierhaus, 1978). It had previously been thought that such a rearrangement of the Rpl10-binding region, potentially induced by Lsg1 GTPase activity, lead to release of Nmd3. However, such a possibility is precluded

by data I present in chapter IV of my thesis. There, I provide evidence that Rpl10 is involved in the release of Tif6, which suggests that Rpl10 loads upstream of Tif6, and thus Nmd3, release. It had been suggested that Rpl10 loads on the large subunit in the nucleus and is part of the binding site of Nmd3 (Gadal et al., 2001). However, mutation in Nmd3 and karyopherins which abrogate the export of 60S subunits do not trap Rpl10 in the nucleus (West, Hedges unpublished data). However, Rpl10 mutants which can not bind the ribosome relocalize to the nucleus (Hofer et al., 2007), maybe suggesting a more complex role for Rpl10.

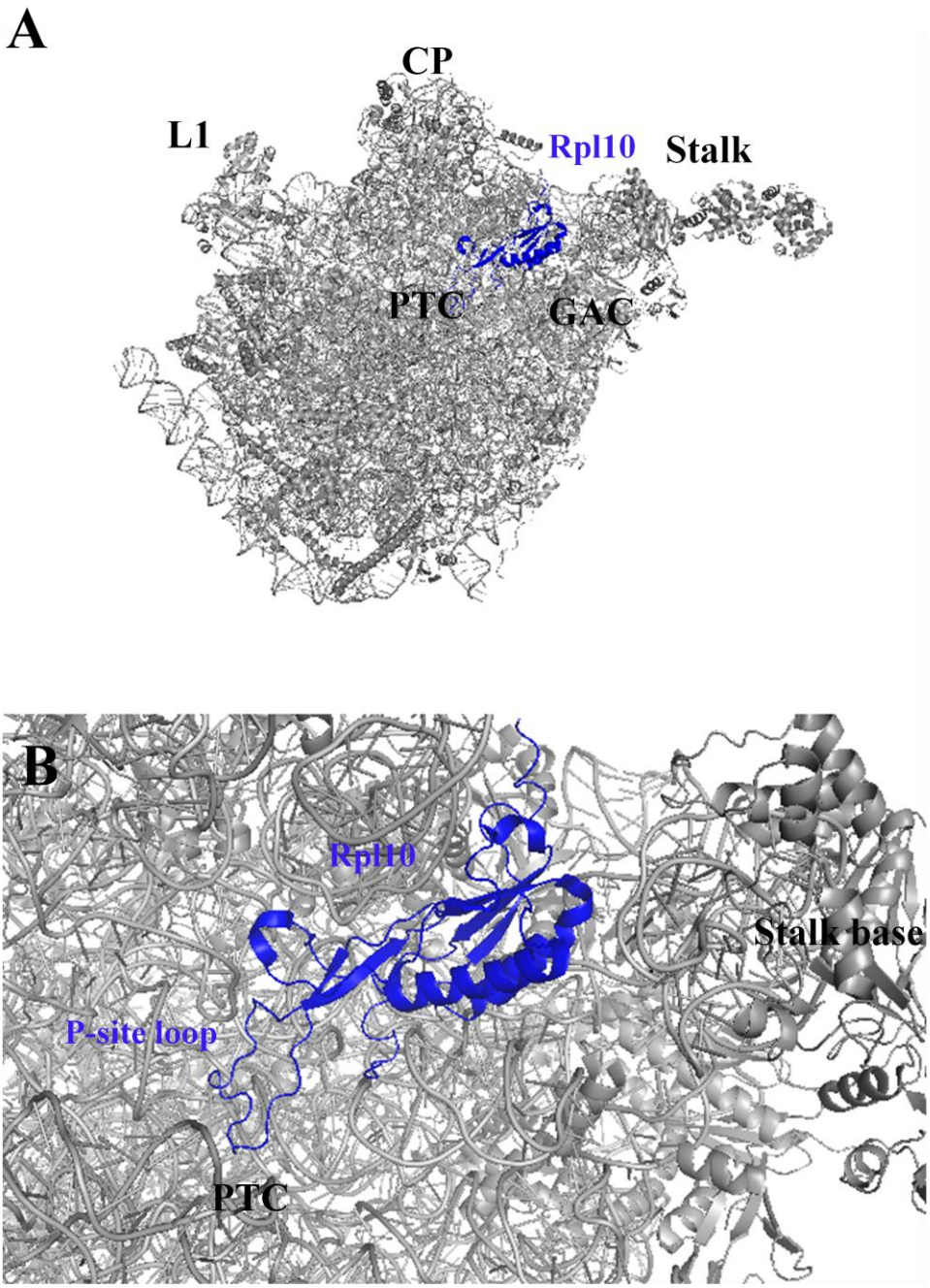

Illustration 1.7 Rpl10 in the large ribosomal subunit
Cryo-EM reconstruction of S*accharomyces cerevisiae* large ribosomal subunit- (A) Rpl10 binds in a cleft between the central protuberance (CP) and the ribosomal stalk. (B) Zoom of (A). The P-site loop of Rpl10 reaches deep into the catalytic core of the 60S subunit. PTC: Peptidyl transferase center. GAC: GTPase activating center. From PDB 3IZS and 3IZF (Armache et al., 2010a, b).

Rpl10 is a globular protein with an internal loop that reaches towards the P-site and hence we refer to it as the P-site loop (Illustration 1.7 B). In L16 the P-site loop is unstructured in solution (Nishimura et al., 2004) but is seen structured in the context of the 80S ribosome containing a P-stie tRNA (Gao et al., 2009). The solution structure of L16 from *T.thermophilus*, is very similar to the ribosome-bound structure of L16 (Gao et al., 2009). Thus binding to the subunit does not appear to induce large conformational changes in L16. Loading of L16 in the bacterial large subunit appears dependent on the GTPase activating center since bacterial large subunits deleted for the SRL, a critical structure for activating GTPases, lack only one protein: L16 (Lancaster et al., 2008). Deletion of the SRL in yeast precludes the export of the mutant subunit (Bussiere unpublished data), hence proper folding of this essential region of the 60S ribosome might represent a quality control step. In yeast, deletion of the P-site loop of Rpl10 (aa102-112) was shown to be required for the release of Nmd3 (Hofer et al., 2007). Crystal structures of the bacterial ribosome show the P-site loop of L16 close to the P-site tRNA, with the N-terminus of L27 bridging the space between the P-site tRNA and the P-site loop and contacting the CCA-end of the P-site tRNA (Gao et al., 2009; Voorhees et al., 2009) (Illustration 1.8 bottom panel). L27 position in the P site suggests an involvement in translation. This is supported by several lines of evidence: ribosomes lacking L27 are impaired for A-site tRNA binding (Wower et al., 1998), a truncation which remove the first three amino acids of L27 reduces the rate of peptide bond formation (Maguire et al., 2005), L27 is stabilized by P-site tRNA binding (Jenner et al., 2010a; Voorhees et

al., 2009) and is seen interacting with the CAA end of both A- and P-site tRNAs (Jenner et al., 2010a; Voorhees et al., 2009). While eukaryotes and archaeons lack L27 they have an elongated P-site loop (Armache et al., 2010b). This extended P-site loop is not resolved in crystal structures of archaeal or eukaryotic ribosomes. However, cryo-EM reconstruction of yeast translating ribosomes show the P-site loop of Rpl10 making contact with the acceptor stem of the P-site tRNA (Illustration 1.8, top panel) (Armache et al., 2010b). Thus, in eukaryotes, it appears that the elongated P-site loop might functionally replace L27. The structures of ribosome-bound Rpl10/L16 highlight the P-site loop (with L27 in prokaryotes) as a structural component of the P-site (Armache et al., 2010a, b; Gao et al., 2009). The location of Rpl10/L16-L27 in the large subunit suggests the possibility that it is involved in translation. In fact, bacterial large ribosomal subunits reconstituted without L16 have reduced catalytic activity and are defective for interaction with the small subunit (Kazemie, 1975; Moore et al., 1975). Furthermore, both L27 and L16 were shown to be involved in the proper placement of tRNA ligands at the peptidyl-transferase center (Harms et al., 2001; Wower et al., 1998) and accordingly an N-terminal truncation of L27 exhibits reduced levels of peptidyl-transferase *in vitro* (Maguire et al., 2005). Crystal structures of bacterial recycling factor (RRF), bound to 70S show RRF deep into the P site contacting L16 and L27, implicating these proteins in ribosome recycling as well (Weixlbaumer et al., 2008; Weixlbaumer et al., 2007; Wilson et al., 2005).

In chapter IV of my thesis I provide compelling evidence that signaling between the P-site, composed in part of Rpl10, and Efl1 occurs. This signaling induces release of the anti-association factor Tif6. Thus, I propose that the translocase-like factor Efl1 interrogates the P-site during 60S biogenesis. A properly formed P-site would signal to Efl1, activating it and inducing a conformational change which drives a faux-translocation event resulting in release of Tif6.

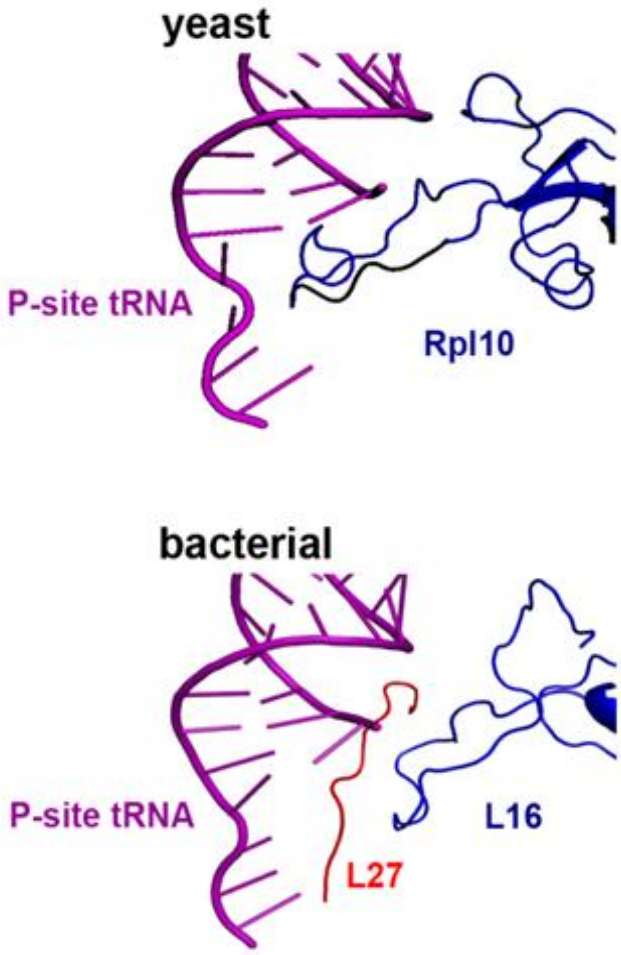

Illustration 1.8 Comparison of the P-site tRNA interactions of L16 and Rpl10. Top panel panel: yeast Rpl10 (blue) and P-site tRNA (purple) (adapted from PDB 3IZC/3IZB/3IZE/3IZF (Armache et al., 2010b). Bottom panel: Bacterial L16 (blue), L27 (red) and P-site tRNA (purple) (adapted from PDB 2WRI/2WRJ (Gao et al., 2009))

1.6 Translation in eukaryotes

In this brief discussion of translation I will focus on the role of EF-G and eEF2 in translocation as it is relevant to understand the role of the translocase-like factor Efl1 in ribosome maturation.

1.6.1 Eukaryotic translation in a nutshell

Translation consists of four steps: initiation, elongation, termination and subunit recycling.

During translation initiation (reviewed in (Acker and Lorsch, 2008; Jackson et al., 2010; Kapp and Lorsch, 2004; Lorsch and Dever, 2010; Rodnina and Wintermeyer, 2009)) the mature 40S subunit, in a complex with initiation factors and Met-$tRNA_i^{Met}$, forms the 43S pre-initiation complex (PIC) (Lorsch and Dever, 2010). The PIC interacts with the 5'-capped of the 3'poly-A-tail-containing mRNA (Kozak, 2002). Upon binding, the PIC scans the mRNA until it reaches the first start codon (AUG). Met-$tRNA_i^{Met}$ is positioned in the P-site of the 40S and interacts with the start codon. GTP hydrolysis by eIF2 signals for release of initiation factors which allows for 60S binding and 80S formation (Acker et al., 2007; Algire et al., 2002; Lorsch and Herschlag, 1999).

Translation elongation consists of three distinct steps (Agirrezabala and Frank, 2009; Kapp and Lorsch, 2004; Rodnina and Wintermeyer, 2009). First the mRNA codon in the A-site of the small subunit is decoded and the corresponding cognate aminoacyl-tRNA (aa-tRNA), delivered by eEF1A (EF-Tu in bacteria), is accommodated. Second, the peptidyl-transferase reaction takes place on the large

subunit, transferring the nascent peptide from the P-site tRNA to the amino acid on the A-site tRNA and forming a peptide bond. Early X-ray crystallography work on the archaeal large subunit (Ban et al., 2000) -supporting previous biochemical evidence (Green and Noller, 1997; Noller, 1991)- confirmed that this reaction is catalyzed solely by the rRNA in the large ribosomal subunit (Nissen et al., 2000), thus owing the ribosome the title of ribozyme. Third, translocation moves the mRNA-tRNA complex relative to the ribosome, from A/P to E/P sites, resetting the A site with a new codon, now free to bind a new cognate aa-tRNA (Agirrezabala and Frank, 2009; Moran et al., 2008). EF-G/eEF2, the translocase, stabilizes the ribosome in a ratcheted state and induces translocation (see translocation section below).

Termination occurs when a stop-codon is present in the A-site and signals the end of the coding sequence. In eukaryotes, the three stop codons are recognized by a single termination factor, eRF1 (Frolova et al., 1999; Song et al., 2000). eRF1 binds the ribosome in a complex with eRF3 (Pisareva et al., 2006), a GTPase. eRF1 induces peptide release by hydrolysis of peptidyl-tRNA at the ribosomal peptidyl transferase center. eRF1 activity is greatly enhanced by eRF3 hydrolysis of GTP which is required for peptide release (Alkalaeva et al., 2006; Fan-Minogue et al., 2008).

Recycling of the ribosome occurs next. This step involves the separation of the 80S ribosome into 40S and 60S subunits and the release of the mRNA and deacetylated P-site tRNA from 40S. Unlike bacteria which use EF-G and ribosome

recycling factor to promote recycling, in eukaryotes ABCE1 activity is required for subunit dissociation (Pisarev et al., 2010). eIF1 promotes the subsequent release of the tRNA from the 40S P-site, while eIF3j promotes release of the mRNA (Pisarev et al., 2007). The involvement of initiation factors in the last step of protein synthesis prepares the 40S subunit for a new round of initiation.

1.6.2 Translocation

The work presented in Chapter 4 describes a molecular signaling pathway from the P-site loop of Rpl10, deep in the catalytic center of the ribosome, to the anti-association factor Tif6 via the translocase-like factor Efll. This pathway highlights an extensive structural and functional probing of the ribosome, especially of the P site, by Efl1. Given the homology between Efl1 and the translocase eEF2 (described in section 1.5.4 Efl1) it is appropriate to describe in more depth the step in translation this factor is involved in (Illustration 1.9).

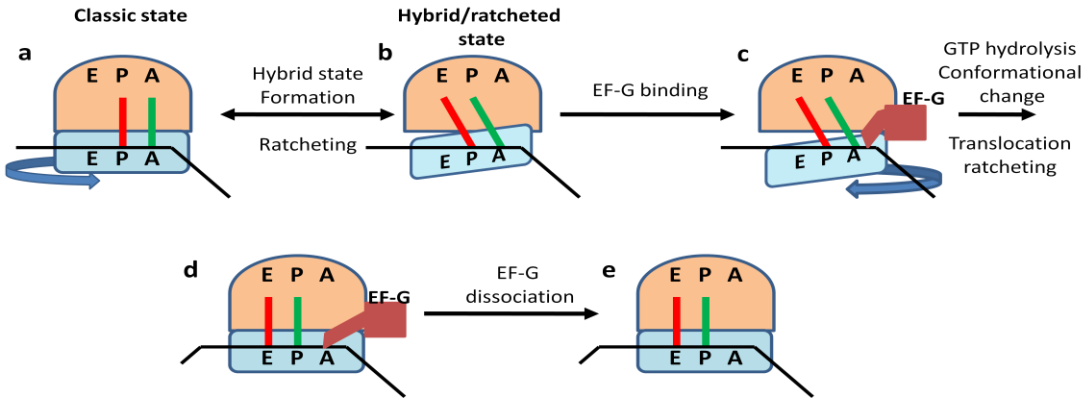

Illustration 1.9 Overview of translocation
(a-b) After peptidyl transferase, tRNAs shift spontaneously to the A/P and P/E states in a ratcheted ribosome. The ribosome oscillates between the classical state (A/A P/P position of the tRNAs)(**a**) and the Hybrid or ratcheted state (A/P and P/E position of the tRNAs) (**b**), to which EF-G (eEF2 in eukaryotes) binds (**c**). After GTP hydrolysis and tRNA movement, ratcheting reverses (**d**) and EF-G dissociates (**e**). See text for details. Adapted from (Schmeing and Ramakrishnan, 2009).

Translocation takes place once the nascent peptide has been transferred from the P-site tRNA to the A-site tRNA. At this point in the translocation pathway, the ribosome is in the classical or pre-translocation state and contains a deacetylated tRNA in the P-site and a peptidyl-tRNA in the A-site. The tRNAs are in the classical state: P/P and A/A on the small subunit/large subunit sites. The pre-translocation ribosome spontaneously undergoes a ratcheting motion in the absence of factors (Blanchard et al., 2004; Cornish et al., 2008), due to a counter clock-wise (CCW) rotation of the small subunit relative to the large subunit (Frank and Agrawal, 2000; Stark et al., 2000). This rotation leads to a hybrid or ratcheted state of the ribosome where the acceptor stems (CCA-ends) of the P and A site tRNAs are repositioned in the E and P sites of the large subunit while their anti-codon stem loop remain in the P and A sites on the small subunit (A/P and P/E position of tRNAs) (Agirrezabala et al., 2008; Julian et al., 2008; Moazed and Noller, 1989). In this state the tRNA/ribosome interactions are mostly unaltered, let alone for the CCA-ends of the tRNA on the large subunit (Frank and Agrawal, 2000; Valle et al., 2003). The post-peptidyl-transferase ribosome naturally oscillates between the classical or unratcheted (A/A P/P) and the hybrid or ratcheted states (A/P P/E) (Blanchard et al., 2004; Cornish et al., 2008). Ratcheting of the ribosome occurs only if the P-site tRNA is deacylated (Valle et al., 2003) -that is only in the post-peptidyl-transferase ribosome- and is required for translocation, as cross-linking the subunits, and thus inhibiting ratcheting, prevents translocation (Horan and Noller, 2007). The translocase (eEF2/EF-G), in complex with GTP, binds to the ratcheted ribosome and

stabilizes it in this state (Frank and Agrawal, 2000; Spiegel et al., 2007). Upon binding, the translocase undergoes a conformational change which rotates domain III and V relative to domain I, G' and II (Agrawal et al., 1998; Valle et al., 2003) . This rotation is required for, and enables, interaction of domain IV with the decoding center of the small subunit. Binding of the translocase/GTP complex induces conformational changes in the ribosome as well: the tip of helix 44 of the small subunit moves and displaces the anti-codon stem loop of the A-site tRNA in the direction of translocation (toward the 3' end of the mRNA) (VanLoock et al., 2000). GTP hydrolysis by the translocase and conformational changes in the ribosome induced by this event, occur before the actual translocation (Rodnina et al., 1997). The role of GTP hydrolysis is not clear, though it has been suggested that it prevents reverse movement of the mRNA/tRNA or allows the ribosome to act as a helicase to unwind mRNA structures (Takyar et al., 2005). After GTP hydrolysis further conformational changes occur in the translocase, which result in domain IV disrupting the interaction of the small subunit with the mRNA and tRNA at the decoding center (Taylor et al., 2007). This allows for rotation of the head of the small subunit. This new conformation permits movement of P-site and A-site tRNA towards the E-site and P-site respectively. The translocase then leaves the ribosome, which is thought to permit the small subunit to back-ratchet and lead to the post-translocation state of the ribosome with E/E and P/P tRNAs and an exposed codon in the A-site (Agirrezabala and Frank, 2009).

Interestingly, in bacteria the Efl1 homologue EF-G is involved in the recycling step alongside ribosome recycling factor (RRF) (Hirashima and Kaji, 1973). In this step, EF-G binds the subunits in a way similar to the way it binds during translocation, albeit to a deacylated hybrid P/E tRNA containing ribosome. Additionally, in archaea, Tif6 and Rpl10 (L10e) are present but not Efl1, inviting the idea that archaeal EF-G might play the role of Efl1 in biogenesis. Hence it seems important to keep in mind the flexibility and various potential roles of translocases, and thus translocases-like proteins, in biogenesis and in translation when attempting to understand the function of these factors in biogenesis.

1.7 Dissertation Objectives

My dissertation is composed of five chapters. In the first one I introduced the structure and composition of the ribosome. I also described relevant aspects of ribosome biogenesis, with emphasis on factors and events relevant to the work presented in subsequent chapters. The second chapter contains a description of the material and methods used in chapters III and IV. Chapter III is entitled: Visualization of the export adaptor Nmd3 on the 60S ribosomal subunit. Nmd3 is an essential export adaptor of the 60S subunit. Nmd3 binds to the ribosome in the nucleolus and is the last known trans-acting factor to be released from the subunit in the cytoplasm. In order to get a better understanding of the molecular events leading to the release of Nmd3 from the 60S subunit I set out to identify the binding site of Nmd3 on 60S. In a collaboration with the Dr Joachim Frank's laboratory (Columbia University), we obtained a cryo-EM model of Nmd3 in a complex with 60S showing

Nmd3 binding to the subunit joining face of the ribosome. I provided biochemical data supporting this result. rRNA protection experiments corroborated the structural data. Furthermore, *in vitro* binding experiments showed Nmd3 binding to the subunit being abrogated by prior 80S formation, consistent with the assigned position of Nmd3 on the subunit binding side of 60S. This work provided the first visualization of an export factor on a ribosomal subunit and was published in JCB in 2010. In chapter IV, Probing the P site during maturation of the 60S ribosomal subunit, I describe work that lead to the discovery of molecular signaling that implies that a faux-translation event occurs during biogenesis and checks the integrity of the P site. The release of the anti-association factor Tif6 requires the translocase-like GTPase Efl1. Based on its homology to the translocases eEF2 and EF-G, Efl1 probably requires the properly assembled ribosomal stalk and the GTPase activating center to be properly formed. I provided data strongly suggesting that this step also involves probing of the P site. My work showed that the ribosomal protein Rpl10 is involved in the release of Tif6. Mutations in a loop of Rpl10 which embraces the P-site tRNA trapped Tif6 on the subunit. These Rpl10 mutants could be suppressed by Tif6 mutants that have weakened affinity for the subunit. Furthermore, mutations in Efl1 which suppress these Rpl10 mutants were also obtained. These suppressing mutations in Efl1 mapped to regions on the translocases eEF2 and EF-G important for conformational changes during translation. These results highlight molecular signaling between the P site, involving a loop of Rpl10, and Tif6, 90Å away. I propose that Efl1 promotes a translocation-like event during biogenesis of the 60S

subunit prior to its first round of *bona fide* translation. In the last chapter of my thesis I address outstanding questions that arose from my work and speculate on the direction future work might take.

Chapter 2

Material and Methods

2.1 Chapter 3 Material and Methods

2.1.1 Strains, plasmids and oligos used in chapter 3

Table 2.1 Strains used in Chapter 3

Strain	Genotype	Source
BJ5464	*Matα ura3-52 trp1 leu2Δ1 his3Δ200 pep4::HIS3 prb1Δ1.6R can1 GAL*	Yeast Genetic Stock Center, Berkeley, CA
AJY2757	*Matα ade2 leu2 ura3 his3 rpl25Δ::HIS3* with pAJ909	This Study

Table 2.2 Plasmids used in Chapter 3

Plasmid	Description	Source
pAJ235	*Gal10::GST-Nmd3 LEU2 CEN*	(Ho et al., 2000a)
pAJ909	*Rpl25-13myc URA3 CEN*	This Study
pAJ1381	*GPD::MBP-HIS$_6$-(TEV)-Nmd3 LEU2 2μ*	This Study

Table 2.3 Oligos used in Chapter 3

Oligo	Sequence
AJO501	ACTGGGCAGAAATCACAT
AJO1060	GTAGATAGGGACAGTGGGAA
AJO1061	GTTCTGCTTACCAAAAATGG
AJO1135	AGAGCCATAATCCAGCGG

2.1.2 Protein Purification

GST-(TEV)-Nmd3: Two liters of AJY1701 were grown in ura raffinose to OD600 0.3. The culture was induced with 20% galactose for 6hrs. Cells were harvested, the pellet washed with 10ml lysis buffer: 500mMKCl, 20mM Tris pH7.5, 0.5% triton, 10%glycerol, 1mM DTT, 1mM EDTA plus protease inhibitors. Cells were resuspended in lysis buffer and crude extract was made using glass ball vortexing. The crude extract was clarified twice and incubated 2hrs at 4oc with 750ml glutathione beads. The beads were washed with 8ml wash buffer: 20mM Tris pH7.5, 500mM KCl, 1mM EDTA, plus protease inhibitors. The protein was eluted with 50mM glutathione in 50mM Tris pH8. Concentration was determined by braddford assay to be 8.5uM.

MBP-(TEV)-his-Nmd3: Four liters of AJY2139 were grown to OD600 0.6 in leu glucose. Cells were harvested, the pellet was washed with 10ml extract buffer: 450mM NaCl, 100mM KCl, 50mM Tris pH 8, 10%glycerol, plus protease inhibitors. Cells were ressuspended in 20ml extract buffer; crude extracts were made using glass bead vortexing and clarified twice. 10mM imidazole and 0.01%NP40 was added to the crude extract. 1.5ml of Ni+ beads bed volume was added to crude extract and rocked 2hrs at 4oc. The beads were washed three times with extract buffer and the protein eluted with 1.5ml of extract buffer supplemented with 250mM imidazole. The eluate was then incubated with 1.5ml of amylose resine for 2hrs at 4oc. The beads were washed with 6ml of extract buffer 2: 20mM Tris pH 7.5, 50mM NaCl, 10% glycerol, plus protease inhibitors. Proteins were eluted with 6ml of extract buffer 2 supplemented with 50mM maltose. Concentration was determined by braddford assay to be 0.75uM.

2.1.3 Ribosome purification:

3 liters of AJY1293 were grown in YPD to an OD600 of 0.8. Cells were washed with 30ml binding buffer (50mM KCl, 20mM Tris pH7.4, 10mM MgCl2, 6mM BME +PI), resuspended in 12.2ml binding buffer. Crude extract was made by glass

bead vortexing and clarified twice. The crude extract was spun over a 2.5ml 1M sucrose cushion in binding buffer and spun 2hr at 32000rpm in an SW28. The pellet was resuspended in 2.5ml binding buffer, stired on ice for 1 hr, shortly clarified and layed over a 250ul 1M sucrose cushion in binding buffer and spun 1h at 80000rpm in a TLA 100. The pellet was resuspended in 1ml dissociation buffer: 0.5M KCl, 8mM MgCl2, 20mM Tris pH 7.4, 6mM BME, plus protease inhibitors and was rocked 5hr at 4oc to dissociate ribosomes. The solution was then layed over a 5-20% sucrose gradient in dissociation buffer and spun 11hr at 23000rpm in an SW28. The gradient was fractionated and the A260 trace taken. The 60S and 40S fractions were respectively pooled, concentrated using an Amicon Ultra 100K and washed with binding buffer: 50mM KCl. 20mM Tris pH7.4, 10mM MgCl2, 6mM BME, plus protease inhibitors. Final concentrations were calculated using extinction coefficient: [60S]=0.14uM, [40S]=0.23uM.

2.1.4 Binding of MBP-Nmd3 and GST-Nmd3 to 60S and 80S:

Cushion assay: 60S was incubated with or without 40S for 1hr at 40c in binding buffer. MBP-Nmd3 was added and binding was allowed to proceed for another hr at 4oc. The reaction was layered on top of a 700ul 60% sucrose cushion in binding buffer and spun 6min at 60,000 rpm in a TLA 100. Supernatant was carefully removed, TCA precipitated and resuspended in 20ul 1x laemmli buffer. The pellet was also resuspended in 20ul 1x laemmli buffer. The samples were ran in a 12% SDS-PAGE gel, transferred to nitrocellulose and protein pattern was visualized by western with anti-Nmd3.

Immunoprecipitation assay: 60S-Rpl25-myc subunits were incubated with increasing amounts of MBP-Nmd3 in binding buffer at 40c for 1hr. Anti-myc antibody was added and incubated for 1hr. ProtA beads were added and incubated for 30minutes. The beads were washed 2X in binding buffer and eluted with 20ul 1X laemmli buffer. 10ul was loaded on 12% SDS-PAGE and coomassie stained.

2.1.5 RNaseV1 protection assays

All reagents were made in DEPC treated water.

RNaseV1 protection assay: 60S was incubated with and without MBP-Nmd3 or GST-Nmd3 in binding buffer (50mMKCl, 20mM Tris pH 7.4, 10mM MgCl2, 6mM BME) for 1 hr at 4^{o}C rocking. The reactions were treated with 0.5ul of 0.1U/ul RNaseV1 (ambion) for 20 minutes at 16oc. 1X TES (10mM Tris pH7.4, 1mM EDTA, 0.1%SDS) and acidphenol:CHCl3 was added. The mixture was vortexed for 1 minute, spun down for 30 seconds. The aqueous phase was transferred to a clean tube and CHCl3 was added. The solution was vortexed for 30 seconds, spun down and the aqueous phase was transferred to a clean tube. The rRNA was ethanol precipitated and resuspended in DEPC treated H2O. Labeled primer was hybridized for 3' at 99^{o}C. The reaction was allowed to cool down to room temperature in the heat block. 34ul of reaction mix was added and incubated at 42 for 1hr. (reaction mix: 5ul 0.1mM DTT, 10ul 2mM dNTPs, 5ul 10x reaction buffer (500mM Tris pH8.3, 0.1M MgCl2, 750mM KCl), 0.2ul RNase inhibitor (NED 40,000U/ml), 13.5 DEPC H2O, 0.5ul Manuscript RT) The reaction was stopped by adding 105ul of RNase reaction mix: 100ug/ul ssDNA and 20ug/ul RNaseA in TEN buffer(100mM NaCl in 1xTE) and incubating 15 min at 370c. DNA was extracted with phenol: CHCl3, ethanol precipitated and resuspended in 10ul urea loading buffer: 50% urea, 1x TBE, 0.05% BPC, 0.05% XCFF. 2.5ul was then ran on a 7M urea gel.

2.1.6 Sequencing reaction

6ug of pAJ718 was incubated with 1/10thvol of 2M NaOH, 2mM EDTA 30min at 37oc. The denatured DNA was ethanol precipitated and resuspended in 4.5ul H2O. Sequencing was then done using USB sequenase version2.0 DNA sequencing kit.

2.2 Chapter 4 Material and Methods

2.2.1 Strains, plasmids and oligos used in chapter 4

Table 2.4 Strains used in Chapter 4

Strain	Genotype	Source
AJY1437	*MATα rpl10::KanMX lysΔ0 met15Δ0 his3Δ0 leu2Δ0 ura3Δ0* pAJ392	This study
AJY1657	*MATa rpl10-G161D ura3 leu2*	(Hedges et al., 2005)
AJY1837	*MATα rpl10::KanMX NMD3-GFP::KanMX CRM1-T539C* pDEQ2#5	(Hedges et al., 2005)
AJY2104	*MATα KanMX::GAL::RPL10 ade2 ade3 ura3 leu2*	(Hofer et al., 2007)
AJY2765	*MATa rpl10::KanMX TIF6-GFP::HIS3 met15Δ0 his3Δ1 leu2Δ0 ura3Δ0* pAJ392	This study
AJY2766	*MATα KanMX::GAL::RPL10 TIF6-GFP::HIS3 ade2 ade3 ura3 leu2*	This study
AJY2767	*MATa KanMX:: GAL::RPL10 ARX1-GFP::HIS3 his3Δ1 leu2Δ0 met15Δ0 ura3Δ0*	This study
AJY2768	*MATα KanMX:: GAL::RPL10 MRT4-GFP::HIS3 his3Δ1 leu2Δ0 met15Δ0 ura3Δ0*	This study
AJY2770	*MATα KanMX::GAL::RPL10 TIF6-6HA::URA3 ade2 ade3 ura3 leu2*	This study
W303	*MATα ade2-1 can1-100 his3-11, leu2-3,112 trp1-1 ura3-1 SSD1-d*	

Table 2.5 Plasmids used in Chapter 4

Plasmid	Description	Source
pDEQ2#5	*P_{Gal1}::RPL10 URA3 CEN*	B.L. Trumpower
pAJ392	*RPL10 URA3 CEN*	This study
pAJ538	*NMD3-13myc LEU2 CEN*	This study
pAJ758 2005)	*nmd3-ILL-AAA-GFP URA3 CEN*	(Hedges et al.,
pAJ1004	*TIF6-GFP URA3 CEN*	This study
pAJ1197 2007)	*RPL10-13myc Leu2 CEN*	(Hofer et al.,
pAJ1315 2005)	*NMD3-I112T,I362T-13myc LEU2 CEN*	(Hedges et al.,
pAJ1777 2007)	*rpl10-102-112Δ-13myc LEU2 CEN*	(Hofer et al.,
pAJ2240	*TIF6-V192F URA3 CEN*	A. Warner
pAJ2522	*RPL10 LEU2 CEN*	This study
pAJ2543	*TIF6 HIS3 CEN*	This study
pAJ2544	*TIF6-V192F HIS3 CEN*	This study
pAJ2545	*EFL1 HIS3 CEN*	This study
pAJ2652	*NMD3 URA3 CEN*	This study
pAJ2653	*NMD3-I112T,I362T URA3 CEN*	This study
pAJ2654	*TIF6-V192F-GFP URA3 CEN*	This study
pAJ2665	*TIF6 URA3 CEN*	This study

Table 2.6 Oligos used in Chapter 4

Oligo	Sequence
AJO268	CGCGGATCCTACCCAACATGCTGAAC
AJO454	GCTGTCGACTCTTTCGCATACAACTG
AJO491	GTGCCATGGCTAGAAGACCAGCT
AJO534	CTGCCCGGGCGGCCGTTTAAACCCATATTCCTTTG
AJO535	GCGCCATGGTATTAATTAATGAGTAGGTTTCAATCAAAG
AJO645	CGTGAGCTCTTGTATCTCTTCACCGAA
AJO646	CCGTGGATCCTAGCTTGAGCAGCAAAGTA
AJO932	CCGTGGGAGCTCATTTGTCGGTGC
AJO933	CGACAAATGAGCTCCCACGGTTAACG
AJO1320	GTCTTACGTATCAACAAGNNNTTGTCTTGTGCCGGTGCG GATAGATTG
AJO1321	GTCTTACGTATCAACAAGATGNNNTCTTGTGCCGGTGCG GATAGATTG
AJO1322	GTCTTACGTATCAACAAGATGTTGNNNTGTGCCGGTGCG GATAGATTG
AJO1323	GTCTTACGTATCAACAAGATGTTGTCTNNNGCCGGTGCG GATAGATTG
AJO1324	GTCTTACGTATCAACAAGATGTTGTCTTGTNNNGGTGCG GATAGATTGCAAC
AJO1352	CGCCCTCGAGAATGAAAGATAATGAACAGC
AJO1353	CGCCGAGCTCGAAAGAATTTTAGTCAGCGC
AJO1367	GCCTCTCGAGCTAGCATTCTGGGCCTCCATGTCGC
AJO1368	CCGCTTGCAAGATGCCCAACC
AJO1369	GGTTGGGCATCTTGCAAGCGG
AJO1384	TGCTGGTACGCGTATCATCGG
F2CORE	TCGATGAATTCGAGCTCGTT
R1CORE	GGTCGACGGATCCCCGGGTT

2.2.2 Strains, plasmids and media

Cells were grown at 30°C in rich media (yeast extract, peptone) or appropriate synthetic drop-out medium with 2% glucose or 1% galactose as the carbon source. Strains, plasmids and primers used in this study are listed in tables 1, 2 and 3, respectively.

AJY2766, 2767 and 2768 were made by amplifying genomic DNA from AJY2104 (Hofer et al., 2007) with oligonucleotides AJO645/646 and transforming the PCR product into Tif6-GFP, Arx1-GFP and Mrt4-GFP strains (Huh et al., 2003) and selecting for $G418^R$ colonies. AJY2765 was made by integrating *TIF6*-GFP::HIS3 (Huh et al., 2003) into AJY1437 (*rpl10*Δ*::*KanMX), derived from sporulating the heterozygous diploid (Research Genetics) containing pAJ392. AJY2770 was made by integrating the PCR product from oligo F2CORE/R1CORE and template pFA6a-HA-K1URA3 (Sung et al., 2008) into AJY2766. pAJ2522 was constructed by amplifying BY4741 genomic DNA with AJO491/268. The product was digested with SalI and BamHI and ligated into the same sites of pAJ1197 (Hofer et al., 2007). pAJ2543 was constructed by amplifying BY4741 genomic DNA with AJO534/454, the product digested with EagI and SalI and ligated into pRS413. pAJ2544 was constructed by digesting pAJ2240 with SstI and XhoI and the fragment was ligated into pRS413. pAJ2545 was constructed by amplifying BY4741 genomic DNA with AJO1352/1353, the product digested with Sst1 and XhoI and ligated into pRS413. pAJ2652 and pAJ2653 were constructed by digesting pAJ538 and pAJ1315 respectively (Hedges et al., 2005) with EagI and XhoI and the fragments were ligated into pRS416. pAJ2654 was constructed by fusion PCR amplifying pAJ2240 with AJO1384/1369 and Tif6-GFP genomic DNA (Huh et al., 2003) with AJO1367/1368 (PCR2). PCR products were combined and re-amplified with AJO1384/1367, digested with XhoI and MluI and ligated into pAJ2240. pAJ2665 was constructed by digesting pAJ1004 with BstEII, and the fragment was ligated into pAJ2240.

2.2.3 Mutagenesis of Rpl10

The P-site loop of Rpl10 was amplified with five different forward primers (AJO1320 through 1324), each containing a single randomized codon, and a common reverse primer (AJO268). The PCR products were cloned as SnaBI to BamHI fragments into pAJ1777, and the resulting pools of vectors were transformed into the *RPL10* shuffle strain AJY1437. Slow growing mutants were identified on 5-FOA-containing medium and sequenced.

2.2.4 Mutagenesis of Efl1

The open reading frame of *EFL1* was randomly mutagenized by PCR using Taq DNA polymerase, wild-type *EFL1* (pAJ2545) as template with oligonucleotides AJO1352 and 1353. The PCR product was co-transformed with gapped (StuI-cut) pAJ2545 into AJY1437 in which wild-type *RPL10* had been replaced with *rpl10-S104D*. Fast growing colonies were selected and *EFL1*-containing plasmids were extracted and sequenced.

2.2.5 Polysome profiles

Sucrose gradient analysis was adapted from (Baim et al., 1985). Briefly, cells were grown to mid-log phase, incubated with 50µg/ml cycloheximide for 10 minutes, harvested on ice, washed and resuspended in buffer C (10mM Tris·HCl, pH7.4, 100mM NaCl, 30mM $MgCl_2$, 50µg/ml cycloheximide, 200µg/ml heparin). Cell extracts were made by vortexing cells with glass beads and clarified twice by centrifugation. 9 A_{260} units were loaded on 7-47% sucrose gradients made in low salt buffer (50mM Tris acetate, pH7.0, 50mMNH_4Cl, 12mM $MgCl_2$, 10mM DTT and 50µg/ml cycloheximide) and centrifuged in a Beckman SW40 rotor for 150 minutes at 40,000rpm. The polysome profiles were obtained by monitoring the A_{260} across the gradients.

2.2.6 Microscopy

Direct fluorescence: Cells were grown to mid-log phase, fixed for 30 min with one-ninth volume of formaldehyde, washed in cold 100mM KPO_4, pH6.6 and resuspended in 100mM KPO_4 pH6.6 and 1.2M Sorbitol. Triton X-100 was added to a final concentration of 0.1% and cells were incubated 5 minutes at room temperature. DAPI was added to a final concentration of 1µg/ml, cells were incubated at room temperature for 1 minute before being washed 3 times and resuspended in phosphate buffered saline. As indicated, cells were treated with LMB: cells were incubated with 0.4µg/ml LMB for 5 minutes at 30°C and then treated as above. For indirect Immunofluorescence, cells were grown and fixed as described above. Cells were treated as described previously (Ho et al., 2000b) using anti-HA antibody (HA.11, Covance) and Cy3-conjugated donkey anti-mouse antibody (Jackson Labs), mounted in Aqua-Poly Mount (Polysciences) and visualized.

2.2.7 Run off assay

Cells were grown in Yeast extract Peptone with 2% glucose to OD_{600} 0.5. Cultures were either treated with LMB as in 2.2.7 or spun down and the pellet resuspended in YP without carbon source, incubated at 30°C for the indicated time and then treated with LMB as in 2.2.7. Quantification of monosome and polysome peaks was done by calculating the area under the curve in Excel.

Chapter 3

Characterization of the nuclear export adaptor Nmd3 in association with the 60S ribosomal subunit.

3.1 Introduction

Eukaryotic ribosomes are produced in the nuclear subcompartment, the nucleolus, in a complex series of precise RNA processing and protein assembly steps. After nucleolar assembly and nucleolar and nucleoplasmic maturation, preribosome subunits are exported to the cytoplasm through the nuclear pore complex ((Fromont-Racine et al., 2003; Hage and Tollervey, 2004; Henras et al., 2008; Johnson, 2009; Zemp and Kutay, 2007). In order for transport substrates to partition into the hydrophobic lumen of the nuclear pore complex, they must recruit specialized receptor proteins that have affinity for nucleoporins (Fried and Kutay, 2003; Kohler and Hurt, 2007; Pemberton and Paschal, 2005; Tran et al., 2007). In yeast, the large ribosomal subunit utilizes four receptors for export: Crm1, recruited by the adaptor protein Nmd3 (Gadal et al., 2001; Ho et al., 2000b), the heterodimeric mRNA export factor Mex67-Mtr2 (Yao et al., 2007), and the noncanonical receptors Arx1 (Bradatsch et al., 2007; Hung et al., 2008) and Ecm1(Yao et al., 2010). Among these factors, only Nmd3 appears to have a conserved role in ribosome export in vertebrates (Thomas and Kutay, 2003; Trotta et al., 2003). Upon reaching the

cytoplasm, Nmd3 needs to be recycled to the nucleus to allow for further rounds of ribosome export. Release of Nmd3 from the large subunit requires the putative GTPase Lsg1 and the ribosomal protein Rpl10 (Hedges et al., 2005; West et al., 2005). Crystal structures of the large ribosomal subunit reveals Rpl10 binding to the subunit in a cleft between the central protuberance and the base of the P0/P1/P2 stalk (Ben-Shem et al., 2010). Rpl10 mutants which trap Nmd3 in the cytoplasm on the large subunit can be suppressed by mutations in Nmd3 which weaken its affinity for the subunit (Hedges et al., 2005; Karl et al., 1999). The work presented in this chapter was undertaken to further our understanding of how Rpl10 and Nmd3 interact on the subunit to the release of Nmd3.

3.2 Background

Nmd3 is a highly conserved protein found throughout eukaryotes and archaea. An in-depth mutational analysis mapped out the multiple domains in Nmd3 (Hedges et al., 2006). Nmd3 is organized in two main regions: the N terminus contains 60S binding domains while the C-terminus contains shuttling sequences (Illustration 3.1). The N terminus of Nmd3 contains four Cys-X_2-Cys repeats, conserved in all Nmd3 orthologs. These repeats are probably zinc binding motifs, similar to treble clef motifs and Type IV zinc fingers. Mutational analysis of these cysteines suggests that the first four coordinate a Zn^{2+}, while the second set coordinates a second Zn^{2+}. Two 60S binding domains have been identified in the N–terminus region of Nmd3. The third and fourth Cys-X_2-Cys repeats surround the first 60S binding domain, and

mutations of the cysteines in these two repeats significantly reduce Nmd3 binding to 60S, suggesting that the second zinc might arrange this binding domain. A second 60S binding domain was identified N-terminal to the shuttling sequences. These binding domains can be mutated to weaken the affinity of Nmd3 for the large ribosomal subunit, bypassing the need for release factors. The C-terminus of Nmd3 contains the shuttling signals, in order: a nuclear localization signal (NLS), a coiled coil and a canonical leucine-rich nuclear export signal (NES). The NLS is composed of a highly basic domain followed by a hydrophobic patch. These two motifs were shown to be sufficient for nuclear localization. The coiled coil enhances the NES function since its deletion sensitizes NES mutants. The leucine-rich nuclear export sequence (IDELLDEL) is predicted to form an amphipathic helix, with the hydrophobic residues critical for Crm1 interaction aligned on one surface (Hedges et al., 2006). Currently, no high-resolution structural information is available on this protein.

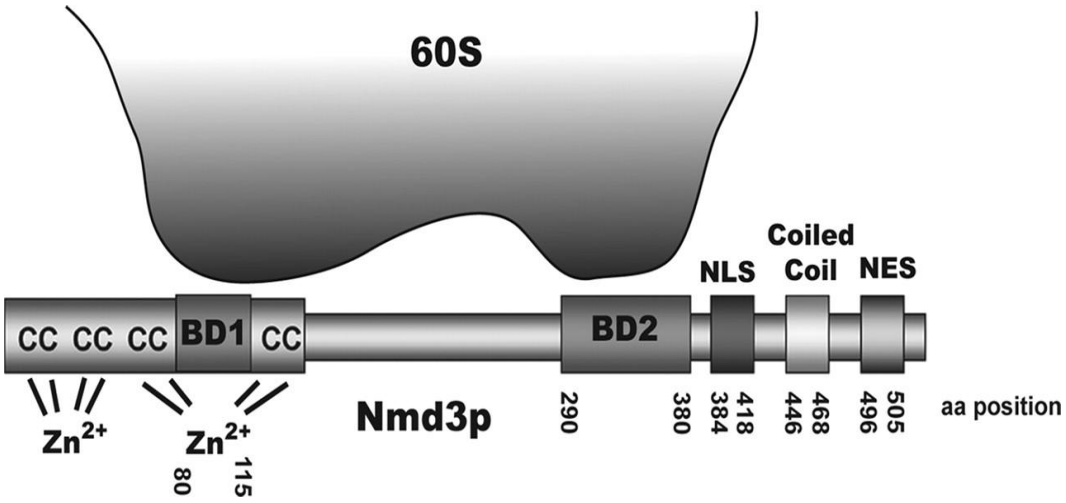

Illustration 3.1 Schematic diagram portraying divalent binding of Nmd3p to 60 S subunits.

CC: Cys-X2-Cys motifs. BD1 and BD2: proposed 60 S binding domains of Nmd3p, based on the observation that suppressor mutations and mutations that weaken Nmd3p-60 S interaction map to these regions..NLS: Nuclear Localization Sequence. Coil: Coiled-coil. NES: Nuclear Export Sequence. The numbers below Nmd3p are the amino acid positions of the approximate boundaries of the indicated domains. Adapted from (Hedges et al., 2006).

The function of Nmd3 in subunit export is conserved from yeast to humans (Thomas and Kutay, 2003; Trotta et al., 2003); however, Nmd3 orthologs are found in archaeal organisms as well. The presence of Nmd3 orthologs in archaea suggests a role in ribosome biogenesis that predates the evolution of the nuclear envelope. In many archaea, Nmd3 is fused to an eIF5A-like domain (Aravind and Koonin, 2000). Although the function of eIF5A is not well understood, *in vitro* eIF5A stimulates the formation of the first peptide bond during translation (Benne et al., 1978; Blaha et al., 2009; Saini et al., 2009). Thus, the physical association of Nmd3p with an eIF5A-like domain in archaea suggests that Nmd3 function is coupled to translation. The cytoplasmic matutration steps of the large ribosomal subunit have been ordered in a coherent pathway (Lo et al., 2010), revealing that the release of Nmd3 is the last step en route to maturation, providing credibility to the idea of Nmd3 function being coupled to translation.

It had been suggested that the ribosomal protein Rpl10 forms the binding site of Nmd3 on the subunit (Gadal et al., 2001). However, genetic and biochemical experiments conducted in our lab indicated that Rpl10, in concert with the conserved cytoplasmic GTPase Lsg1p, is involved in the release of Nmd3 from 60S subunits in the cytoplasm rather than Nmd3 binding to the subunit in the nucleus (Hedges et al., 2005; West et al., 2005). Mutations in Rpl10 and Lsg1 trap Nmd3 on the 60S subunit in the cytoplasm, preventing its recycling to the nucleus, and thus depleting the nuclear pool of Nmd3 and trapping pre-60S subunits in the nucleus. Overexpression of Nmd3 restores subunit export in these mutants, and rescues the growth defect

(Zuk et al., 1999), indicating that the major defect in these mutants is the lack of export of nascent 60S subunits. As mentioned above, mutations in Nmd3 which weaken its affinity for the ribosome allow for release of Nmd3 independently of Rpl10 and Lsg1, and suppress the growth defect of these mutants (Hedges et al., 2005; Karl et al., 1999).

Yeast Rpl10 belongs to the L10e family of ribosomal proteins and is orthologous to bacterial L16. Cryo-EM reconstruction of *S. cerevisiae* ribosome shows Rpl10 located in the deep cleft between the central protuberance and the GTPase-associated center at the base of the P-protein stalk (L7/L12 stalk in prokaryotes) (Armache et al., 2010a, b), corresponding to the position of L16 in *Escherichia coli* (Schuwirth et al., 2005).

To address the molecular mechanism by which the export adaptor protein Nmd3 interacts with the large subunit, I collaborated with Dr Joachim Frank's laboratory to obtain a 3D reconstruction of a 60S subunit in complex with Nmd3. The helix 95 region at the intersubunit surface of the large subunit was identified as the anchoring site of Nmd3. An extended part of the protein reaches close to the ribosomal protein Rpl10. However, no direct interaction with the Rpl10 site is detected. I provided supporting biochemical data that corroborate the structural results. This study provided the first structural description of an export factor in complex with the large subunit.

3.3 Results

3.3.1 Nmd3 binds stoichiometrically with the 60S subunit

The Nmd3 protein used in this work was expressed as a fusion to maltose binding protein (MBP). MBP-Nmd3 fully complemented an *nmd3* deletion mutant (West, unpublished data), indicating that the fusion protein is functional in vivo. Cleavage of MBP from Nmd3 destabilized the protein and reduced 60S binding. Consequently, all work was performed with the intact fusion protein. Previously, reconstitution of the Nmd3–60S complex using a GST-Nmd3 fusion (Ho et al., 2000a)) was shown. However, because this protein dimerizes 60S subunits (West, unpublished data) and thus would presumably occlude the binding surface of Nmd3 from visualization, I used it in this work only as a control for specificity of RNase footprinting.

To examine the interaction of Nmd3 with 60S subunits, I used a rapid coimmunoprecipitation technique. A fixed amount of epitope-tagged subunits (60S-Rpl25-13xmyc) was bound to protein A beads and incubated with increasing amounts of MBP–Nmd3. After binding, the beads were washed extensively, and bound proteins were eluted and separated by SDS-PAGE. As the ratio of Nmd3 to 60S was increased, the amount of Nmd3 bound to 60S increased accordingly, reaching a maximum of 1:1, even at 81-fold excess of Nmd3 relative to 60S (Fig 3.1). This result suggests that Nmd3 binds to the 60S subunit as a monomer and to a single site on the subunit.

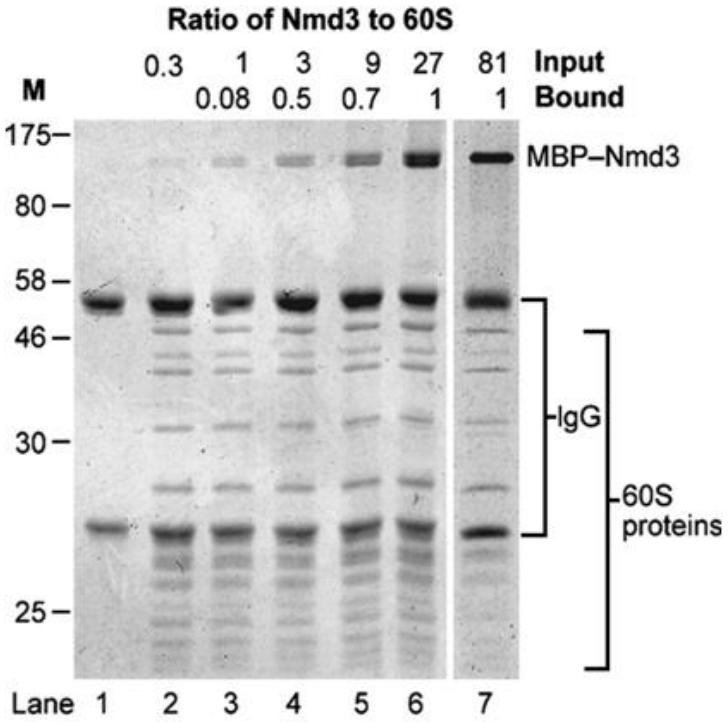

Figure 3.1 MBP-Nmd3 binds stoichiometrically to 60S subunits

Increasing amounts of MBP-Nmd3 were incubated with Rpl25-myc–containing 60S subunits and immunoprecipitated with anti-myc antibody and protein A beads. Bound proteins were eluted in Laemmli sample buffer, separated on 12% SDS-PAGE, and stained with Coomassie brilliant blue. See Materials and methods for details. Lane 1 shows MBP-Nmd3 without 60S; lanes 2–7 show 60S-myc with increasing amounts of MBP-Nmd3 as indicated. The molar ratio of Nmd3 to 60S subunits is given for the input and bound samples. Quantification of protein levels was done using ImageJ (Rasband, W.S., ImageJ, U.S.National Institutes of Health, Bethesda, Maryland, USA, http://imagej.nih.gov/ij/, 1997-2011).

3.3.2 Localization of Nmd3 protein on the 60S subunit

To obtain a more detailed picture of how Nmd3 interacts with the large subunit, collaborators in Dr Joachim Frank's laboratory used cryo-electon microscopy (cryo-EM) and single particle image reconstruction. Cryo-EM maps depicting the 60S subunit alone and in complex with the MBP-Nmd3 fusion protein were obtained at resolutions of 18 Å and 16 Å, respectively (Fig 3.2 A and C). A comparison of the two maps clearly shows an extra density attached to the intersubunit side of the large subunit covering the region extending from the Rpl1 stalk base to the P-protein stalk base of the 25S r-RNA.

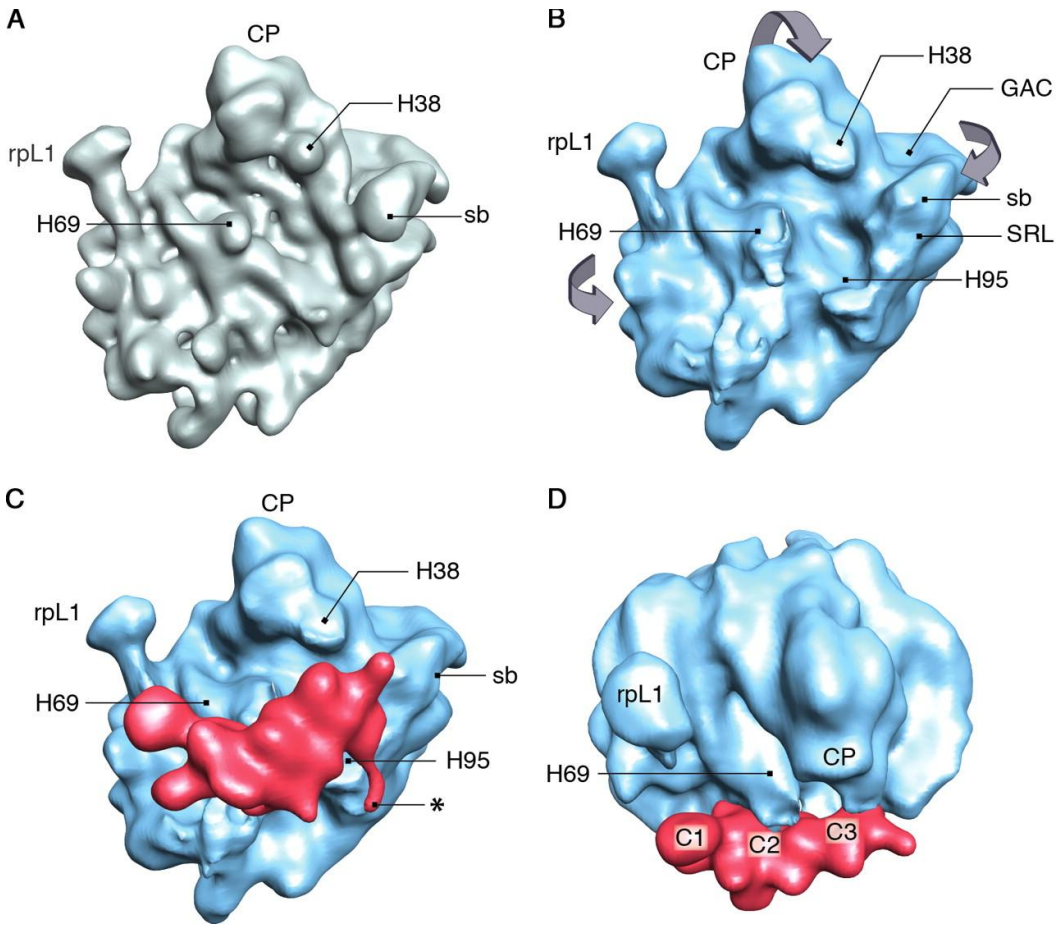

Figure 3.2 Visualization of MBP-Nmd3 binding to the 60S subunit
(A) Intersubunit side view of the control 60S subunit. (B) Intersubunit view of the segmented 60S part of the MBP-Nmd3–60S reconstruction. Significant conformational changes are seen in the GAC, the SRL, the CP, and the region around the peptidyl-transfer center. The stalk base (sb), the L1 stalk (rpL1), and 25S rRNA helices 38, 69, and 95 (H38, H69, and H95) are also labeled. The direction of the motion of the intersubunit surface of the 60S subunit after MBP-Nmd3 binding is marked with arrows. (C) Intersubunit side view of the MBP-Nmd3–60S subunit complex. The segmented density attributed to the MBP-Nmd3 combined mass is colored red, whereas the 60S subunit is colored blue. The asterisk denotes the thread of density (see Identification of Nmd3–60S subunit interactions for details). (D) Top view of the complex showing three connections (C1, C2, and C3) of the MBP-Nmd3 mass (red) with the 60S subunit (blue).

Because the Nmd3 protein was purified with the MBP tag, it is expected that the extra density contains both MBP and Nmd3 as the intact fusion protein. Indeed, the molecular mass of this extra density (about 110KD) calculated from the volume it occupies is substantially larger than the known molecular mass of Nmd3 (59 kD) and close to the expected size of MBP-Nmd3 (103 kD). In addition, biochemical results rule out the possibility of the presence of two copies of Nmd3 (Fig 3.2). Therefore, the additional mass can be attributed to the presence of the MBP tag (molecular mass ~44 kD). These results suggest that the entire MBP-Nmd3 fusion protein is visualized in the cryo-EM map. The current resolution does not allow the modeling of MBP into the mass attributed to MBP-Nmd3. The position of Nmd3 at the interface of the 60S subunit is incompatible with subunit joining, which is consistent with the observation that Nmd3 does not bind to the 80S ribosome in vivo (Ho and Johnson, 1999) or in vitro (see below and Fig 3.5).

The conformational changes in the MBP-Nmd3–bound 60S subunit relative to the control 60S subunit are shown in Fig 3.2 (A and B). Significant displacement was observed in the following regions: (a) the base of the L1 stalk, (b) the GAC and the sarcin–ricin loop (SRL; domain VI of the 25S rRNA), and (c) the CP and the region around the peptidyl-transfer center. In all of these regions, ribosome density was shifted toward the MBP-Nmd3 density. Of particular note, the cleft between the CP and the GAC was narrower in the complex than in the control map. Overall, the changes on the intersubunit side of the 60S subunit can be likened, in their tendency, to the grip of a hand around an object (MBP-Nmd3) on its palm (primary binding

sites are H69 and H95 of 25S rRNA; for brevity, rRNA helices of 25S rRNA will be denoted by "H") (Fig 3.2 C and D). The part of the extra density designated by a star (Fig 3.2 C) is probably not the fusion protein but rather represent a conformational change in the 60S subunit itself, around the Rpl23 region.

The L1 stalk, containing protein Rpl1, is seen in the open position (Valle et al., 2003) in both complex and control maps in which the protein part (Rpl1) of the mushroom-shaped head is partially visible. In contrast, the extended part of the acidic P-protein stalk region and the protein Rpl12 (L11p) at the stalk base are neither visible in the control nor in the 60S subunit map of our complex.

3.3.3 Biochemical characterization of 60S subunit–ligand interactions

To seek supporting evidence for the position of MBP-Nmd3 on the 60S subunit, helices appearing to make contact with the mass assigned to MBP-Nmd3 in the cryo-EM map were probed for altered sensitivity to RNaseV1, a nuclease specific for double-stranded RNA. In these assays, 60S subunits were incubated alone, with MBP-Nmd3, or with GST-Nmd3 and treated with RNaseV1. The GST-Nmd3 reactions were used to control for MBP-specific effects. After RNaseV1 treatment, the rRNA was extracted, and reverse transcription was performed using radio-labeled primers. Primer extension reactions were compared with a DNA sequencing ladder to identify the positions of cleavages.

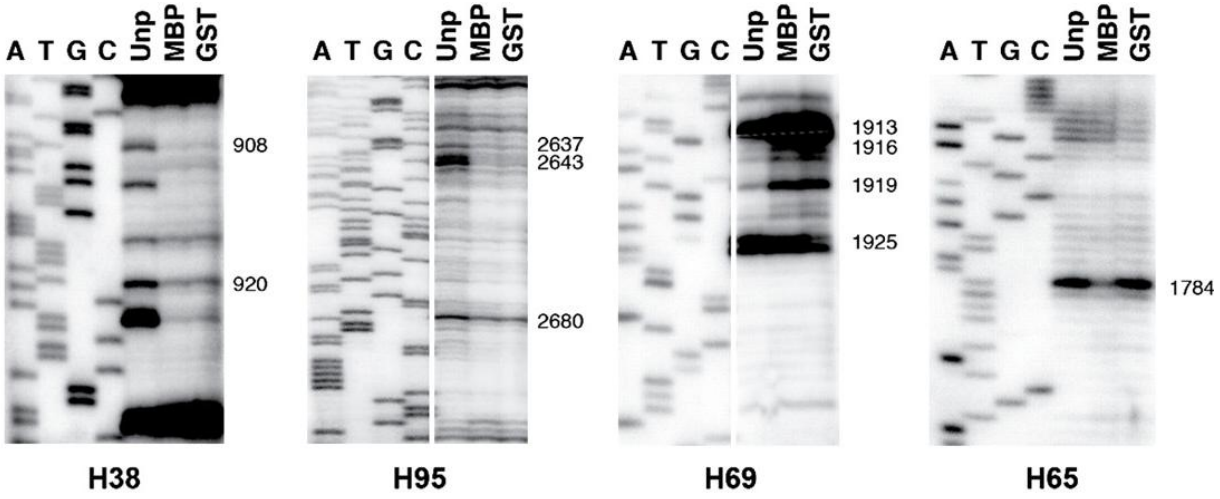

Figure 3.3 rRNA protection: MBP-Nmd3 interaction with helices H38, H65, H69, and H95 of 25S.

(A) 60S subunits were incubated with no protein, MBP-Nmd3, or GST-Nmd3 and treated with RNaseV1. The rRNA was extracted, and primer extension reactions were performed to identify regions of altered sensitivity to RNaseV1. Sequencing reaction lanes are marked by the dideoxynucleotide present in the mixture. Primers used were H38, AJO1061; H65, AJO501; H69, AJO1060; and H95, AJO1135. Numbers indicate positions (*E. coli* numbering) of nucleotides showing major alteration in sensitivity to RNaseV1. Unp, unprotected (no Nmd3); MBP, MBP-Nmd3; GST, GST-Nmd3

Protection by both MBP- and GST-Nmd3 against RNaseV1 was observed for H38 at four positions (Fig 3.3). Two of these positions (bases 1045 and 1054) correspond to *E. coli* 23S bases 908 and 920. MBP- and GST-Nmd3 binding also protected three positions in H95 against cleavage. These positions (3003, 3009, and 3047) correspond to *E. coli* 23S bases 2637, 2643, and 2680 (Fig 3.3). A strong enhancement of RNaseV1 cleavage was observed with both Nmd3 fusion proteins (i.e., GST- and MBP-Nmd3) at three positions in H69, nt 2253, 2256, and 2259 (corresponding to *E. coli* 23S nt 1913, 1916, and 1919). Furthermore, a GST-Nmd3–specific protection was seen in H69 at position 2265 (corresponding to *E. coli* 23S position 1925), and an MBP-Nmd3–specific RNaseV1 protection was observed at position 2142 of H65 (corresponding to *E. coli* 23S nt 1784). Primer extension analysis did not reveal significant changes in other regions of 25S, 5.8S, or 5S rRNA.

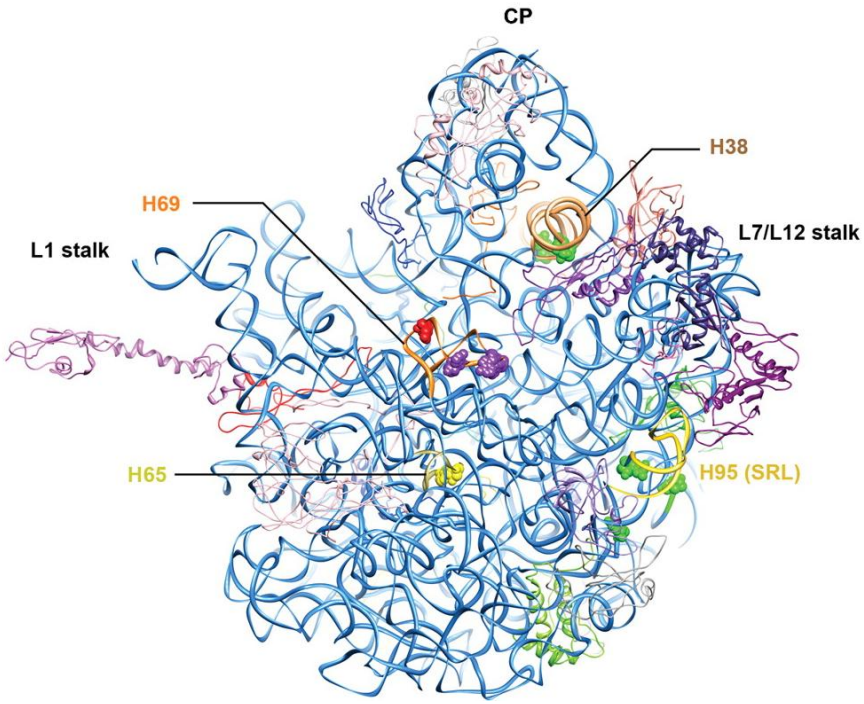

Figure 3.4 MBP-Nmd3 interaction with 60S as inferred from rRNA protection . An interface view of the 50S subunit of the 70S *E. coli* crystal structure (PDB ID 2AW4) showing the position of the helices concerned. Nucleotides marked in green are protected from RNaseV1 by Nmd3; nucleotides in purple show enhancement of cleavage upon interaction with Nmd3; the nucleotide in red shows protection from RNaseV1 cleavage by GST; and the nucleotide in yellow is protected from RNaseV1 cleavage by MBP.

H38 is part of 25S rRNA domain II, which accounts for most of the solvent-side surface of the large subunit. However, the tip of this helix (A-site finger), adjacent to the CP, protrudes toward the subunit interface side and participates in the formation of the intersubunit bridge B1a. In contrast, H65 and H69 belong to domain IV, which accounts for most of the intersubunit surface of the large subunit. H69 is positioned at the center of the large subunit interface and participates in the formation of two essential intersubunit bridges, B2a and B2b (Yusupov et al., 2001). H65 is also exposed to the subunit surface on the intersubunit side. H95 (SRL; rRNA domain VI) is situated below the P-protein stalk base region (Ban et al., 2000)), and part of it is exposed to the solvent (Fig 3.4)). Based on the protection assay results, a tentative identification of the positions for MBP and Nmd3 in the density can be made. These results suggests that the SRL/CP proximal part of the differential mass observed in the cryo-EM structure accounts for Nmd3, whereas the distal part close to H65 likely represents the MBP portion of the fusion protein.

3.3.4 80S formation prevents Nmd3 binding to the ribosome

Nmd3 binds to free 60S subunits but not to 40S subunits or 80S complexes in vivo, suggesting that its binding site may be blocked by the presence of the 40S subunit (Ho and Johnson, 1999)). The cryo-EM result assigns the subunit joining face as the binding site of Nmd3 on the 60S subunit. Hence, one would expect the formation of 80S to prevent binding of Nmd3 to 60S. To test this I compared the binding of Nmd3 to purified 60S subunits versus 80S ribosomes. MBP-Nmd3 was incubated alone,

with 60S subunits, or with preformed 80S ribosomes, and reactions were separated by centrifugation through sucrose cushions. Under these conditions, free Nmd3 remained entirely in the supernatant Fig 3.5 lanes 1 and 2), whereas in the presence of 60S subunits, Nmd3 quantitatively cosedimented with the subunits (Fig 3.5 lanes 3 and 4). In contrast, Nmd3 did not cosediment with preformed 80S ribosomes, but rather remained in the supernatant fraction (Fig 3.5 lanes 5 and 6). These results are consistent with the cryo-EM data and Nmd3 binding to the subunit joining face of the large ribosomal subunit.

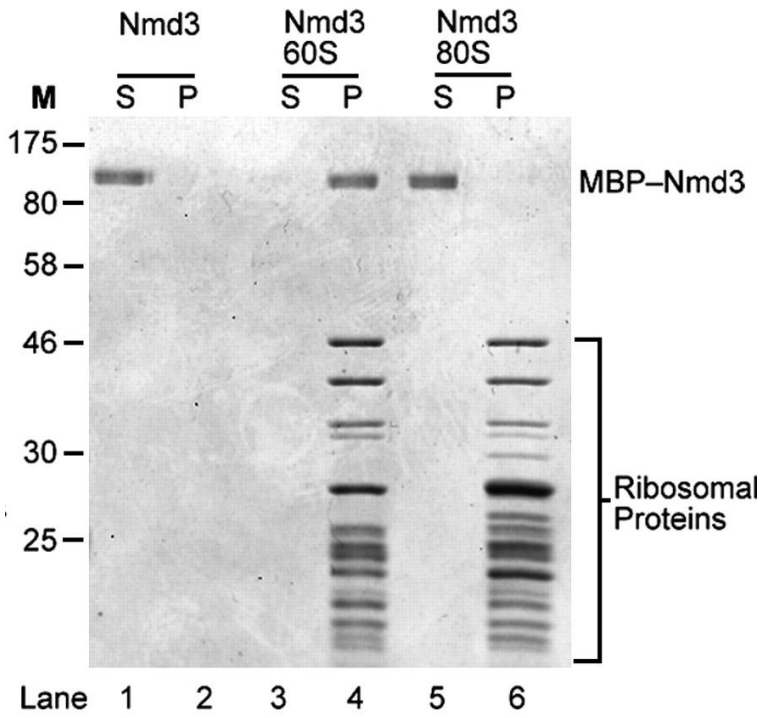

Figure 3.5 80S formation prevents Nmd3 binding.
MBP-Nmd3 was incubated alone (lanes 1 and 2), with 60S (lanes 3 and 4), or with 80S subunits (lanes 5 and 6). Samples were layered over 60% sucrose cushions and centrifuged. Supernatants (S) and pellets (P) were separated on a 12% SDS-PAGE, and proteins were visualized by Coomassie staining. (A and B) The positions of molecular mass markers (M) are given in kilodaltons.

3.4 Discussion

3.4.1 Nmd3 binding to the 60S ribosomal subunit

The results presented here clearly assign the Nmd3 binding site to the subunit joining face of the 60S ribosomal subunit. With the binding of Nmd3, the interface of the 60S subunit containing Rpl10 is apparently pulled toward the ligand. The resulting conformational change of the 60S subunit may reflect strain induced by Nmd3 binding. Although there is no direct interaction between the isolated mass and the 60S subunit at the Rpl10 region visible at this resolution of the cryo-EM map, the morphological features at the Rpl10-binding site and H38 regions in the 60S subunit appear different in the complex as compared with the control 60S subunit map (Fig 3.3). However, the resolution of the maps does not allow for accurate modeling of Rpl10 inside the density.

As mentioned previously, it had been suggested that Rpl10 forms the binding platform of Nmd3 on the subunit (Gadal et al., 2001). However, the binding site assignment for Nmd3 on the subunit presented here clearly refutes this notion since Nmd3 is not seen making contact with Rpl10.

Nmd3 binding alters the conformation of the ribosome. In the cryo-EM map, the ribosome can be seen pulled toward Nmd3 (Fig 3.3). Nmd3 is conserved in archaea, although it lacks the shuttling sequences, suggesting an additional function besides export. In the absence of Nmd3, 60S subunits are extremely unstable (Ho and Johnson, 1999). Thus, Nmd3 binding to 60S subunit might hold the nascent

subunit in a conformation that stabilizes it. Furthermore, the observed tightening of the ribosome around the ligand might also facilitate transport through the nuclear pore complex.

The binding of Nmd3 to the 60S subunit induces a conformational change in the Rpl23 region which can be observed in the MBP-Nmd3/60S cryo-EM reconstruction despite the relatively low resolution (Fig 3.3 B star). The binding site of the anti-association factor Tif6 was identified in a similar fashion (Gartmann et al., 2010). The binding site of Tif6 involves mostly Rpl23 alongside the SRL and to a lesser extent Rpl24. The conformational change observed in the Rpl23 region upon Nmd3 binding implies allostery between the binding sites of Nmd3 and Tif6. The release of Tif6 is a pre-requisite for the release of Nmd3(Lo et al., 2010). Thus, the presence of Tif6 on the subunit, bound to the Rpl23 region, might prevent a conformational change of the ribosome in this region required for the release of Nmd3, resulting in entrapment of Nmd3 on the 60S subunit.

3.4.2 Nmd3 binding to mature versus nascent subunits

The cryo-EM map presented in this study is of Nmd3 (fused with MBP) in complex with a mature 60S subunit. However, during ribosome assembly in eukaryotes, Nmd3 initially binds to pre-60S particles in the nucleus to direct their export to the cytoplasm (Gadal et al., 2001; Ho et al., 2000b). After export, the pre-60S particle undergoes a series of maturation steps involving the release of trans-acting factors and the assembly of certain ribosomal proteins (Panse and Johnson, 2010) and

culminates in the release of Nmd3 (Lo et al., 2010). The release of Nmd3 depends on the presence of ribosomal protein Rpl10 and the activity of the GTPase Lsg1 (Hedges et al., 2005). Rpl10 is required for release of Tif6, prior to release of Nmd3 (See Chapter 4). Thus, at the time of Nmd3 release, the subunit is presumably mature. The reconstituted MBP-Nmd3/60S complex, which contains Rpl10, may represent a late intermediate of 60S maturation, after Rpl10 loading but before Nmd3 release. Hence, the structure presented here might not be an accurate reflection of the native Nmd3-pre-60S complex. This could be resolved by purifying native Nmd3-pre-60S complexes from crude extract.

It has been previously suggested that both Nmd3 and Lsg1 can bind to mature subunits as well as nascent subunits (Ho and Johnson, 1999). Considering that Nmd3 is the last factor released from the nascent subunit, its binding to mature subunits could simply be a reversal of this step. Mutations in translation factors, which affect translation, inhibit release of Nmd3 from the subunit (Lo, unpublished data). This implies that translation is necessary for release of Nmd3. Since release of Nmd3 is necessary for large subunits to enter the translating pool –Nmd3 does not sediment with 80S or polysomes- Nmd3 release and translation appear to co-regulate each other. This interplay between Nmd3 release and translation suggests that Nmd3 binding to mature subunit could represent a mean of inhibiting 60S from entering the translating pool under conditions where the cell cannot support translation, for example during stress response induced by low energy (NTPs) or nutrient levels.

3.4.3 Nmd3 release and Rpl10 accommodation

It had been suggested that Rpl10 loading is involved in released of Nmd3 (Hedges et al., 2005; West et al., 2005). However, in Chapter 4 I describe a new role for Rpl10 in release of Tif6. Release of Tif6 is a prerequisite for release of Nmd3. Thus Rpl10 loading appears to occur prior to or concomitantly with the release of Tif6, before release of Nmd3. Reported physical interactions between Lsg1 mutants which impair Nmd3 release and an Rpl10 truncation support the notion that release of Nmd3 involves or induces conformational change in the large ribosomal subunit. A truncation of Rpl10 (Rpl10-N187) lacking its C-terminus, does not immunoprecipitate with wild-type Lsg1, suggesting that it does not interact with the 60S ribosomal subunit (West et al., 2005). In Lsg1, K349 is in the G1 (Walker A) motif (GX_4G**K**S/T), that is required for coordination and catalysis of GTP (Saraste et al., 1990). *lsg1-K349T* is a dominant negative Lsg1 mutant which traps RPL10-N187 on the subunit and allows for co-immunoprecipitation with the mutant LSG1 (West et al., 2005). Thus, it appears that Rpl10-N187 loads prior to activation of Lsg1 GTPase, and is not stably accommodated into the subunit in WT Lsg1. The fact that Rpl10-N187 is not co-immunoprecipitated with WT LSG1 but is seen in LSG1-K349T immunoprecipitation suggests that a conformational change of the ribosome in the Rpl10-binding-site region occurs upon activation of Lsg1 GTPase activity during release of Nmd3. This conformation change induces release of Rpl10-N187 which is unstably associated with 60S. Consequently, Lsg1 induced rearrangement of the ribosome which leads to release of Nmd3 could represent a final Rpl10

accommodation step. The fact that Nmd3 bound to the 60S ribosomal subunit shows a tightening of the subunit towards the ligand, concurs with a conformational change involved with or induced by release of Nmd3.

Chapter 4

Probing the P site during maturation of the 60S ribosomal subunit

4.1 Introduction

Accurate translation is crucial for proper protein function and, consequently, for the viability of all cellular processes. The complexity of ribosome structure (Bashan and Yonath, 2008; Ramakrishnan, 2002; Schmeing and Ramakrishnan, 2009; Steitz, 2008) would appear to present an extreme challenge to a cell to ensure the correct assembly and function of the ribosome. Because defects in assembly would likely lead to reduced function and fidelity of the ribosome, strategies must have evolved to ensure the proper function of newly assembled ribosomes. However, the mechanism(s) that cells employ to monitor the correct assembly of their ribosomes is largely unknown.

Eukaryotic ribosomes are largely preassembled in the nucleus, requiring more than 200 trans-acting factors (Fromont-Racine et al., 2003; Kressler et al., 2010; Tschochner and Hurt, 2003). The premature subunits are then exported to the cytoplasm where they undergo final maturation steps prior to becoming translation-competent. Maturation of the pre-60S subunit involves the recycling of export factors, the removal of placeholder proteins, and the assembly of several critical

ribosomal proteins (Henras et al., 2008; Panse and Johnson, 2010; Staley and Woolford, 2009; Strunk and Karbstein, 2009; Zemp and Kutay, 2007).

The order of events of the cytoplasmic maturation pathway of the 60S subunit has been recently established (Lo et al., 2010) and found that it is a highly ordered progression of events. Two different ATPases carry out one series of protein exchanges, leading to the release of the export receptor Arx1 (Demoinet et al., 2007; Hung and Johnson, 2006; Lebreton et al., 2006a; Meyer et al., 2007; Pertschy et al., 2007). The ribosome stalk is a feature that is critical for recruiting and activating translation factors (Gao et al., 2009) } . It is assembled separately and requires the removal of the placeholder Mrt4 (Kemmler et al., 2009; Lo et al., 2009; Rodriguez-Mateos et al., 2009) which blocks the binding of the stalk protein P0. These two series of events are prerequisite for the function of the GTPase Efl1, which together with Sdo1releases the subunit anti-association factor Tif6 (Becam et al., 2001; Menne et al., 2007; Miluzio et al., 2009; Senger et al., 2001). In the last known step, which depends on the prior release of Tif6, the export adaptor Nmd3 is released from the ribosome by the concerted action of the GTPase Lsg1 and the ribosomal protein Rpl10 (Hedges et al., 2005; Kallstrom et al., 2003; West et al., 2005).

4.2 Background

The GTPase Efl1 is homologous to the translation elongation factor eEF2 (EF-G in prokaryotes) (Senger et al., 2001), while Sdo1 is orthologous to the human SBDS protein (Luz et al., 2009; Shammas et al., 2005), mutations in which cause

Shwachman-Bodian-Diamond syndrome, an autosomal recessive bone marrow failure disease (Bodian et al., 1964; Moore et al., 2010; Shwachman et al., 1964) . During translation, the growing polypeptide chain is transferred from the P-site tRNA to the A-site tRNA. However, this is a dynamic process; the peptidyl tRNA rapidly shifts to the hybrid A/P position through a natural ratchet-like motion of the subunits (Agirrezabala et al., 2008; Blanchard et al., 2004; Cornish et al., 2008; Frank and Agrawal, 2001; Julian et al., 2008). EF-G is recruited to the GTPase-associated center (GAC) of the ribosome by the L7/L12 stalk (Mohr et al., 2002) and stabilizes the ribosome in the ratchet-like intersubunit rotated state (Spiegel et al., 2007). GTP hydrolysis by EF-G (Rodnina et al., 1997) induces a conformational change in the protein (Czworkowski et al., 1994; Stark et al., 2000) that drives translocation. The anticodon ends of the tRNAs along with the mRNA are shifted with respect to the decoding center of the small subunit, thereby resetting the A site.

It has previously been suggested that cytoplasmic assembly of the P0-P1-P2 protein stalk (the eukaryotic equivalent of L10-L7-L12) is necessary for recruitment and activation of Efl1 to induce the release of Tif6 (Lo et al., 2010). Thus, the GTPase activity of Efl1 could act during a quality control check of the ribosome prior to translation initiation (Lo et al., 2010; Senger et al., 2001). Such a mechanism would monitor assembly of the GAC, including the stalk and the sarcin-ricin loop, thereby providing a structural check for a critical functional center of the ribosome. According to this model, Efl1 utilizes the known function of the stalk, in recruiting and activating GTPases during translation, for a biogenesis-specific function.

Here I show that a loop of the large-subunit protein Rpl10 is also intimately involved in the release of Tif6 from the 60S subunit by Efl1. This loop, which is refered to as the P-site loop, reaches in toward the catalytic center of the ribosome where it contacts the acceptor stem of the P-site tRNA (Armache et al., 2010b; Gao et al., 2009; Voorhees et al., 2009). Mutations in this loop prevent the release of Tif6, 90Å away. Mutations in Efl1 that are predicted to facilitate a conformational change analogous to conformational changes that eEF2 undergoes during translocation, bypass the effects of these P-site loop mutations. My data suggest that in addition to interrogating the correct assembly of the stalk, Efl1 interrogates the P-site of the ribosome in a more rigorous assessment of the integrity of the 60S subunit assembly than previously recognized. The utilization of a translocation-like factor during biogenesis to assess both the status of ribosome assembly and, specifically, the status of the P site suggests that the newly assembled ribosome undergoes a "test drive" before being released into the active pool of ribosomes engaged in translating mRNAs.

4.3 Results

4.3.1 Rpl10 is required for the release of Tif6 as well as Nmd3 from nascent 60S subunits.

It was previously shown that Rpl10 is required for the release of the nuclear export adapter Nmd3 (Hedges et al., 2005; West et al., 2005). However, this is only one of multiple cytoplasmic maturation events that the 60S subunit undergoes. The large

ribosomal subunit cytoplasmic maturation events were recently ordered into a coherent pathway (Lo et al., 2010). This study prompted me to revisit the role of Rpl10, asking if it is required solely for the release of Nmd3 or if it affects other steps as well. I first determined if depletion of Rpl10 affected the release, and hence the recycling to the nucleus, of any of the known shuttling 60S subunit biogenesis factors. A galactose-inducible promoter was integrated into the *RPL10* locus in strains expressing GFP-tagged Mrt4, Arx1, Tif6 or Nmd3. Mrt4, Arx1 and Tif6 display nuclear localization at steady state but are mislocalized to the cytoplasm under conditions that prevent their release from the subunit ((Lo et al., 2010) and references therein). However, to monitor Nmd3, which is predominantly cytoplasmic, a leptomycin B (LMB) -sensitive *CRM1-T539C* mutant was used. Crm1 is the nuclear export receptor for Nmd3. Thus, in the presence of LMB the export of Nmd3 is blocked and it accumulates in the nucleus. As expected, when grown in non-repressing conditions (galactose) Mrt4, Arx1 and Tif6 localized to the nucleus, indicating that they were shuttling (Fig 4.1, left panel). Nmd3 also could be trapped in the nucleus by the addition of LMB, indicating that it was also shuttling (Fig 4.1, left panel). Upon repression of *RPL10* by addition of glucose, Mrt4 and Arx1 remained nuclear (Fig. 4.1, right panel), whereas Nmd3 became cytoplasmic, as has been shown previously (Hedges et al., 2005; West et al., 2005). Surprisingly, repression of *RPL10* also resulted in the re-localization of Tif6 from the nucleus to the cytoplasm.

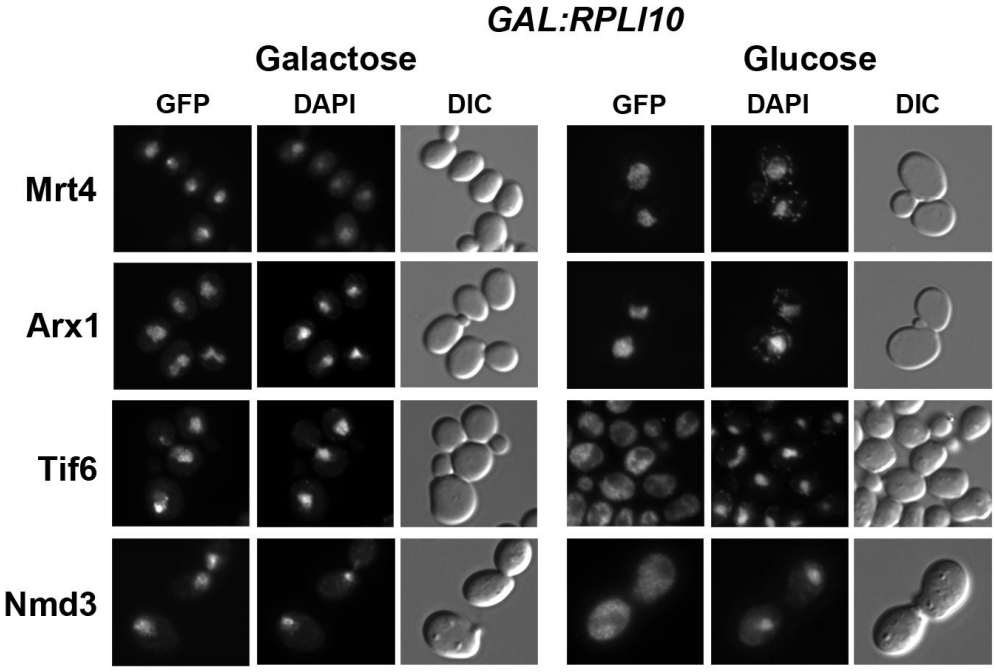

Figure 4.1 Rpl10 is required for recycling of Tif6 to the nucleus
The localization of Mrt4, Arx1, Tif6 and Nmd3 was examined in the presence (galactose) or absence (glucose) of ongoing Rpl10 expression. AJY2766 (P_{GAL1}-*RPL10 TIF6-GFP*), AJY2767 (P_{GAL1}-*RPL10 ARX1-GFP*), and AJY2768 (P_{GAL1}-*RPL10 MRT4-GFP*) were grown in galactose to mid-log phase, the cultures were split in two and for one, Rpl10 expression was repressed for 2 hours by the addition of glucose. GFP-tagged proteins were visualized by microscopy. AJY1837 *(*P_{GAL1}-*RPL10 NMD3-GFP crm1-T539C*) was treated as above with the addition of LMB following glucose addition.

This result indicates a failure in Tif6 recycling, either because of a defect in reimport or a failure to release it from cytoplasmic 60S subunits. To distinguish between these possibilities, I monitored the sedimentation of Tif6 in sucrose gradients under conditions of *RPL10* expression or repression (Fig. 4.2). In both conditions, Tif6 sedimented strictly at the position of free 60S subunits, indicating that Tif6 remains bound to the subunit in the cytoplasm when *RPL10* expression is repressed.

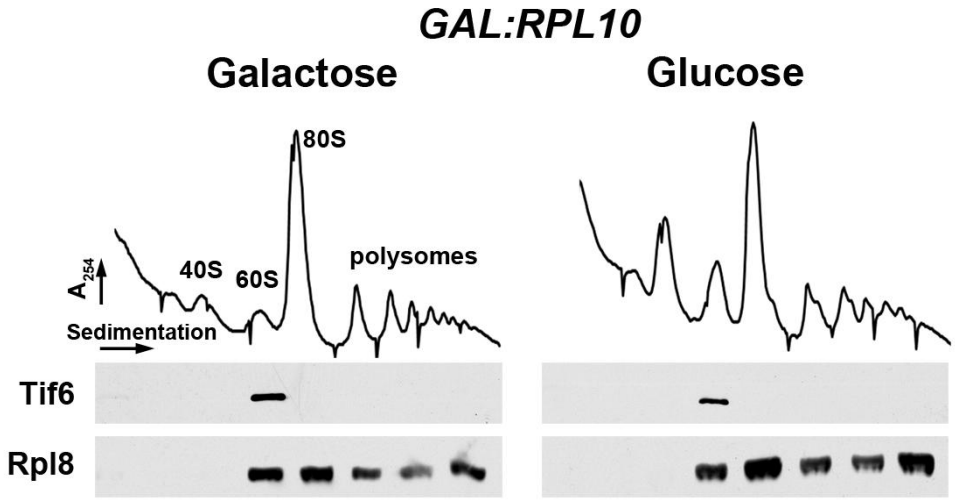

Figure 4.2 Tif6 remains bound to 60S subunit upon depletion of Rpl10
Sucrose gradient sedimentation of Tif6. AJY2766 (P_{GAL1}-*RPL10 TIF6-GFP*) was cultured as described in (A). Crude extracts were prepared and fractionated by sucrose gradient sedimentation. The position of Tif6 in gradients was monitored by western blotting using anti-GFP antibody. Anti-Rpl8 was used to monitor the position of 60S subunits.

4.3.2 The P-site loop of Rpl10 is required for the release of Tif6.

In a previous mutational analysis of Rpl10 (Hofer et al., 2007), an internal loop (aa102-112) that is required for the release of Nmd3 was identified. Rpl10 (L16 in bacteria) is located in a cleft between the central protuberance and the P0/P1/P2 ribosome stalk (Illustration 4.1).

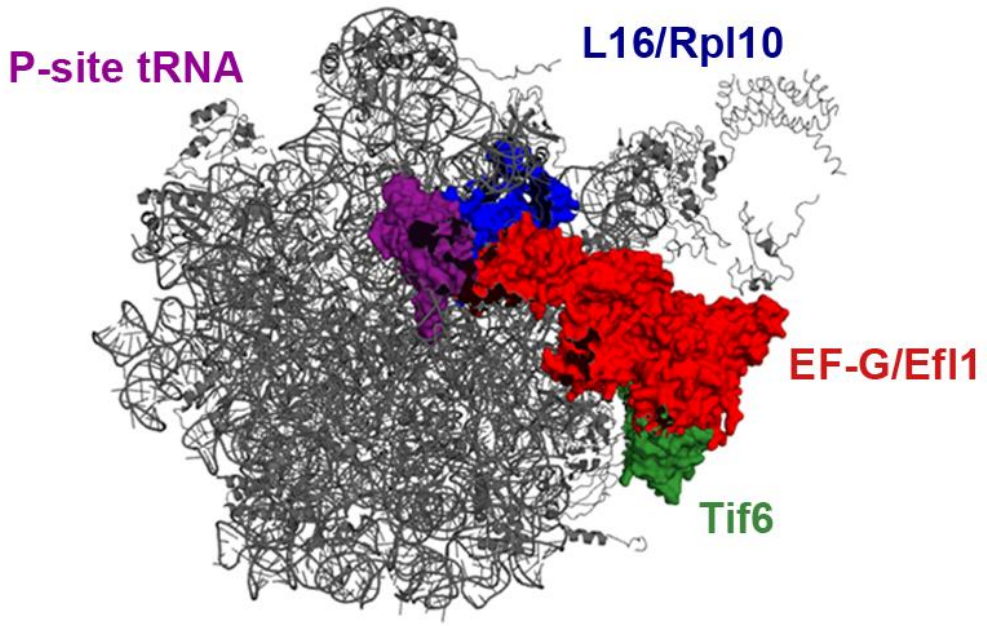

Illustration 4.1 Position of the relevant protein on the large ribosomal subunit
A composite image of the large subunit showing the expected relative positions of L16/Rpl10 (blue), P-site tRNA (purple), EF-G/Efl1 (red) and Tif6 (green) was made by docking yeast Tif6 (PDB 2X7N) (Gartmann et al., 2010) onto the bacterial 50S subunit with EF-G (PDB 2WRI/2WRJ) (Gao et al., 2009). The similarities between L16 and Rpl10 and EF-G and Efl1 suggest that the bacterial proteins can be used as proxies for the eukaryotic structures.

High-resolution crystal structures of the bacterial ribosome show that in L16, this loop extends towards the P site and, together with L27, embraces the P-site tRNA (Illustration 4.2 lower panel) (Gao et al., 2009; Voorhees et al., 2009). Thus I refer to this loop of Rpl10 as the P-site loop. Archaeons and eukaryotes lack L27 but have an elongated P-site loop (Illustration 4.2) that may functionally replace L27 (Schmeing et al., 2009; Voorhees et al., 2009). This extended P-site loop has not been resolved in crystal structures of archaeal or eukaryotic ribosomes but has recently been modeled by cryo-EM of translating eukaryotic ribosomes, where it is seen making contact with the acceptor stem of the P-site tRNA (Armache et al., 2010b) (Illustration 4.2 upper panel).

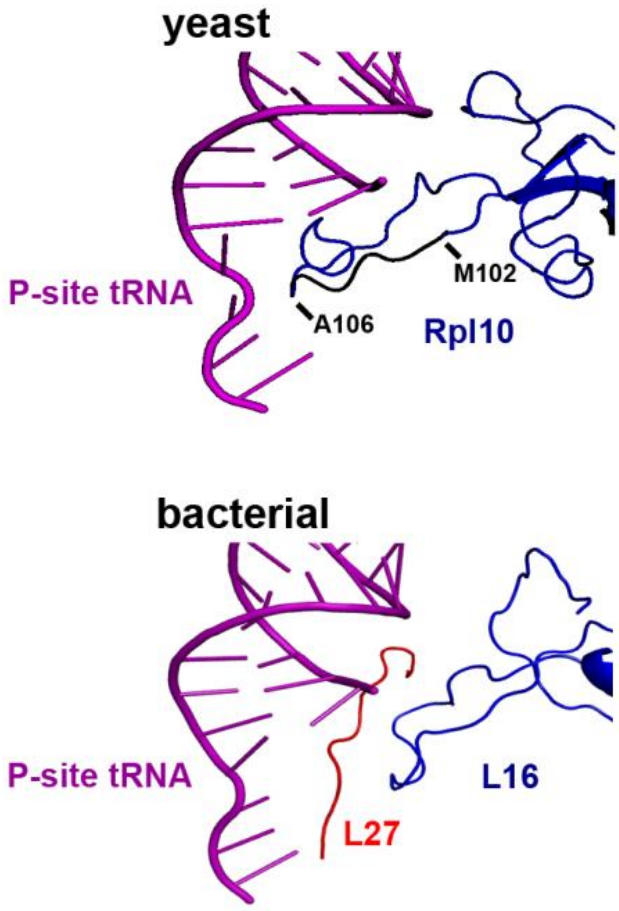

Illustration 4.2 Comparison of the P-site tRNA interactions of L16 and Rpl10. Top panel panel: yeast Rpl10 (blue) and P-site tRNA (purple) (adapted from PDB 3IZC/3IZB/3IZE/3IZF (Armache et al., 2010b) Mutated residues in the P-site loop are indicated in black. Bottom panel: Bacterial L16 (blue), L27 (red) and P-site tRNA (purple) (adapted from PDB 2WRI/2WRJ (Gao et al., 2009))

Deletion of the P-site loop (*rpl10-*Δ*102-112*) is lethal and blocks the recycling of Nmd3 (Hofer et al., 2007). I asked if the release of Tif6 was also blocked by mutations in the P-site loop of Rpl10. I introduced a plasmid carrying the *rpl10-Δ 102-112* allele into strains containing a glucose-repressible *RPL10* and GFP-tagged shuttling factors. Upon repression of wild-type *RPL10* so that only *rpl10-*Δ*102-112* continues to be expressed, Mrt4 and Arx1 remained nuclear while Tif6 and Nmd3 became cytoplasmic (Fig. 4.3, right panel, glucose).

\

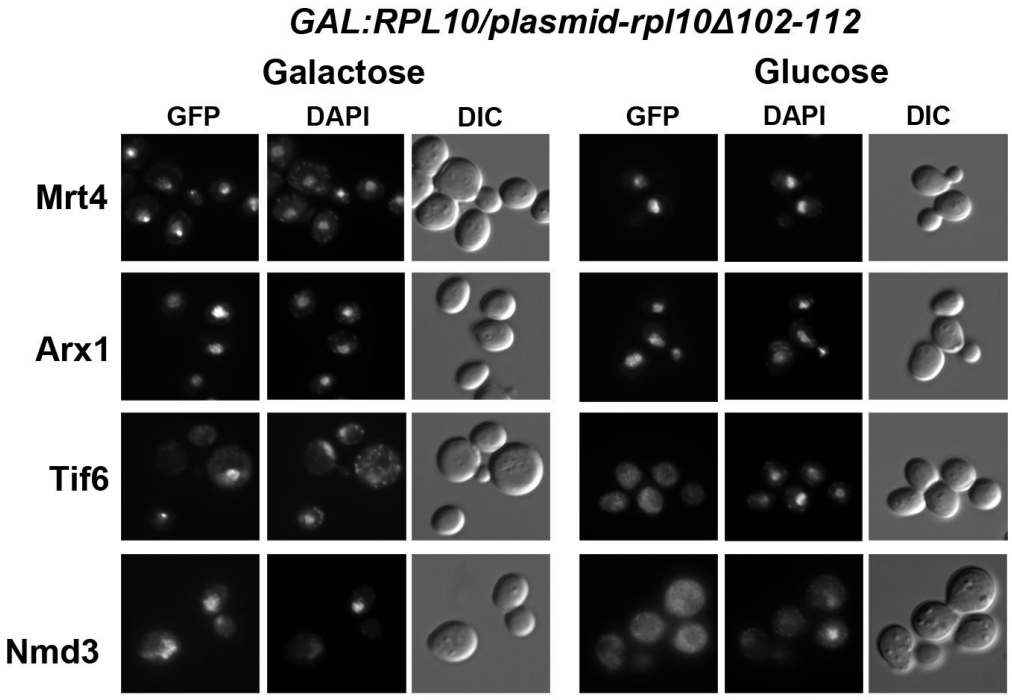

Figure 4.3 The P-site loop of Rpl10 is required for release of Tif6 from 60S subunits

The Rpl10 P-site loop is required for release of Tif6 from 60S subunits. The GFP-tagged strains described in Fig 4.1 were transformed with a vector (pAJ1777) expressing mutant *RPL10* deleted of the P-site loop (*rpl10-*Δ*102-112*). GFP fluorescence of the tagged proteins was monitored under conditions of Rpl10 expression (galactose) or repression (glucose) as in Fig4.1.

To ensure that deletion of the Rpl10 P-site loop and not simply depletion of wild-type *RPL10* was responsible for the cytoplasmic entrapment of Tif6, I also monitored the localization of Tif6-GFP in cells upon over-expression of *rpl10-Δ102-112*. This mutant is strongly dominant-negative when overexpressed and caused mislocalization of Tif6 to the cytoplasm (Fig 4.4). Thus deletion of the P-site loop had an effect similar to repression of *RPL10* in preventing the release of both Tif6 and Nmd3 from 60S subunits. These results reveal an unexpected role for Rpl10 in 60S subunit biogenesis, implicating the P-site loop, deep in the catalytic center of the ribosome, in the release of Tif6.

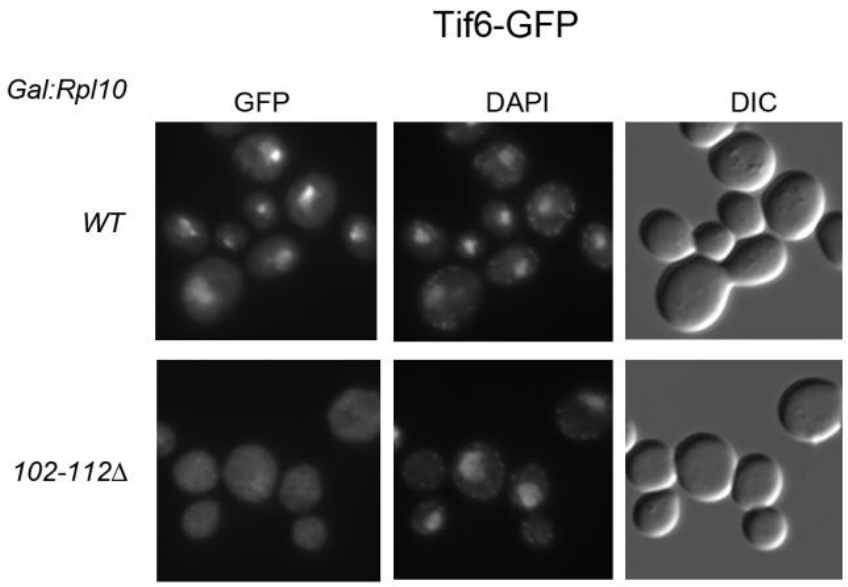

Figure 4.4 Overexpression of Rpl10-Δ*102-112* traps Tif6 in the cytoplasm
A Tif6-GFP strain (AJY) was transformed with pAJ1781 (*Gal::Rpl10-(TEV)-myc*) and pAJ1782 (*Gal::rpl10-Δ102-112-(TEV)-myc*). Cells were grown in Raffinose and overexpression of plasmid born alleles was induced for 2 hours by addition of galactose. Tif6-GFP localization was monitored by microscopy.

4.3.3 Mutations in the P-site loop of Rpl10 exhibit two distinct phenotypes.

Rpl10 P-site loop mutagenesis

To further investigate the function of the P-site loop of Rpl10 I targeted the P-site loop for mutagenesis. Initially, pairs of codons were randomized by oligonucleotide-directed mutagenesis and mutant pools were screened for viable but slow growing mutants. I obtained a few double mutants in the first 5 codons of the loop (102-106), and one single mutant (A106R), but could not obtain viable mutations in the last six codons, perhaps suggesting a more conserved and essential function for the second half of the loop. In order to obtain single mutants, a second screen was set up. Sucheta Arora, while rotating in our laboratory conducted this screen. In that screen, the first five amino acids of the loop (aa 102-106) were individually targeted for mutagenesis in a similar fashion. 21 mutants exhibiting slower than wild-type growth were identified (Fig 4.5).

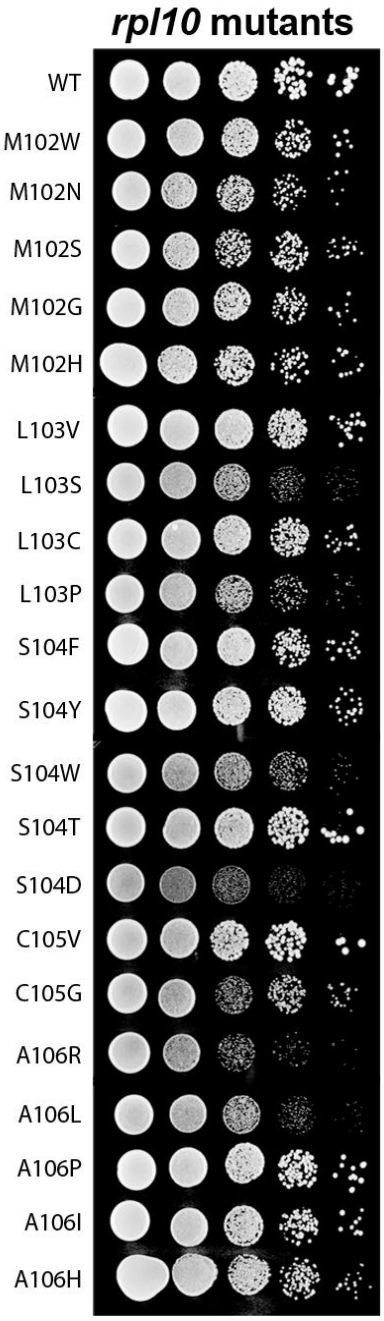

Figure 4.5 Growth assay of the *rpl10* P-site loop mutants.
Ten-fold serial dilutions of AJY1437 (*rpl10*Δ*::KanMX*) containing either wild-type (pAJ2522) or P-site loop mutants as the sole source of Rpl10 were spotted onto YPD and grown two days at 30°C.

Polysome profile analysis reveals two classes of Rpl10 P-site loop mutant

To further investigate the effect of these mutations on ribosome biogenesis or translation, polysome profiles were determined for the mutants. Cell extracts were sedimented through sucrose gradients and UV absorbance along the gradients was monitored. Two distinct classes of mutants emerged from this study. Class I (biogenesis) mutants, including *rpl10-M102N, M102G, M102H, S104D, S104F, S104Y, S104W, C105G, A106I,* and *A106P,* displayed halfmers (Fig 4.6). These are mRNAs that contain a 48S initiation complex that has not yet joined with the 60S subunit, indicative of a defect in biogenesis and/or subunit joining. *rpl10-S104D* was the most extreme example of this class of biogenesis mutants. Class II mutants, including *rpl10-M102W, M102S, L103V, L103S, L103P, A106R, and A106H,* lacked halfmer polysomes and exhibited higher free 60S than 40S peaks (Fig 4.6). *rpl10-A106R* had the strongest phenotype in this class. A few of the mutants, e.g. *rpl10-S104T* and *C105V*, exhibited polysome profiles nearly identical to wild-type (Fig 4.6), correlating with their modest growth defects. Interestingly, different mutations of the same residue sometimes resulted in drastically different phenotypes. For example, *rpl10-A106P* is a biogenesis mutant, *rpl10-A106R* is a Class II mutant, and *rpl10-A106L* shows elements of both phenotypes.

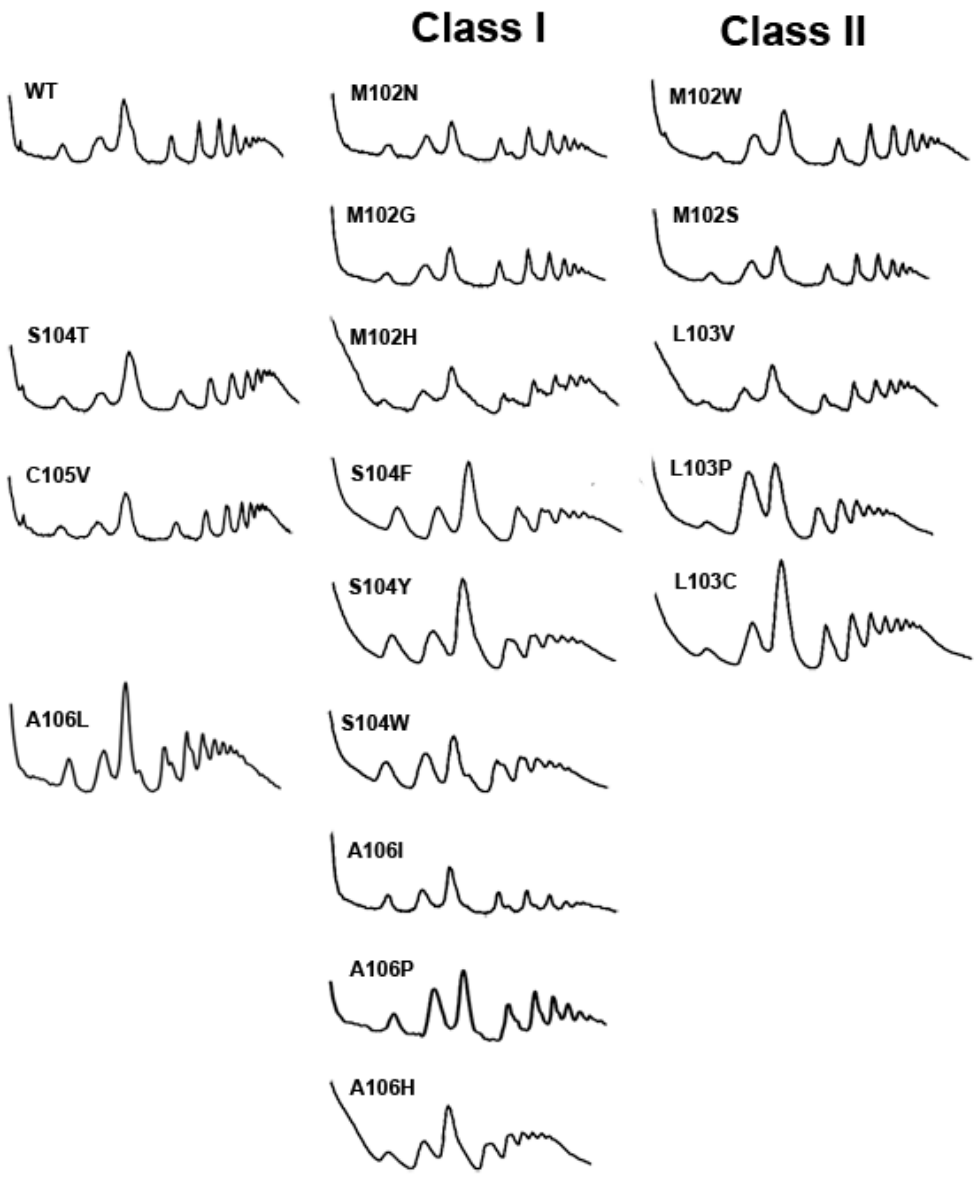

Figure 4.6 Two classes of Rpl10 P-site loop mutants based on their polysome profiles.
AJY1437 containing wild-type (pAJ2522) or P-site loop mutant Rpl10 was grown in YPD to mid-log, incubated with cycloheximide and collected on ice. Crude extracts were made and ran through 7-47% gradients and A_{260} was monitored along the gradients.

The Rpl10 P-site loop mutants sequester both Nmd3 and Tif6 in the cytoplasm

I monitored the localization of Nmd3 and Tif6 in strains containing the P-site loop mutants as the sole copy of Rpl10. The fifteen mutants tested all trapped Tif6 in the cytoplasm to various degrees when compared to wild-type Rpl10 (Fig. 4.7, left panels). Similarly, these mutants had various effects on the release of Nmd3 from 60S (Fig 4.7 right panels). However, the mutants exhibiting the most severe growth defects all relocalized Nmd3 to the cytoplasm. While the class I mutants appear to affect subunit biogenesis specifically (see below) the defect in the class II mutants appears more complex in nature.

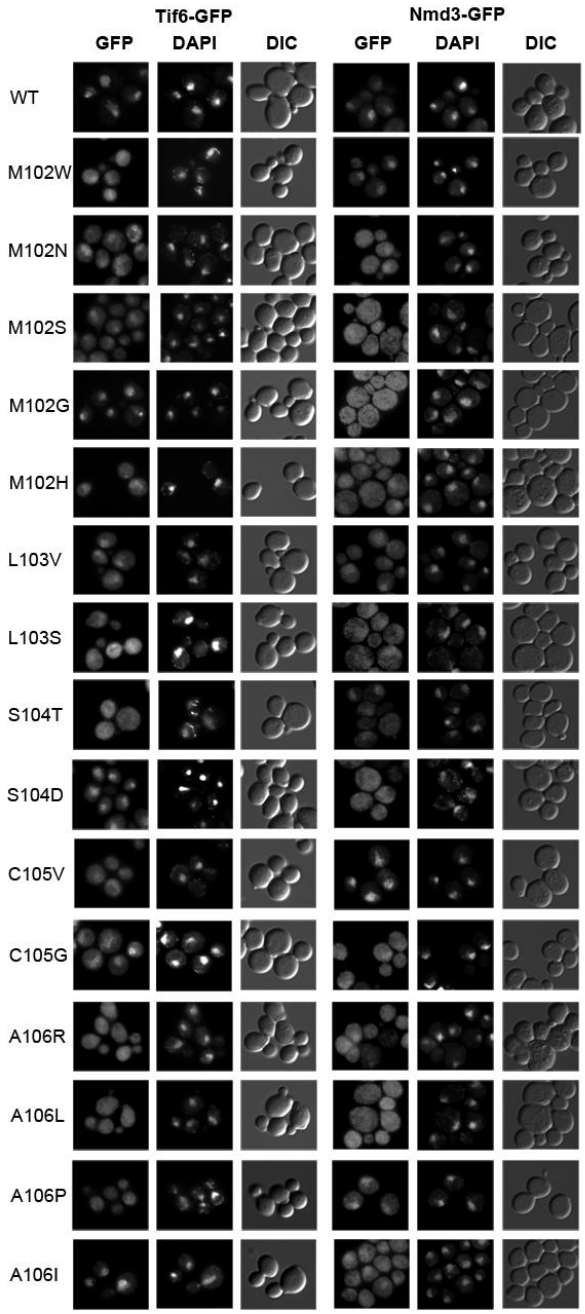

Figure 4.7 Localization of Nmd3 and Tif6 in Rpl10 P-site loop mutants
AJY2765 (*TIF6-GFP rpl10*Δ*::KanMX*) and AJY1837 (*NMD3-GFP CRM1-T539C rpl10*Δ*::KanMX*) containing wild-type (pAJ2522) or the indicated P-site loop mutants were prepared for microscopy as described in Materials and Methods. AJY1837 was incubated with LMB prior to fixing.

4.3.4 Mutations in *TIF6* suppress the biogenesis class of *rpl10* P-site loop mutants.

As shown above, *rpl10* loop mutants are defective for the release of Tif6 and its recycling to the nucleus. *EFL1*, encoding an eEF2-like GTPase, is also required for efficient release of Tif6 from the subunit (Becam et al., 2001; Senger et al., 2001). Dominant mutations have been identified in *TIF6* that suppress the severe growth defect of *efl1* mutants. These mutations weaken the affinity of Tif6 protein for the subunit, obviating the need for Efl1 (Becam et al., 2001; Menne et al., 2007; Senger et al., 2001).

Tif6 mutant suppresses the growth defect of the biogenesis class of Rpl10 P-site loop mutants

I asked if one such mutant, *TIF6-V192F*, could suppress the effects of the *rpl10* P-site loop mutations. Remarkably, *TIF6-V192F* suppressed the growth defect of the biogenesis mutants (*rpl10-S104D* and *C105G*) but not Class II mutants (*rpl10-A106R* and *L103S*) (Fig 4.8).

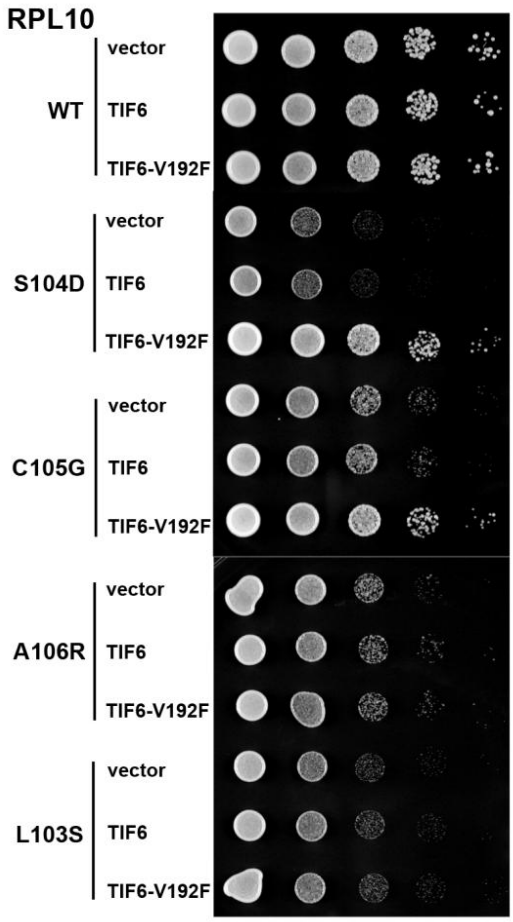

Figure 4.8 Growth suppression of Rpl10 P-site loop mutants by Tif6-V192F

The *rpl10* deletion strain (AJY1437) containing wild-type (pAJ2522) or mutant *RPL10* and either vector (pRS413), wild-type *TIF6* (pAJ2543) or *TIF6-V192F* (pAJ2544) were grown in selective media and ten-fold serial dilutions were spotted onto plates and incubated 2 days at 30°C.

Tif6 mutant suppresses Class I Rpl10 P-site loop mutant polysome defect

This suppression of growth was reflected in improved polysome profiles of the *rpl10* biogenesis mutants, indicated by the loss of halfmers and increased polysome levels (Fig 4.9).

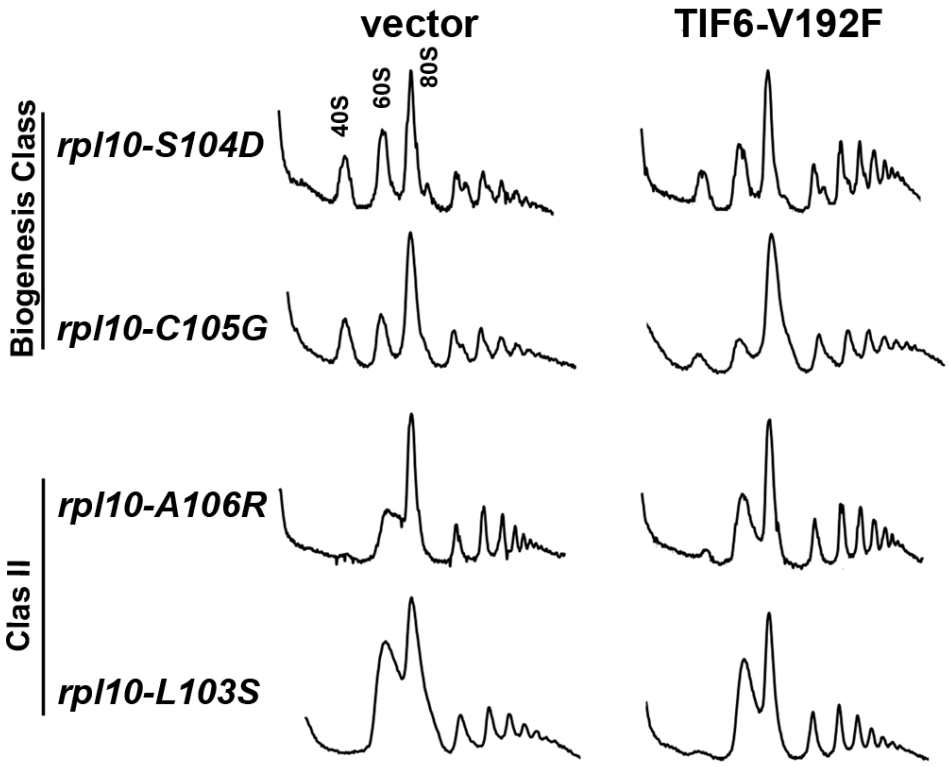

Figure 4.9 Tif6-V192F suppresses class I mutant polysome defect
Extracts were prepared from the *rpl10* deletion strain (AJY1437) containing *rpl10* P-site loop mutants and either Vector (pRS413) or *TIF6-V192F* (pAJ2544) and sedimented through 7-47% sucrose density gradients. A_{260} was monitored along the gradient.

Tif6-V192F recycles in Class I Rpl10 P-site loop mutants

I also monitored the localization of wild-type Tif6 or Tif6-V192F in these strains. Tif6-V192F recycled to the nucleus in the *rpl10* biogenesis mutants *rpl10-S104D* and *C105G*, which it suppressed, but not in the Class II mutants *rpl10-A106R* and *L103S*, which it did not suppress (Fig 4.10). The suppression of *rpl10-S104D* and *C105G* by *TIF6-V192F* implies that the primary defect in the biogenesis class of mutants is caused by the persistence of Tif6 on the large subunit.

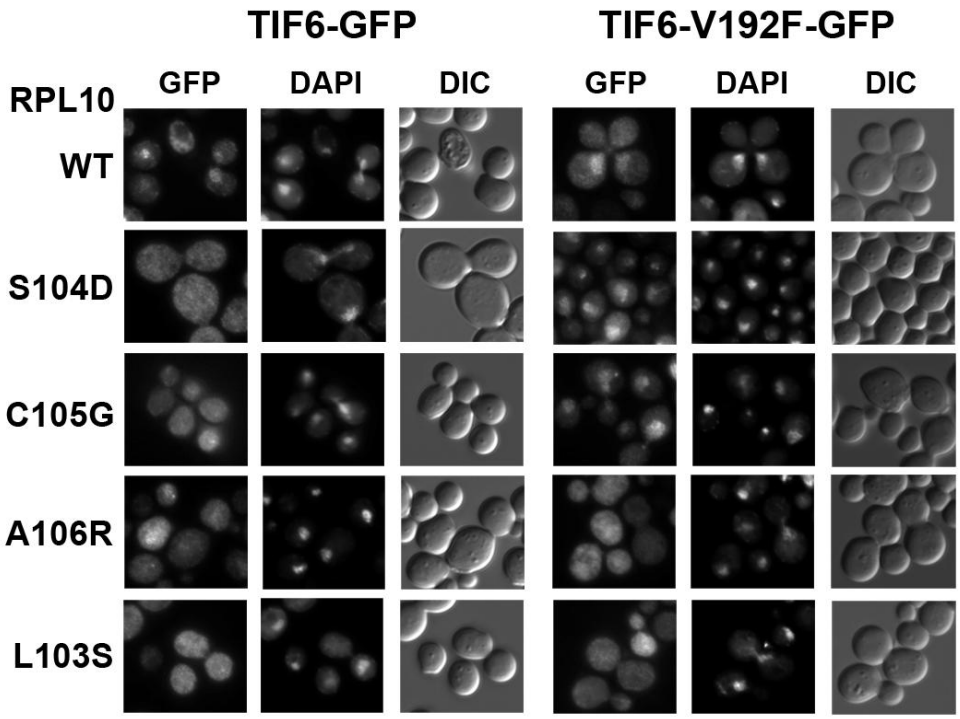

Figure 4.10 Tif6-V192F recycles in Class I Rpl10 P-site loop mutants
The *rpl10* deletion strain (AJY1437) containing wild-type (pAJ2522) or mutant *RPL10* and vector harboring either wild-type *TIF6-GFP* (pAJ1004) or *TIF6-V192F*-GFP (pAJ2654) were grown in selective media. Cells were fixed with formaldehyde and stained with DAPI prior to visualization.

4.3.5 Rpl10 is independently involved in release of Tif6 and Nmd3 from the large subunit.

Mutations in the P-site loop of Rpl10 prevent the release of both Tif6 and Nmd3. Because the release of Tif6 is required for the subsequent release of Nmd3 (Lo et al., 2010), mutations in the P-site loop of Rpl10 may only indirectly impinge on the release of Nmd3.

Rpl10 P-site loop is specifically required for release of Tif6

I monitored the localization of Nmd3 in *rpl10* P-site loop mutants containing vector, wild-type *TIF6* or the suppressing allele, *TIF6-V192F*. These strains also contained the LMB-sensitive *crm1-T539C* mutation. In the biogenesis mutant *rpl10-S104D*, Nmd3 recycled to the nucleus only in the presence of *TIF6-V192F* (Fig 4.11). Because the recycling of Nmd3 was restored by mutant Tif6, the effect of *rpl10-S104D* on Nmd3 recycling is likely an indirect consequence of blocking Tif6 release, upstream of Nmd3 release. In the Class II mutant *rpl10-A106R* Nmd3 localization was not altered by the presence of *TIF6-V192F* and remained cytoplasmic (Fig 4.11). These results demonstrate that the P-site loop of Rpl10 is needed specifically for the release of Tif6.

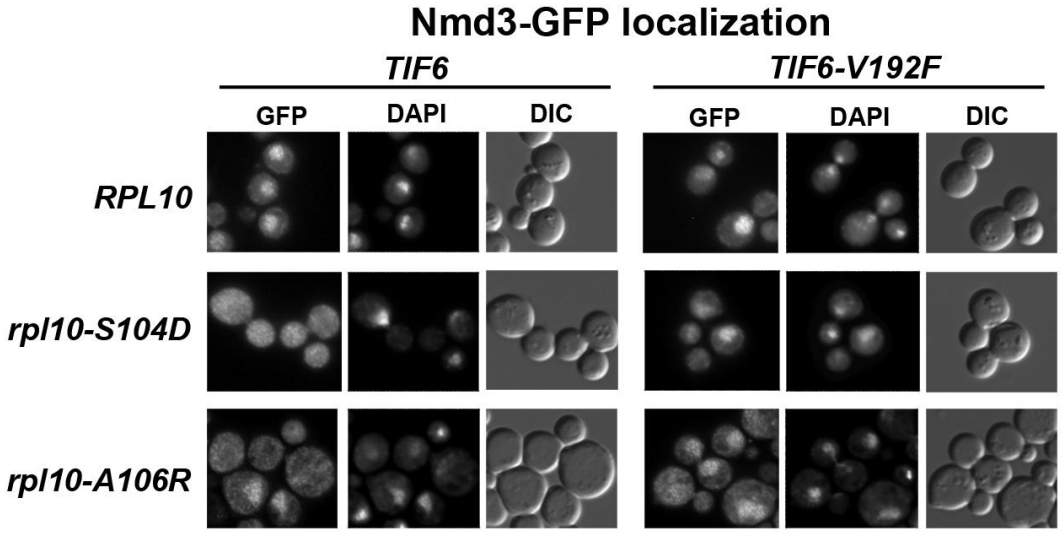

Figure 4.11 Tif6-V192F allows for release of Nmd3 from 60S subunit in Rpl10 Class I mutant

AJY1837 *(NMD3-GFP CRM1-T539C rpl10Δ::KanMX*) containing wild-type (pAJ2522) or mutant *RPL10* and wild-type (pAJ2543) or mutant *TIF6* (pAJ2544) were grown in selective media to mid-log phase and treated with LMB prior to fixation and preparation for microscopy.

Rpl10 P-site loop is independently involved in Tif6 and Nmd3 release from the 60S subunit,

The result that the P-site loop of Rpl10 indirectly affects the release of Nmd3 appears contradictory to previously published results which suggest that Rpl10 is required for the release of Nmd3. Those experiments used depletion of Rpl10 as well as point mutations in Rpl10 that could be suppressed by mutations in Nmd3 that weakened its affinity for the ribosome (Hedges et al., 2005; Hofer et al., 2007). My current results raise the possibility that Rpl10 affects Nmd3 only indirectly, through the release of Tif6. To distinguish between these possibilities I tested for allele-specificity of genetic interaction using the temperature-sensitive *rpl10-G161D* mutant, which is suppressed by *NMD3-I112T,I362T* (Hedges et al., 2006). I introduced wild-type copies of *TIF6* or *NMD3* or the suppressing alleles *TIF6-V192F* and *NMD3-I112T,I362T* in *rpl10-G161D*, *rpl10-S104D* and *rpl10-A106R* strains. I observed strong allele-specificity: *rpl10-G161D* was suppressed only by *NMD3-I112T,I362T,* whereas *rpl10-S104D* was suppressed only by *TIF6-V192F* and not by the *nmd3* mutant. *rpl10-A106R* was not suppressed by either *TIF6* or *NMD3* alleles (Fig 4.12 A). In accordance with these results *rpl10-G161D* relocalized an Nmd3 NES mutant to the cytoplasm but did not affect Tif6 localization. These results show that Rpl10 has separate functions in the release of Tif6 and Nmd3 (Fig 4.12B).

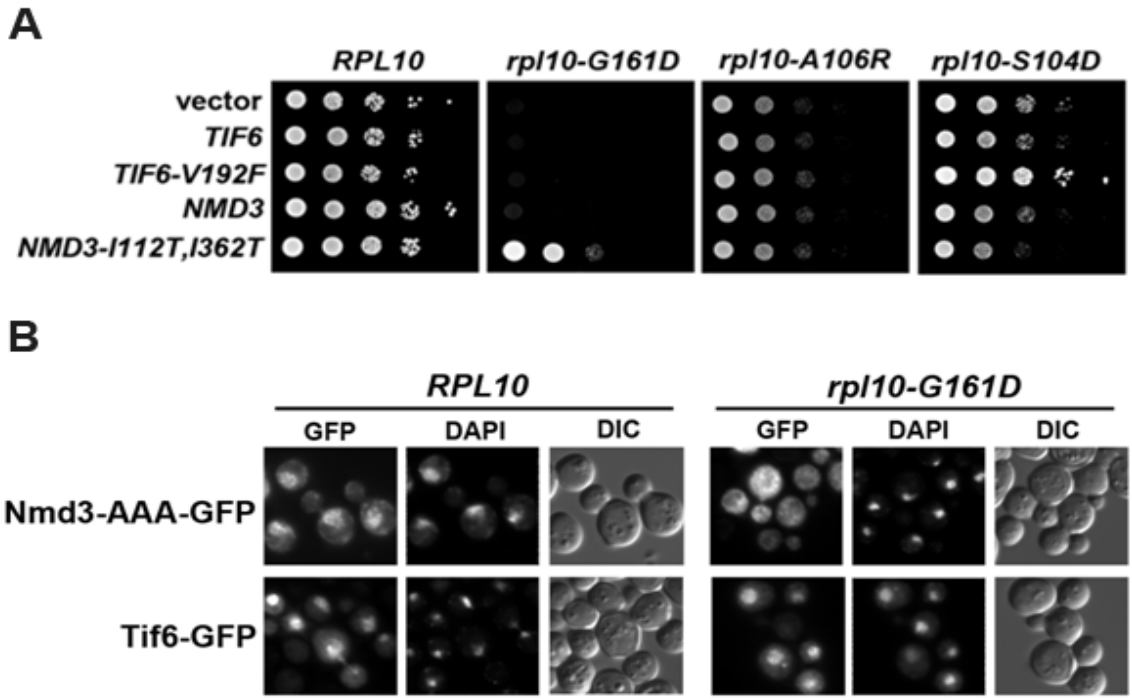

Figure 4.12 Rpl10 is independently involved in release of Tif6 and Nmd3 from the large subunit.
(A) AJY1657 (*rpl10-G161D*) and AJY1437 with wild-type (pAJ2522) or mutant Rpl10 were transformed with vector (pRS416), wild-type (pAJ2665) or mutant (pAJ2240) *TIF6* or wild-type (pAJ2652) or mutant (pAJ2653) *NMD3*. The strains were grown in selective media, ten-fold serial dilutions were spotted on plates and incubated for two days at 30°C. (B) *rpl10-G161D* affects Nmd3 release specifically. W303 or AJY1657 (*rpl10-G161D*) were transformed with pAJ758 (*nmd3AAA-GFP*) or pAJ1004 (*TIF6*-GFP). The cells were grown to mid-log phase, fixed with formaldehyde, and stained with DAPI prior to microscopy.

4.3.6 Mutations in *EFL1* suppress *rpl10* P-site loop mutants.

Mutations in EFL1 suppress rpl10 P-site loop mutants growth phenotype.

The functional interaction between Rpl10 and Tif6 suggests the presence of molecular signaling in the ribosome from the P-site loop of Rpl10 to Tif6 in the region of the SRL and Rpl23 (Gartmann et al.). Efl1 is a GTPase that is closely related to the translation factor eEF2 (Becam et al., 2001) that promotes ribosome translocation. I reasoned that if Efl1 is involved in signaling from Rpl10 to Tif6 then I should be able to find dominant mutations in Efl1 that would be activated for the release of Tif6 regardless of the status of Rpl10. To isolate such mutants, I carried out a random mutagenesis of *EFL1* and screened for mutants that could suppress the growth defect of the biogenesis-specific mutant *rpl10-S104D*. I identified 16 *EFL1* mutants that suppressed, to various degrees, the slow growth of *rpl10-S104D* (Fig 4.13).

These mutants suppressed only the biogenesis class of P-site loop mutants; no suppression of the growth defect of *rpl10-A106R* was observed (Fig 4.14), similar to the specificity of suppression by *TIF6-V192F*.

The level of suppression of the slow growth phenotype of *rpl10-S104D* by the mutant *EFL1-F250S,A669G* was comparable to that of *TIF6-V192F* (Fig 4.15) and approached the growth of wild-type.

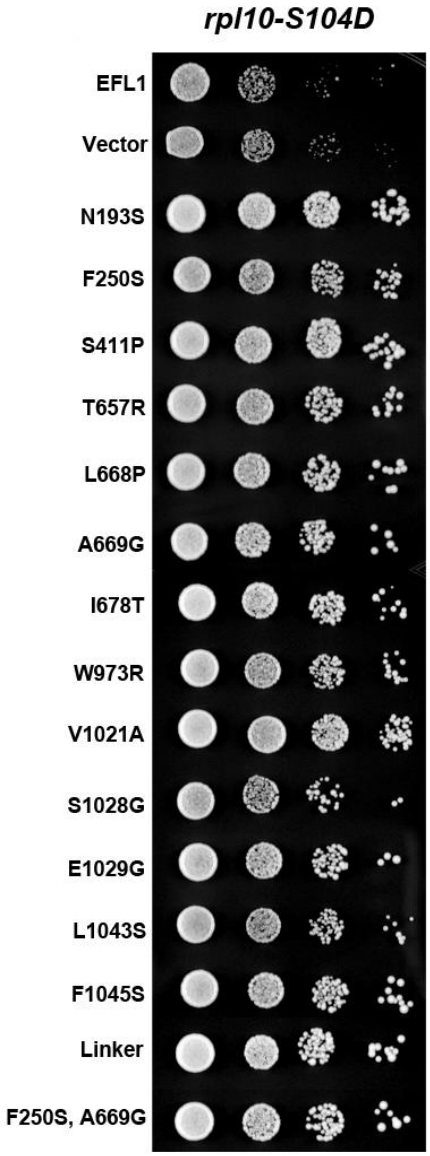

Figure 4.13 Efl1 mutants suppress Rpl10 P-site loop mutant *rpl10-S104D*.
AJY1437 (*rpl10*Δ*::KanMX*) with *rpl10-S104D* and either vector (pRS416), wild-type (pAJ2545) or suppressing allele of *EFL1*, was grown in selective media. Serial dilutions were spotted on plates and grown for two days at 30°C.

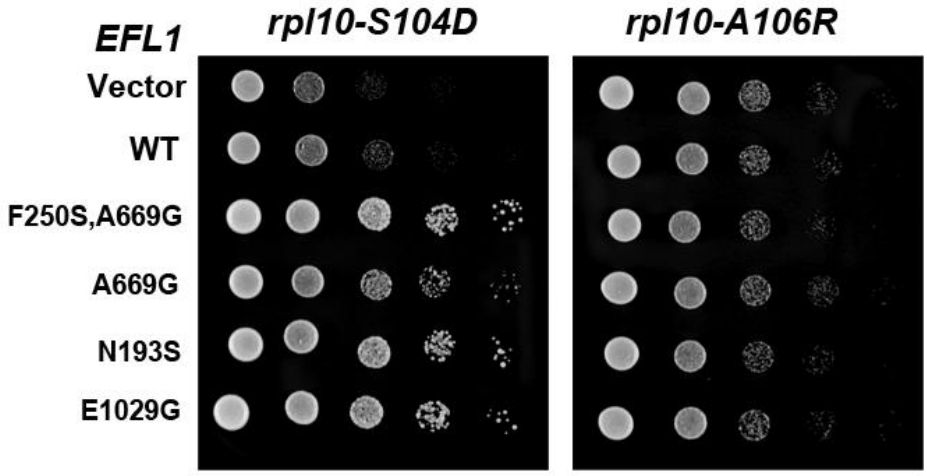

Figure 4.14 Efl1 mutants suppress specifically Class I Rpl10 P-site loop mutant *rpl10-S104D*.
AJY1437 (*rpl10*Δ*::KanMX*) with *rpl10-S104D* or *rpl10-A106R* and either vector (pRS416), wild-type (pAJ2545) or suppressing allele of *EFL1*, was grown in selective media. Serial dilutions were spotted on plates and grown for two days at 30°C.

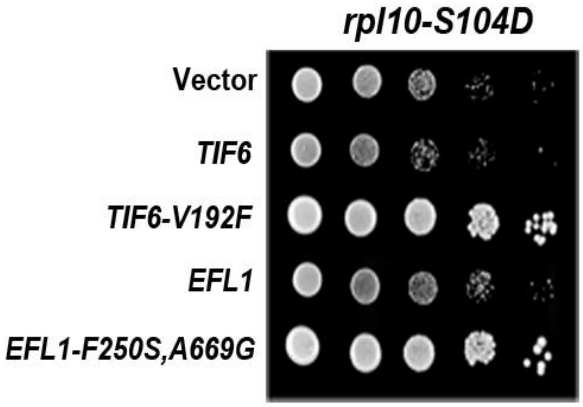

Figure 4.15 Comparison of Efl1 and Tif6 mutant alleles suppression of *rpl10-S104D* AJY1437 (*rpl10*Δ*::KanMX*) with *rpl10-S104D* and either vector (pRS416), wild-type (pAJ2543) or suppressing alleles of *TIF6* (pAJ2544) or wild-type (pAJ2545) or suppressing allele of *EFL1*, was grown in selective media. Serial dilutions were spotted on plates and grown for two days at 30°C.

Mutations in EFL1 suppress rpl10 P-site loop Class I mutants polysome profile defect.

Suppression was also observed in the polysome profiles of these strains; the halfmer phenotype of *rpl10-S104D* was alleviated and the level of polysomes was increased (Fig. 4.16). These *EFL1* alleles did not improve the polysome profile of *rpl10-A106R* (Fig. 4.16), congruent with the lack of growth suppression of this mutant.

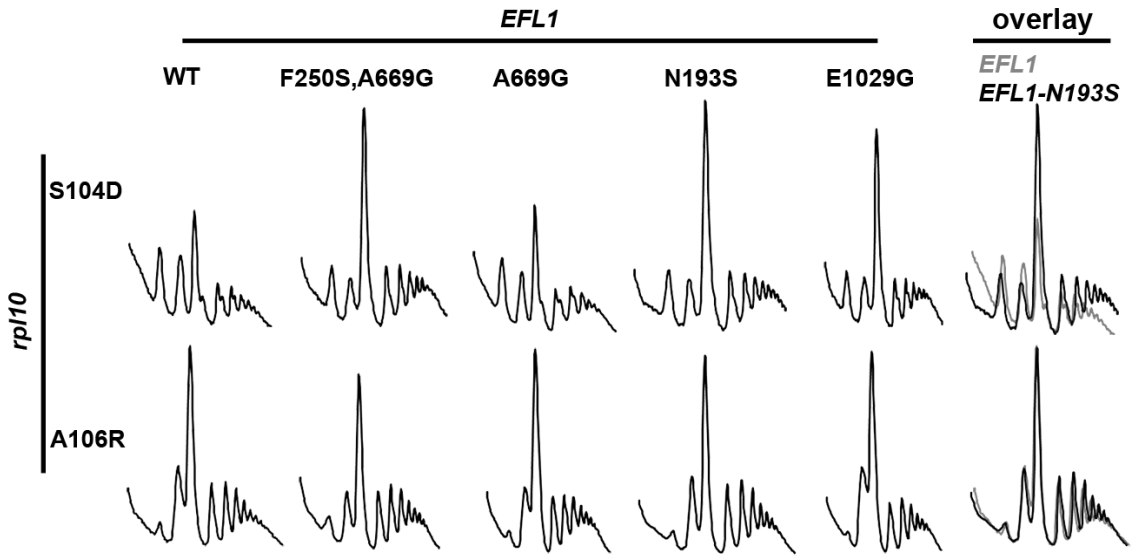

Figure 4.16 Efl1 mutants rescue the polysome defect of Class I Rpl10 P-site loop mutants specifically

AJY1437 *(rpl10Δ::KanMX*) with *rpl10-S104D* or *rpl10-A106R* with vector (pRS413), wild-type (pAJ2545) or mutant *EFL1*was grown in selective media to mid-log phase, incubated with 50µg/ml cycloheximide for 10 minutes and harvested on ice. Crude extracts were fractionated by sedimentation through 7-47% sucrose gradients. A_{260} was monitored along the gradient. Far right: for comparison, profiles for *rpl10-S104D* (upper) or *rpl10-A106R* (lower) with wild-type *EFL1* or *EFL1-N193S* were overlayed

Efl1 suppressor allows for release of Tif6 in Rpl10 P-site loop mutant.

The localization of Tif6 in an *rpl10-S104D* mutant strain was monitored in the absence or presence of an Efl1 suppressing mutant. Due to genetic interaction between the GFP tag on Tif6 and the suppressing alleles of Efl1 (data not shown) I monitored Tif6 localization via indirect immunofluorescence (IF). P_{GAL1}*-RPL10 TIF6-HA* with *rpl10-S104D* on a plasmid and either empty vector or a suppressing allele of Efl1 (*EFL1-F250S,A669G*) was grown in galactose and genomic Rpl10 expression was repressed for 4 hours by addition of glucose before visualization of Tif6 localization by IF. In the presence of empty vector, Tif6 is trapped in the cytoplasm as previously seen, while in the presence of a suppressing allele of Efl1 it is redistributed to the nucleus (Fig 4.17), indicating that the Efl1 suppressing alleles allow for the release of Tif6 regardless of the status of the P-site.

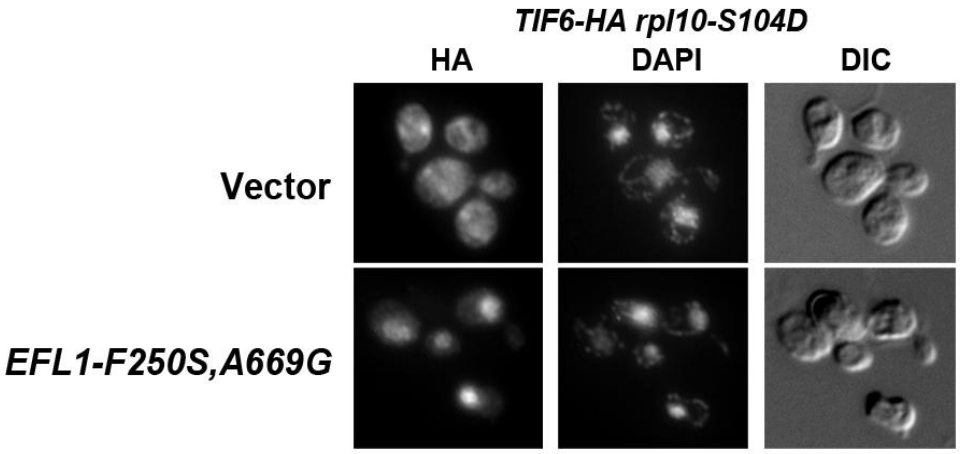

Figure 4.17 Efl1 suppressor allows for release of Tif6 independently of Rpl10 P-site loop status

AJY2770 (*P_{GAL1}-RPL10 TIF6-3xHA)* containing *rpl10-S104D* and either empty vector (pRS413) or a suppressing allele of *EFL1* (*EFL1-F250S,A669G*) was grown to mid-log phase in galactose and expression of genomic *RPL10* was repressed by addition of glucose for 4 hours, revealing the *rpl10-S104D* phenotype. Localization of TIF6-3xHA was monitored by indirect immunofluoresence using an anti-HA antibody (see Materials and Methods).

These data argue for a role of the Rpl10 P-site loop in Efl1 mediated release of Tif6. I suggest that the status of the P-site is probed by Efl1, activating its GTPase activity and resulting in release of Tif6. Mutations in the P-site loop that disrupt Efl1 signaling could be suppressed by mutations in Tif6 that enable its release from the ribosome independently of Efl1 (e.g. Tif6-V192F) or by mutations in Efl1 that render its activation independent of upstream signaling. The proposed molecular pathway can be seen in Illustration 4.3, with a P-site tRNA as a place-holder for the P site.

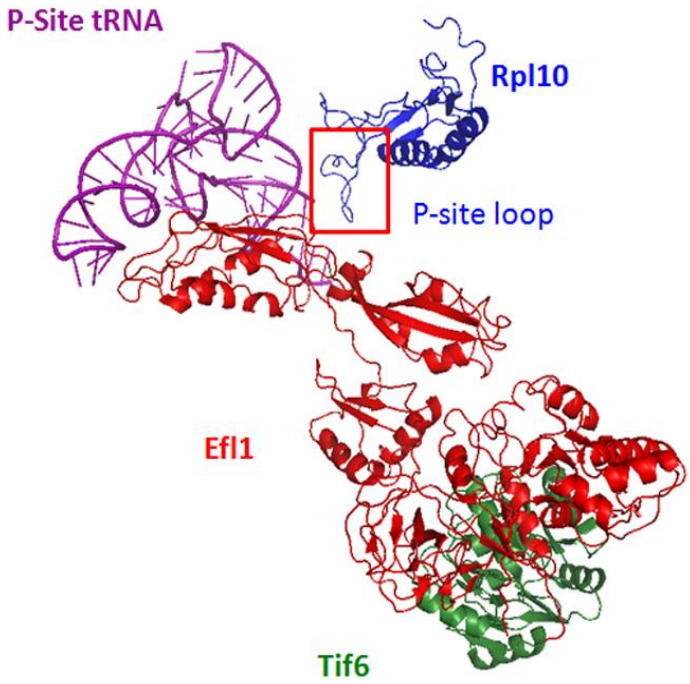

Illustration 4.3 Ribbon diagram of the molecular linkage between the P-site loop of Rpl10 and Tif6.
L16 in blue, P-site tRNA in purple, EF-G in red and yeast Tif6 in green. PBD accession numbers: 2WRI/2WRJ (Goa et al) and 2X7N (Gartmann et al). The red box highlights the P-site loop of Rpl10. Derived from Fig 4.3.

4.3.7 Efl1 mutations induce a conformational change similar to conformational change the translocase undergoes during translocation.

To better understand how Efl1 mutants suppress Rpl10 P-site loop mutants I modeled the *EFL1* suppressor mutations on the structure of eEF2 (Fig 4.18). eEF2 is a multidomain protein that undergoes a large conformational change that is thought to drive ribosome translocation (Jorgensen et al., 2003). The anti-fungal translation inhibitor sordarin inserts between domains III and V and traps eEF2 in a post-translocation conformation (Jorgensen et al., 2003; Spahn et al., 2004). Similarly, fusidic acid traps bacterial EF-G on the ribosome in a post-translocation state, although it binds in a different subunit interface (Agrawal et al., 1998; Ermolenko et al., 2007; Gao et al., 2009; Spahn et al., 2004). One cluster of *EFL1* suppressing mutations (S411P, T657R, L668P, A669G) mapped to domain II at the interface with domain III while I678T mapped to the same interface but in domain III. One additional mutation in this region arose from a 36 base-pair DNA inversion, altering amino acids 664 to 675 that comprise the linker between domains II and III. Crystal structures of bacterial EF-G in complex with fusidic acid reveal that it binds in the interface of domains II and III, although at a position offset from the *efl1* suppressing mutations (Agrawal et al., 1998; Gao et al., 2009). A second cluster of mutations (W973R, V1021, S1028G, E1029G, L1043S, F1045S) mapped to domain V at the interface with domain III. These mutations correspond in position to the sordarin binding site in eEF2(Jorgensen et al., 2003; Spahn et al., 2004). Notably, these mutations map to dynamic domain interfaces that are involved in the conformational

change that eEF2 undergoes during translocation. Mutations in these domain interfaces could favor a conformation change in Efl1 required for its activity and normally induced by signaling from the P-site. Thus by shifting the equilibrium between two conformations and favoring an eEF2-post-translocation-like conformation, the Efl1 suppressor mutations could allow for release of Tif6 independently of the status of the P-site. A couple of other mutations, namely N193S and F250S (subcloned form *EFL1-F250S,A669G*) mapped in domain one of Efl1. F250S lays in the G' subdomain of Efl1. In EF-G the G' subdomain interacts with the stalk and is involved in activation of GTP hydrolysis (Nechifor et al., 2007). A mutation in this domain might activate GTP hydrolysis independently of signaling from the P-site and similarly, albeit in a different fashion from the other suppressing mutations, induce release of Tif6. N193S lays in an Efl1-specific loop not conserved in eEF2 or EF-G but could suppress Rpl10 mutations in a fashion similar to that of F250S

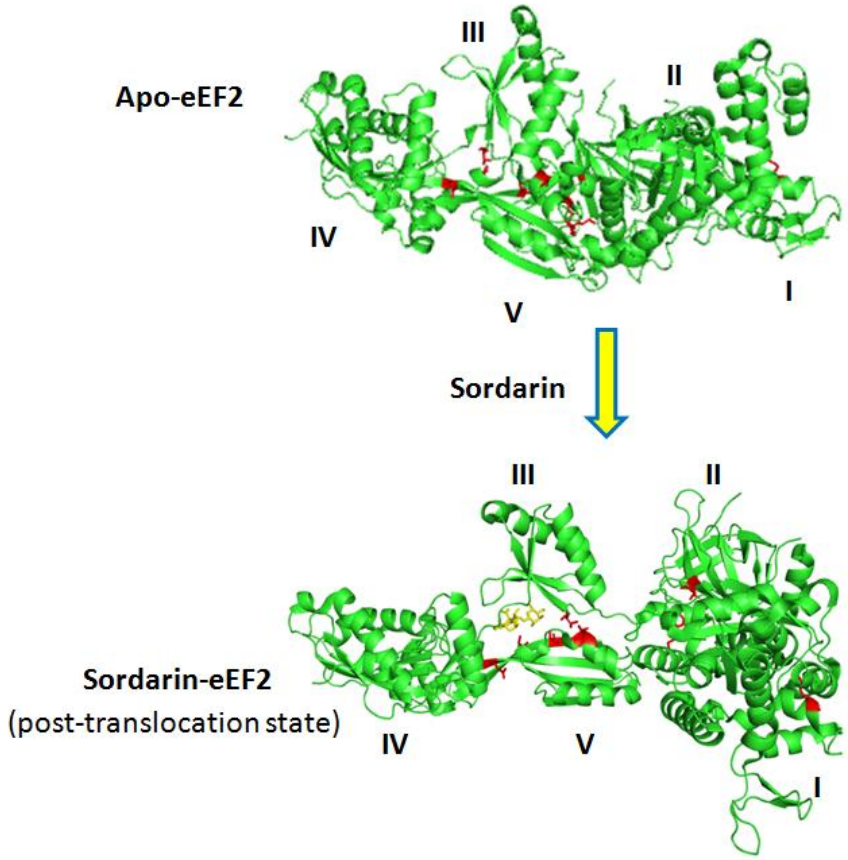

Figure 4.18 Efl1 suppressor mapped to the apo and sordarin-bound structures of eEF2.

Apo- (top) and sordarin- (bottom) bound structures (adapted from PDB 1NOU/1NOV(Jorgensen et al., 2003)) with Efl1 suppressing mutations in red. Yellow: Sordarin. Efl1 domains are indicated in roman numeral.

4.3.8 Modeling of Efl1 and Suppressing Efl1 mutants

Modeling Efl1

In order to further support the model that the *rpl10-S104D* suppressing mutations in Efl1 induce a conformation change in Efl1 during biogenesis similar to changes observed in translocases during translocation, I collaborated with Yasser Hashem from the Dr Joachim Frank's laboratory (Columbia University). Yasser built atomic models of Efl1 by homology to eEF2 in two different conformations, apo eEF2 and sordarin-bound eEF2 (Derek J Taylor, 2007; Jorgensen et al., 2003). As mentioned above, sordarin traps eEF2 in an extended conformation that mimics an intermediate of translocation. I refer to the corresponding conformation of Efl1 as "translocational". As expected, modeled Efl1 in the apo and translocational forms is similar to eEF2 in the apo and sordarin-bound forms. The apo and translocational conformations display changes in the interfaces between domains III and V and between domains III and II (Fig 4.19).

As expected, most of the Efl1 mutations that suppress the P-site loop mutant *rpl10-S104D* map to dynamic domain interfaces that are involved in the conformational change that eEF2 and EF-G undergo during translocation. I678T in domain III and W973R, V1021, S1028G, E1029G, L1043S and F1045S in domain V, mapped to the hydrophobic core of the III-V interface (Fig 4.20) while S411P, T657R, L668P and A669G mapped to domain II at the hydrophobic core of the III-V interface.

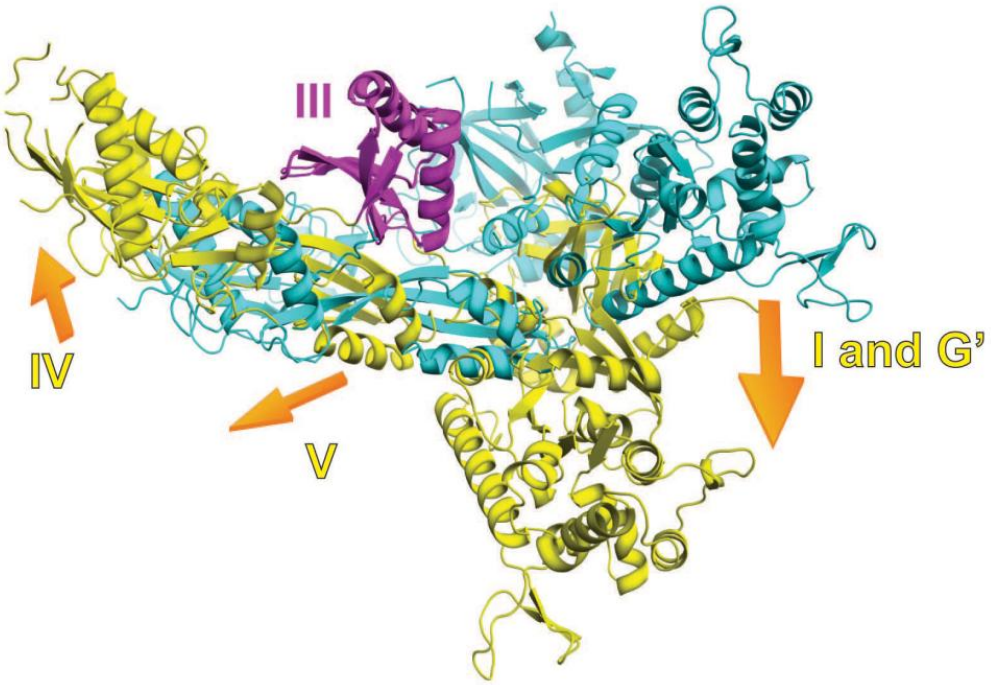

Figure 4.19 Efl1 models in the apo and post-translocational conformations
A superimposition on domain III (in purple) of Efl1 in two conformations, the apo (in cyan) and the post-translocational (in yellow) conformations. The orange arrows indicate the direction of movement of domains I, G', IV and V, relative to domain III, in the post-translocational conformation. The inserts unique to Efl1 are not displayed.

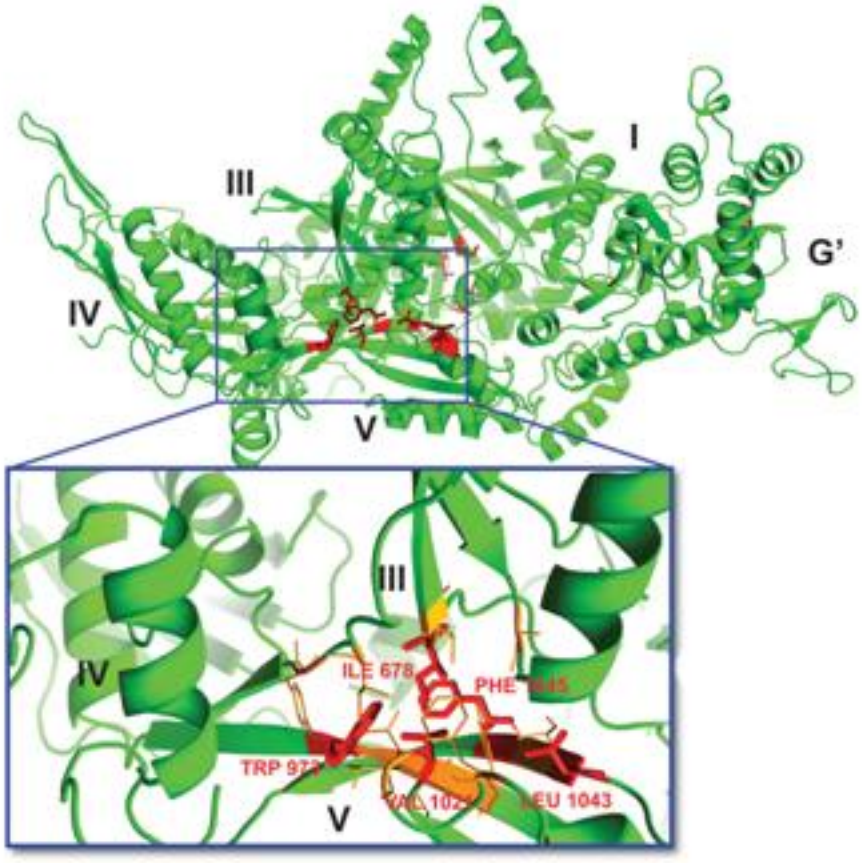

Figure 4.20 Efl1 suppressor mutations mapped on the Efl1 model in the apo conformation.
Efl1 model in the apo conformation, residues in red highlight the positions of single-residue mutations that suppress *rpl10-S104D*. Box: zoom on the hydrophobic core of domains III and V of Efl1 in the apo conformation. Residues in red sticks are the inner residues of the hydrophobic core and designate the positions of the single-residue mutations. Residues in orange lines are additional hydrophobic residues surrounding the inner residues of the hydrophobic core.

efl1 suppressor mutations disrupt domain interfaces that promote conformational changes in eEF2.

To investigate the hypothesis that the mutations in Efl1 promote a conformational change, Yasser studied the hydrophobic-core mutations by molecular dynamics simulations in explicit solvent. He first built a reduced model that comprised domains III and V, and part of domain IV of wild-type Efl1 in the apo conformation. He then introduced mutations that affect the innermost residues of the hydrophobic core, at the interface between domains III and V. His results are summarized in figure 4.21, for one of the mutants, *EFL1-V1021A*. In a nutshell, simulations of the dynamics of the interface between domains III and V show that each mutant disrupts the hydrophobic core of the interface, causing domain IV and V to pivot around domain III. This repositioning of domains IV and V in the mutant Efl1 proteins is analogous to that observed in the translocational eEF2 conformation. Thus, this molecular dynamics study strongly supports a model in which a shift in the equilibrium of Efl1 conformation toward the more extended translocational conformation promotes suppression of defects in the P-site loop of Rpl10.

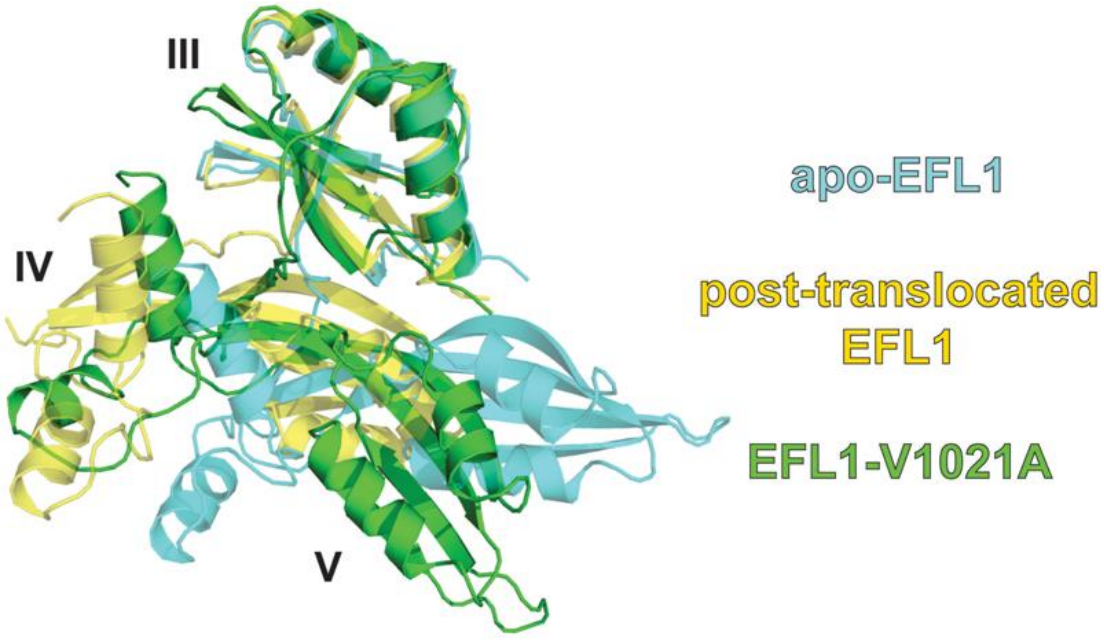

Figure 4.21 Efl1 suppressing mutations induce a conformation change analogous to change translocases undergo during translocation.
A superimposition on domain III of Efl1 in the apo (in blue), and post-translocational (in yellow) conformations, and of the suppressor mutant *efl1-V1021A* (in green). Only domain III, V and part of domain IV are shown.

4.3.9 Rpl10 P-site loop mutants affect translation

Rpl10 P-site loop mutant have a defect in translation

The data presented above provides compelling evidence of a molecular pathway existing between the P-site, in part made of Rpl10 P-site loop, and Tif6 via the translocase-like GTPase Efl1. The Rpl10 P-site loop Class I biogenesis mutants have a defect in release of Tif6 which can be suppressed by mutations in Efl1 or Tif6 which enable for release of Tif6 independently of upstream signaling. However, the Class II mutants, which also trap Tif6 in the cytoplasm, are not suppressed by Efl1 or Tif6 suppressing alleles. Considering the position of the P-site loop near the acceptor stem of the P-site tRNA, it is plausible that the Class II Rpl10 P-site loop mutants affect translation, possibly peptidyl transferase, and/or termination. In order to address this possibility, I monitored the effect of the Rpl10 P-site loop mutants on translation using a ribosome run off assay. Upon glucose depletion translation initiation is rapidly inhibited (Ashe et al., 2000). This allows one to monitor the rate of completion of translation in the absence of novel translation initiation. In this assay, translation initiation was inhibited by glucose depletion prior to treating cells with cycloheximide to trap translating ribosomes on mRNAs. Polysome profiles were then determined. The ratio of polysomes to monosomes before and after glucose depletion was calculated, enabling me to compare the relative polysome retention in wild-type versus mutant Rpl10 strains. Wild-type *RPL10*, *rpl10-S104D* or *rpl10-A106R* strains were grown in rich medium with glucose. Cells were collected with cycloheximide, or spun down, resuspended in glucose-free media,

incubated one or six minutes and collected with cycloheximide. Polysome profiles were determined (Fig 4.22 A) and levels of monosomes (80S) or polysomes calculated by integrating the area under the curves. Ratios of polysomes/monosomes were calculated for each profile and normalized to the ratio obtained in the presence of glucose (Fig 4.22 B). In wild-type Rpl10, one minute after glucose depletion a 70% decrease in polysome/monosome is observed, reaching 80% decrease six minutes after glucose depletion, indicating a 30 and 20% polysome retention after one and six minute glucose depletion respectively. In contrast, in the case of the Class II Rpl10 P-site loop mutant *rpl10-A106R*, a 68 and 40% polysome retention is observed after one and six minute glucose depletion, respectively. This increased polysome retention indicates that in the *rpl10-A106R* strain ribosomes stay on mRNAs longer than ribosomes in wild-type Rpl10 strain. Such a translation defect, resulting in polysome retention, could be due either to a defect in elongation, leading to ribosomes translating slower and hence taking longer to transit along an mRNA, or to a termination defect, similarly leading to an increase of retention of ribosomes on mRNAs. Surprisingly, the Class I biogenesis mutant *rpl10-S104D*, exhibited a more severe translation defect, with 83 and 68% polysome retention after one and six minute glucose depletion respectively.

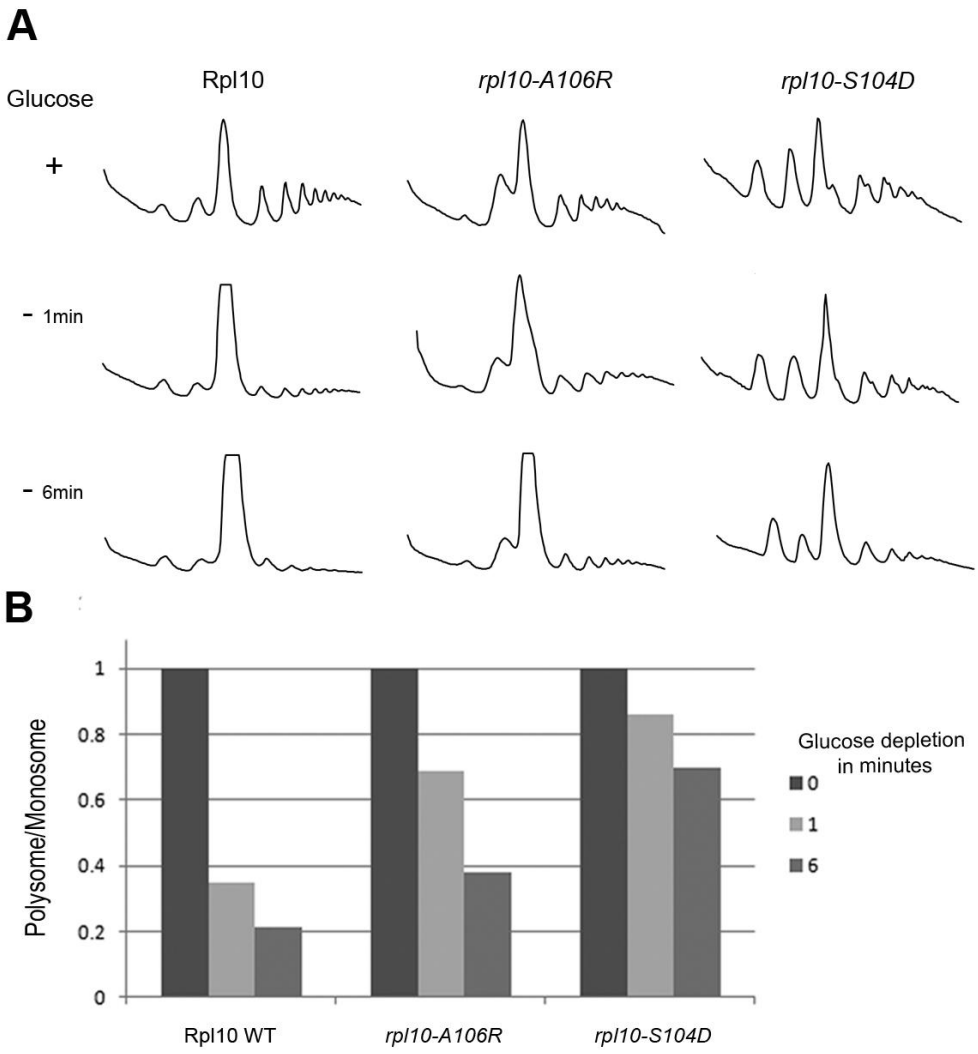

Figure 4.22 Rpl10 P-site loop mutants exhibit a translation defect
(A) AJY1437 (Rpl10::Kan) with wild-type or mutant Rpl10 was grown in selective media with 2% glucose. At mid-log media was exchanged for selective media without carbon source. At time 0, 1 or 6 minutes after glucose depletion 50µg/ml cycloheximide was added to the culture. Crude extracts were made and ran over 7-47%sucrose gradients. A_{260} was monitored across the gradient. (B) Quantification of the experiment in A. Polysome over free 80S ratio was standardized to $t_{0.}$

Rpl10 class I P-site loop mutant translation defect is suppressed by Efl1 and Tif6 mutants

It would appear that the Rpl10 P-site loop mutants affect both biogenesis (trapping Tif6 and Nmd3 on cytoplasmic subunits) and translation (polysome retention). The Class I biogenesis mutant *rpl10-S104D* growth defect is equally well suppressed by Tif6 and Efl1 mutants, restoring growth to almost wild-type levels (Fig 4.17), while the Class II mutant *rpl10-A106R* is not suppressed by these Efl1 and Tif6 alleles. The translation defect of *rpl10-S104D* is severe and would most likely result in a significant growth impairment, however, as mentioned above suppression by Efl1 or Tif6 mutants restore close to wild-type growth levels in this Rpl10 mutant, suggesting that these Efl1 and Tif6 alleles also suppress the translation defect observed. Indeed the translation defect of *rpl10-S104D* is completely resolved in the presence of either EFL1-F250S,A669G or TIF6-V192F (Fig 4.23 A) In the *rpl10*-S104D strain, in the presence of vector only, after three minutes glucose depletion, a 74% polysome retention is observed, however in the presence of either Efl1 or Tif6 suppressing allele, the polysome retention decreased to close to 20%, comparable to the polysome retention observed in wild-type Rpl10 strains (Fig 4.23 B). In contrast to the Class I biogenesis mutant, the Class II mutant *rpl10-A106R* did not show a change in polysome retention in the presence of Efl1 or Tif6 mutants, in agreement with the lack of growth suppression.

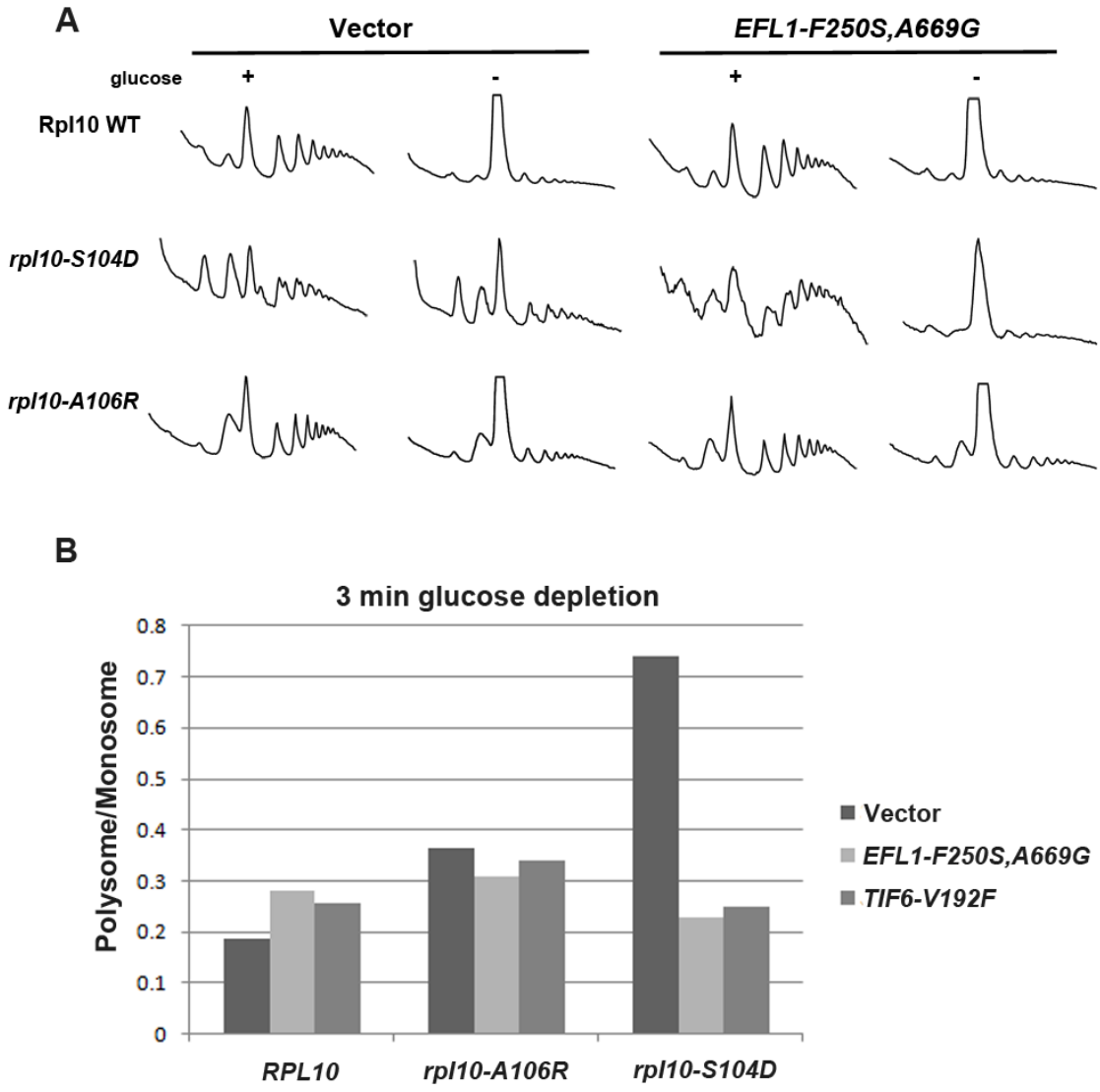

Figure 4.23 Rpl10 P-site loop biogenesis mutant translation defect is suppressed by Tif6 or Efl1 mutant

(A) AJY1437 (Rpl10::Kan) with wild-type or mutant Rpl10 and Vector or suppressing Efl1, treated as in Fig 4.25. Glucose was depleted for 3 minutes before addition of cycloheximide. (B) Quantification of AJY1437 (Rpl10::Kan) with wild-type or mutant Rpl10 and Vector or suppressing Efl1 or Tif6, treated as in Fig 4.25. Polysome over free 80S ratio was standardized to $t_{0.}$ polysome/monosome ratios for t_{3min} are shown.

Given the position of the P-site loop of Rpl10, close to the P-site tRNA, it is not surprising that the Rpl10 P-site loop mutants affect translation. However, the fact that a translation defect can be suppressed by mutations in ribosome biogenesis factors is surprising. Furthermore, this argues that in the case of the Class I Rpl10 P-site loop mutants, it is not the mutation in the P-site loop itself which directly causes the translation defect, since even when suppressed, the mutated P-site loop is still present in the ribosome, but rather an indirect effect linked to the release of Tif6. I reasoned that the impaired release of a biogenesis factor (for example Tif6 or Nmd3) from the maturing 60S subunit could lead to the persistence of that factor on the translating ribosome, somehow perturbing the proper functioning of the translation machinery and resulting in a translation defect. To test this possibility crude extracts from wild-type Rpl10, *rpl10-S104D* and *rpl10-A106R* strains were analyzed by sucrose gradients sedimentation and the presence of Tif6, Nmd3 and the Lsg1 was monitor along the gradient. The sedimentation pattern of these factors was similar in wild-type and mutant Rpl10 strains, indicating that the translation defect observed in the Rpl10 P-site loop mutants is not due to one of these factors persisting on 60S subunits during translation (data not shown).

4.4 Discussion

Here, I provide compelling evidence that maturation of the large ribosomal subunit involves extensive probing of the structure and function of the nascent subunit. I showed that the large ribosomal protein Rpl10 and more specifically its

unstructured P-site loop is involved in relaying information about the state of the ribosome via the P-site to the GTPase Efl1, resulting in release of Tif6.

4.4.1 The P-site loop of Rpl10

The P-site loop of Rpl10 is conserved. In archaeal 50S crystal structure the P-site loop is not resolved indicating that it is unstructured (Ban et al., 2000). Recently, a high-resolution cryo-EM reconstruction of the translating eukaryotic ribosomes revealed the P-site loop of Rpl10 extending toward the acceptor stem of the P-site tRNA (Armache et al., 2010b). In contrast to eukaryotes and archaea, the P-site loop of L16 (the prokaryotic ortholog of Rpl10) is shorter. In accordance with this, crystal structures of bacterial 50S (Gao et al., 2009; Schmeing et al., 2009) reveal the P-site loop of L16 not extending as far as the eukaryotic P-site loop. A bacterial-specific ribosomal protein, L27, threads through 50S, runs parallel to the P-site loop and fills the space between the L16 P-site loop and the P-site tRNA. It would appear that the longer P-site loop of eukaryotic Rpl10 has evolved to compensate for the loss of L27. Recent structures of bacterial ribosomes in pre- and post-peptidyl transfer states suggest that the N-terminus of protein L27 stabilizes the acceptor stems of both A and P-site tRNAs (Voorhees et al., 2009). This is consistent with the observations that L27 can be cross-linked to the 3'-ends of tRNAs in bacteria (Kirillov et al., 2002) and that the absence of L27 leads to reduced peptidyl transferase activity (Maguire et al., 2005). Presumably the role of L27 is fulfilled by the elongated P-site loop of Rpl10 in eukaryotes, though this remains to be demonstrated.

4.4.2 Rpl10 P-site loop Class II mutants

The polysome profile of Class I Rpl10 P-site loop mutants exhibit half-mers, indicative of a large ribosomal subunit biogenesis or subunit joining defect. These mutants trap Tif6 on the subunit in the cytoplasm, which indirectly leads to a lack of release of Nmd3. Mutations in Tif6 or Efl1 can suppress this class of mutants by inducing release of Tif6 independently of signaling from the P-site. Mutants of the second class similarly trap Tif6 and Nmd3 in the cytoplasm but are not suppressed by mutations in Tif6 or Efl1. Furthermore, they prevent release of Tif6-V192F, which bypasses the Tif6 release block in the Class I mutants. The Class II mutants clearly affect biogenesis but somehow this defect is not reflected in their polysome profiles which exhibit an unusually high free 60S peak, a very low free 40S peak, polysome levels comparable to wild-type and a lack of half-mers. Class II mutants could affect Tif6 release in a way similar to the Class I mutants, albeit more severely, or possibly in an as-of-yet unknown fashion – the later being supported by the unusual Class II mutants polysome profiles.

4.4.3 What occupies the P-site during biogenesis?

Crystal structure of translating ribosome shows the P-site loop of L16 in close proximity to the acceptor stem of the P-site tRNA and domain IV of EF-G in contact with the anticodon loop of the P-site tRNA (Fig 4.20)(Gao et al., 2009). It seems likely that during translation the P-site loop of Rpl10 communicates with eEF2/EF-G via a tRNA present in the P site. The question then is: what is in the P site during

biogenesis? The data presented in this chapter suggests that during biogenesis the P-site loop of Rpl10 conveys information to Efl1 about the state of the P site. This could occur via a tRNA in the P site, either as a standalone tRNA or as part of the 48S initiation complex, which would imply that the last steps of biogenesis (Tif6 and Nmd3 release) occur during subunit joining. A tRNA would seem to be the ideal substrate for testing the function of the ribosome and could facilitate assembly of the P site. Alternatively, another factor could be located in the P-site in lieu of a tRNA, but playing the same role of relaying information from the P-site of Rpl10 to Efl1. Sdo1 is required for release of Tif6 alongside Efl1 (Menne et al., 2007). The structure of human and archaeal Sdo1 has been solved (de Oliveira et al., 2010; Savchenko et al., 2005; Shammas et al., 2005) and has been likened to that of a tRNA (Ng et al., 2009). Thus, Sdo1 could act as a tRNA mimic, to test the P site for tRNA binding and, perhaps for its ability to support tRNA translocation.

4.4.4 Efl1 is a eukaryote-specific factor.

Efl1 appears to have evolved from the translation elongation factor eEF2 as a specialized factor required for 60S subunit maturation. Efl1 works in conjunction with Sdo1 to release Tif6 (Becam et al., 2001; Menne et al., 2007; Senger et al., 2001). All three of these factors are conserved throughout eukaryotes. However, archaea lack Efl1 but have Sdo1 and Tif6. Assuming that the mechanism of the release of Tif6 is fundamentally conserved, it is likely that archaeal EF-G acts in

biogenesis to release TIf6, in addition to its canonical role as an elongation factor. Bacteria have neither Sdo1 nor Tif6.

What distinguishes Efl1 from eEF2? In yeast the two proteins share 40% sequence identity, which extends throughout the entire protein. However, Efl1 contains several insertions that are not present in eEF2. The most conspicuous difference, an insertion of 160 aa in domain II, can be deleted without any significant impairment in protein function (Johnson unpublished). Presumably, differences in the structures of the two proteins allow Efl1 but not eEF2 to be recruited to pre-60S subunits. However, it remains a possibility that the two proteins retain some overlap in function. Efl1 is not essential, leaving open the possibility that eEF2 can function in its place, albeit inefficiently. Such functional overlap has recently been reported for the divergent release factors Dom34 and Hbs1, which act primarily on stalled ribosomes but have retained the ability to act on terminating ribosomes, the substrate primarily of eRF1 and eRF3 (Shoemaker et al., 2010).

4.4.5 Ribosome biogenesis and translation coupling?

The Class I Rpl10 P-site loop mutants exhibit a translation defect. This is not surprising given the location of the P-site loop deep in the catalytic center of the subunit. However, this translation defect is suppressed by mutations in either Efl1 or Tif6, implying that the P-site loop mutations are not directly responsible for the translation defect. It would appear that the effect of the P-site loop mutant in Tif6 release during maturation is the cause of the translation defect. This raises the

question of how events that take place during ribosome maturation can affect translation.

A conformation defect- The Rpl10 P-site loop mutants described here are viable, indicating that in the absence of proper signaling from the P-site, Tif6 and Nmd3 are released at some rate less than wild-type and recycle to the nucleus to support further rounds of ribosome biogenesis and subunit export. The results of chapter III suggest that a large conformation change on the large subunit occurs upon Nmd3 binding (Sengupta et al., 2010). It ensues that a significant conformational change would also occur upon Nmd3 release. The data presented in this chapter argues for the release of Nmd3 from the subunit being independent of proper signaling from the P site, but require release of Tif6. Release of Tif6 via improper P site signaling might be followed by an inappropriate release of Nmd3, resulting in aberrant rearrangement of the ribosome, somehow leading to the observed translation defect.

Biogenesis factors moonlighting as translation factors?- The fact that a translation defect can be suppressed by mutations in biogenesis factors suggests that these factors might be directly involved in translation. In bacteria the Efl1 homologue EF-G is involved in the ribosome recycling step of translation alongside ribosome recycling factors (RRF) (Hirashima and Kaji, 1973). In this step, EF-G binds the subunits in a way similar to the way it binds during translocation, albeit to a deacylated hybrid P/E tRNA containing ribosome. This raises the interesting possibility that Efl1 and Tif6 might be similarly involved in recycling. Although it

would seem unlikely that both Efl1 and Tif6 are involved in elongation, in sucrose gradient centrifugation experiments Sdo1 is seen sedimenting at the position of 60S but also of 80S and polysomes ((Menne et al., 2007) and Bussiere unpublished data) suggesting a potential role of the Tif6 release factor in translation.

4.4.6 Quality control in ribosome assembly: functional vs structural proofreading

The ribosome is a complex ribonucleoprotein structure whose assembly involves extensive RNA processing, folding, and protein assembly. It is singly responsible for decoding the genome. Considering the mechanisms of fidelity that are in place to monitor the integrity of mRNAs (Balagopal and Parker, 2009), one would anticipate that there are mechanisms to ensure the proper assembly of the ribosome as well. Two general strategies can be envisioned for assessing the correct assembly of ribosomes. One is "structural proofreading" in which progression through a given step in the assembly pathway depends on the correct assembly of a specific structure. It has been previously suggested that recruitment of the export adapter Nmd3 could promote structural proofreading if its recruitment depended on the correct folding and/or assembly of a multivalent binding site (Johnson et al., 2002; West et al., 2005). Alternatively, the correct assembly of ribosomes could be assessed at a functional level. Inactivating mutations have been introduced into the large and small subunit ribosomal RNAs in yeast (LaRiviere et al., 2006). The consequence of such mutations is the accelerated degradation of the mutant ribosomes, indicating a

surveillance mechanism able to detect functionally defective ribosomes (Lafontaine, 2010). Such ribosomes are cleared by the non-functional RNA Decay (NRD) pathway. Clearing defective small subunits requires the release factor-related proteins Hbs1 and Dom34, which presumably recognize stalled translating ribosomes (Cole et al., 2009). However, the elimination of defective large subunits uses a different set of factors and appears to be initiated by ubiquitylation of the defective ribosomal particles dependent on Mms1 and Rtt101 (Fujii et al., 2009).

Probing the P-site during biogenesis to induce release of the anti-association factor Tif6 provides a functional and structural check of the ribosome prior to its utilization in translation. As mentioned above this check is rather extensive since it requires various elements of the ribosome to be in place: (i) a functional and properly assembled stalk must recruit Efl1, (ii) if the parallel with translocases holds, binding and activation of Efl1 requires a properly structured GTPase activating center, (iii) Rpl10 must be properly accommodated in the ribosome and (iiii) correct signaling via the P-site, in part made of the P-site loop of Rpl10, to Tif6 via Efl1 must occur, probably involving proper occupancy of the P site by either a tRNA or another factor, possibly Sdo1.

Chapter 5

Prospective

5.1 Introduction

In chapter 3, I have described the visualization of the export adaptor Nmd3 on the large ribosomal subunit. A 16Å cryo-EM map of Nmd3 in complex with the large subunit assigned the subunit joining face of the 60S subunit as the binding site of Nmd3. Nmd3 contacts 60S, mostly via interaction with rRNA, at two positions: H69 in front of the peptidyl transferase center and H95 at the base of the ribosomal stalk. The ribosomal protein Rpl10 is necessary for Nmd3 release from the large subunit alongside the putative GTPase Lsg1 (Hedges et al., 2005; West et al., 2005). The assigned Nmd3 mass is observed close to but not in contact with Rpl10.

In chapter 4, I provided compelling evidence that maturation of the large ribosomal subunit involves extensive probing of the structure of the nascent subunit. I showed that the large ribosomal subunit protein Rpl10 and more specifically its unstructured P-site loop is involved in transduction of information about the state of the ribosome, most likely through a moiety in the P site, to the GTPase Efl1, resulting in release of Tif6. Mutations in the P-site loop of Rpl10 prevent the release of Tif6. Mutations in Tif6 which weaken its affinity for the subunit bypass the need for upstream signaling and suppress these Rpl10 mutants. Likewise, mutations in Efl1

favoring a conformational change similar to changes observed in translocases during translation allowed for release of Tif6 independently of upstream signaling.

In the present chapter I will address questions that arose from my work.

5.2 How do Nmd3 and Efl1 access the ribosome simultaneously?

During biogenesis the nascent ribosome is a binding platform for a multitude of tran-acting factors (Henras et al., 2008; Panse and Johnson, 2010). To address how these factors fit simultaneously on the ribosome will require extensive structural work on various native purified pre-60S species as well as crystal structures for trans-acting factors such as Nmd3. In chapter 3 I described the binding site of Nmd3 as a fusion to a maltose binding protein (MBP) on the large subunit. I conducted RNase footprinting experiments comparing the protection of MBP-Nmd3 with GST-Nmd3, which enabled a tentative assignment for the MBP fusion and the Nmd3 moiety. Nmd3 appears to bind the joining face of the large subunit (Illustration 5.1 upper panel) and span from the center of this face via H69 (Illustration 5.2 left panel C2,) to the base of the ribosomal stalk via H95 (Illustration 5.2 left panel C3) and Rpl12 (Illustration 5.2 right panel C3). Nmd3 binds to the nascent large subunit in the nucleus and is the last known biogenesis factor to be release prior to translation. Efl1 is required for the release of Tif6, the release of which is a pre-requisite for Nmd3 release. Hence Efl1 and Nmd3 must bind to the subunit simultaneously.

Structural work on EF-G and eEF2 shows the translocase binding to the base of the stalk at the GTPase activating center around the SRL (Illustration 5.1 lower

panel). Strikingly, it would appear that Nmd3 and the translocase, and by homology Efl1, occupy overlapping space on the subunit. It has been suggested that Nmd3 binding to the subunit is divalent (Hedges et al., 2006), and the structural work presented in chapter 3 is in agreement with this idea (Sengupta et al., 2010). The data presented in chapter 4 describes a molecular pathway which enables signaling from the P-site loop of Rpl10 in the P site to induce release of Tif6 via activation of Efl1. If this model is right, domain IV of Efl1 would interact with a moiety in the P site. However, the Nmd3 density is seen atop the peptidyl transferase center, and thus the P site. So, how does Efl1 interact with the P site in the presence of Nmd3 on the subunit? When paying close attention to the cryo-EM map of Nmd3 in complex with the large ribosomal subunit it becomes evident that the Nmd3 mass curves away from the surface of 60S between its points of contact with the subunit (C2 and C3) (Illustration 5.2 A and B left panel). C2 contacts H69 and C3 contacts H95. One can envision that the space provided by the curvature of the Nmd3 density away from 60S allows for domain IV of Efl1 to reach towards the P site nesting under the bridge formed by Nmd3.

This position of Nmd3 relative to Efl1 on the subunit may address another concern. That is, what does Efl1 bind to in lieu of the small subunit? During translation, the translocase interacts with both subunits of the ribosome and these interactions are necessary for inducing conformational changes essential for its function (See Chapter 1, translocation) (Agirrezabala and Frank, 2009; Gao et al., 2009; Moran et al., 2008). However, during biogenesis, since Tif6 has been

characterized as an anti-association factor (Raychaudhuri et al., 1984; Russell and Spremulli, 1979; Si and Maitra, 1999; Valenzuela et al., 1982), Efl1 presumably interacts with the large subunit alone. The translocase-like GTPase Efl1 presumably behaves like a translocase during biogenesis. This raises the question of what replaces the small subunit and provides the interactions that, by homology, would be crucial for its function? In particular, domains II and III make extensive contacts with the small subunit If Efl1 were to fit under the bridge formed by Nmd3 between its contact points with the subunit, Nmd3 could in part replace the small subunit and provide the necessary interactions to support the function of Efl1 as a translocase mimic during biogenesis. These predicted interactions between Nmd3 and specific domains of Efl1 could be tested experimentally, for example by yeast two-hybrid.

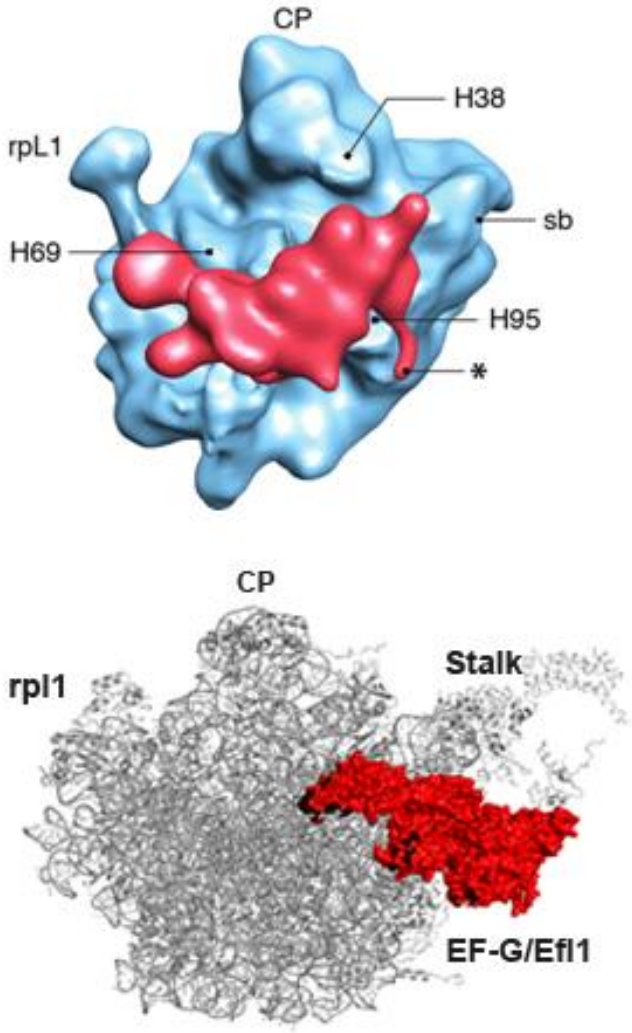

Illustration 5.1 Comparison of Nmd3 and Efl1 proposed interaction with the large ribosomal subunit
Upper panel: intersubunit side view of the cryo-EM of MBP-Nmd3 (red) bound to 60S (blue) (Sengupta et al., 2010). CP: central protuberance, SB: stalk base.
Lower panel: intersubunit side view of the crystal structure of EF-G (red) bound to 50S (grey). Adapted from (Gao et al., 2009).

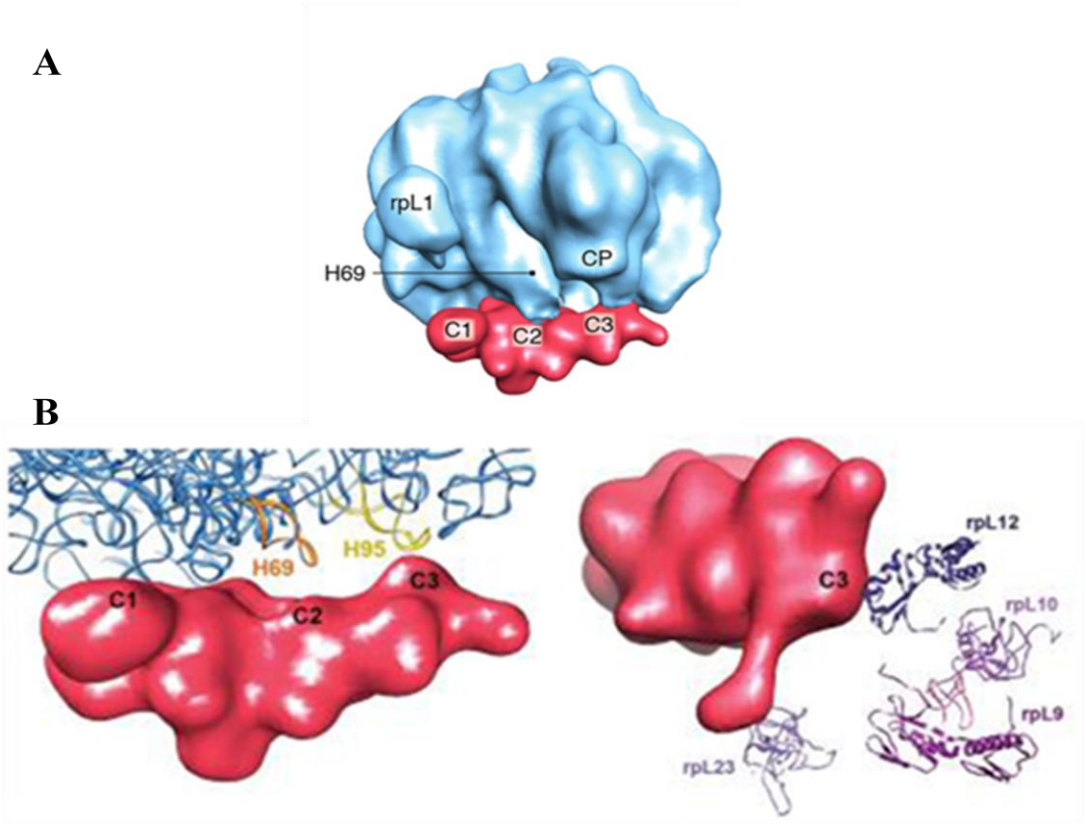

Illustration 5.2 Nmd3 interaction with the large ribosomal subunit
(A) Crown view of the cryo-EM of Nmd3 bound to 60S. (B) Close up view of the quasiatomic structure of the 60S subunit (PDB 1S1I (Spahn et al., 2001)) with the MBP-Nmd3 density showing connections with the rRNA helices (left panel) and nearby proteins (right panel). (Sengupta et al., 2010). CP: central protuberance, C1/C2/C3: connections of MBP-Nmd3 with the subunit.

5.3 How extensively is the large ribosomal subunit checked during maturation?

The activation of Efl1 via signaling by a moiety in the P site requires a structurally and functionally sound 60S subunit. The activation of Efl1 necessitates numerous elements to be in place on the ribosome. (i) Rpl10 needs to be loaded properly and its P-site loop must allow for signaling from the P site. (ii) A properly assembled ribosome stalk is required for release of Tif6 (Lo et al., 2010). Given the homology between Efl1 and translocases, the ribosome stalk is probably required for recruitment and activation of Efl1. (iii) If Efl1 loads onto the ribosome similarly to its homolog eEF2, a properly folded SRL environment at the GPTase activating center is required for docking of Efl1. (iv) Integrity of the P site, in part structurally composed of Rpl10 P-site loop, is tested by requiring information to be transduced, presumably from a moiety in the P site, to Efl1, inducing its GTPase activity and leading to release of Tif6 and subsequent release of Nmd3 from the subunit. I propose that the activation of Efl1 via the P site moiety, and involving Rpl10, mirrors events that take place during translation. Most likely, the Rpl10 P-site loop plays a structural role rather than a functional one, and mutations in this loop could disrupt the structural integrity of the P site. Such disruption could change the geometry of the P site and affect positioning of the moiety present in the P site, for example, during translation, by inducing a non-favorable state of the P-site tRNA for peptityl-transferase reaction or for activation of eEF2. Similarly, during biogenesis, mutations in the P-site loop of Rpl10 would structurally disrupt the P site and could affect the proper accommodation or movement of the moiety present in the P site at

that time. In chapter 4 I proposed that the Shwachman-Bodian-Diamond-Syndrome (SBDS) homolog Sdo1 binds to the P site during biogenesis and plays the role of a tRNA mimic during the faux-translocation event that involves probing of the P site by Efl1 and induces the release of Tif6. Structurally, Sdo1 size and shape are very close to that of a tRNA (Ng et al., 2009) (Illustration 5.3 upper panel) and consequently Sdo1 can easily be modeled in the P site of the large ribosomal subunit (Illustration 5.3 lower panel). Hence, Sdo1 could be used to check the integrity of the P site during the Tif6 release step. If that were the case and the P site is probed prior to translation, one wonders why only one out of the three tRNA binding sites on the large subunit would be checked in this fashion. That the P site be checked during biogenesis makes sense since it is the first site occupied on the ribosome during initiation of translation: the P site is where initiating tRNA first binds, positioning its acceptor stem in the catalytic center. However, some published data hints at a possibly more comprehensive check of the ribosome during biogenesis. Published data suggests that the archaeal Sdo1 ortholog physically interacts with the L1 stalk protein Rpl1 (Rpl5/Rpl1 in yeast) (Ng et al., 2009). The L1 stalk interacts with P and E site tRNAs and facilitates the movement of tRNAs from the P site to the E site, and subsequent release from the E site, during elongation (Cornish et al., 2009; Fei et al., 2008; Trabuco et al., 2010). The reported interaction of the L1 stalk protein with Sdo1 hints at the potential movement of Sdo1 from the P site to the E site during biogenesis, maybe as a way to release Sdo1. If this model were to be correct, it would reveal a much more extensive check of the ribosome during ribosome

maturation, involving mobile structures (L1 stalk and P0/P1/P2 stalk), a translocase-like factor (Efl1) and the movement of a tRNA mimic from P site to E site on the large subunit.

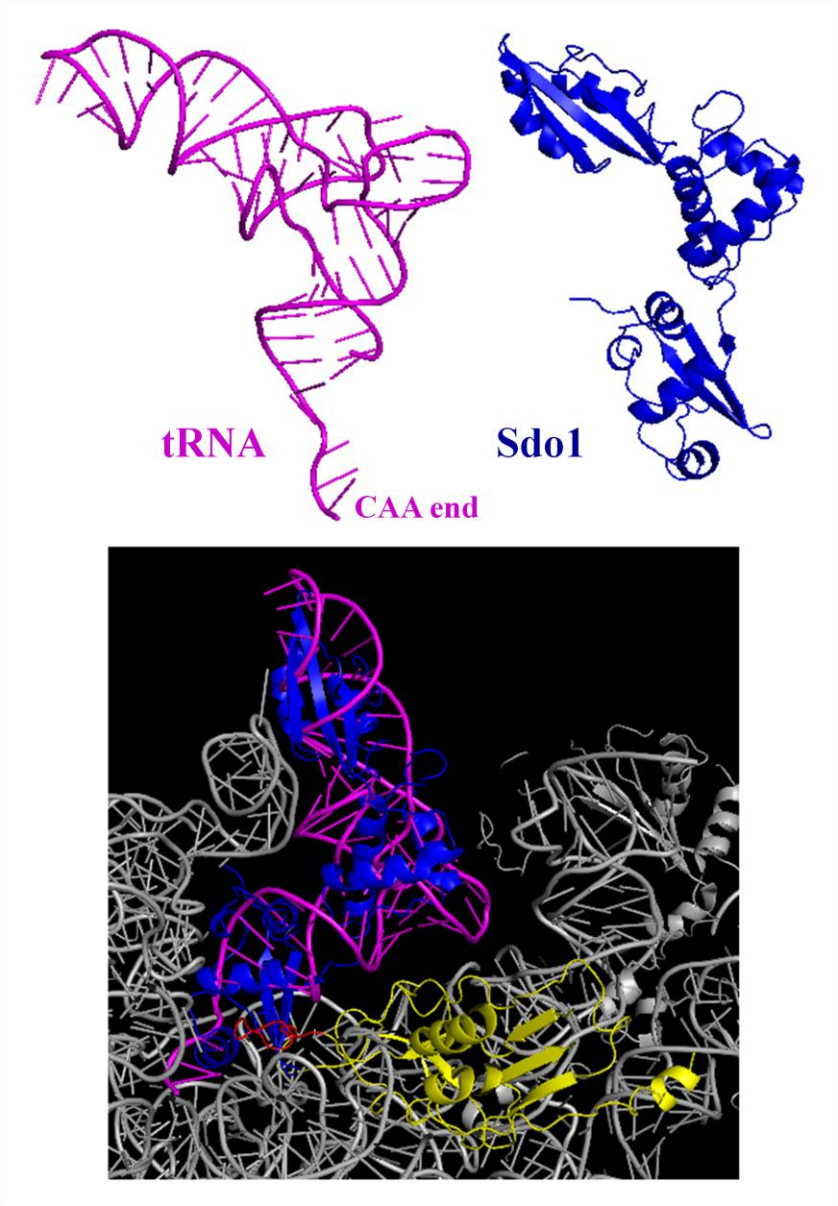

Illustration 5.3 Sdo1 a tRNA mimic?
Upper panel: Comparison of archaeal Sdo1 (blue) (PDB 2WBM (Ng et al., 2009) and tRNA (purple) (PDB 3IZC, 3IZF (Armache et al., 2010a, b)). Lower panel: Hand fitting of archeal Sdo1 (blue) in the P site containing a tRNA from yeast (purple) (PDB 3IZC, 3IZF (Armache et al., 2010a, b)). Yellow: Rpl10, red: Rpl10 P-site loop, grey: 60S ribosome.

5.4 What signals for degradation of defective ribosomes?

Probing the P-site during biogenesis provides a functional or structural quality control of the large ribosomal subunit prior to its utilization in translation. If such an extensive quality control occurs, one question that arises concerns the fate of the subunits that are deficient for signaling and fail in the release of Tif6. Recognition and degradation of defective ribosomal subunits are active processes in the nucleus (Allmang et al., 2000; Dez et al., 2006; Lafontaine et al., 1998; Zanchin and Goldfarb, 1999). LaRiviere et al described a novel cytoplasmic degradation pathway termed non-functional rRNA decay (NRD) which targets subunits containing deleterious rRNA mutations (LaRiviere et al., 2006). One of the mutations used in that study (U2585A) is of a conserved residue in the catalytic center that is essential for peptidyl transfer. Ribosomes containing this mutation enter the cytoplasm but are not seen associated with translating ribosomes (LaRiviere et al., 2006). This phenotype might indicate that these mutant ribosomes fail at subunit joining and do not enter the translating pool. U2585A is at the heart of the PTC and is unlikely to be monitored directly at the rRNA level but rather could be detected indirectly during cytoplasmic maturation when failing to proceed through one of the steps and, for example, leading to the retention of a biogenesis factor. Potentially, this ribosomal subunit somehow "marked" by that factor would be recognized as defective and targeted for degradation. Mutations in Rpl10 P-site loop trap Tif6 and Nmd3 on free 60S subunits and accumulate unusual levels of free 60S relative to free 40S levels. I predict that U2585A rRNA-containing ribosomes, similarly to Rpl10 P-site loop

mutants, accumulate a biogenesis factor, potentially Tif6 and/or Nmd3. These free 60S subunits could represent a pool of ribosome recognized as defective and targeted for degradation. These mutant ribosomes recognized as defective in the cytoplasm might be turned over more slowly than mutant ribosomes degraded in the nucleus, potentially representing a challenge to the cytoplasmic degradation machinery, specifically for 60S degradation, and resulting in the observed free 60S accumulation relative to free 40S.

The GUARD complex and ubiquitination of ribosomal or ribosome-associated proteins have been linked to the degradation of NRD ribosome (Fujii et al., 2009). However, the ribosomal cytoplasmic surveillance system, that is the means by which a ribosome is deemed non-functional, and the machinery involved in the degradation of these ribosomes still remains unknown. The Rpl10 P-site loop mutants generated in my thesis work could provide unique reagents to understand the pathway of eliminating defective ribosomes. These mutants could be used in genetic screens to identify suppressors of P-site loop mutants or synthetic sick/lethal mutants that could help identifying factors involved in the ribosome degradation machinery.

Work presented in chapter 4 suggests that Class II P-site loop mutant-containing ribosomes are viable and are able to translate, though probably slower than wild-type Rpl10-containing ribosomes. If these mutant ribosomes are mostly targeted for degradation before entering the translating pool and thus decrease the overall ribosome levels available for translation in the cell, resulting in a growth defect, then mutants in the surveillance mechanism that allow for a higher percentage of these

ribosomes to partake in translation could suppress the P-site loop mutants growth defect. Such suppressors would be expected to rescue the free subunit imbalance observed in the Class II mutants. On the other hand, if the Class II P-site loop mutant-containing ribosomes targeted for degradation are non-functional, mutations in the surveillance machinery would allow these ribosomes to join the translating pool, which would result in a more severe translation and thus growth defect. Determining the fate of these defective ribosomes will be important for establishing if the release of Tif6 represents a quality control check in 60S maturation.

References

A, A., Brazhnikov, E., Garber, M., Zheltonosova, J., Chirgadze, Y., al-Karadaghi, S., Svensson, L.A., and Liljas, A. (1994). Three-dimensional structure of the ribosomal translocase: elongation factor G from Thermus thermophilus. EMBO J *13*, 3669-3677.

Acker, M.G., Kolitz, S.E., Mitchell, S.F., Nanda, J.S., and Lorsch, J.R. (2007). Reconstitution of yeast translation initiation. Methods Enzymol *430*, 111-145.

Acker, M.G., and Lorsch, J.R. (2008). Mechanism of ribosomal subunit joining during eukaryotic translation initiation. Biochem Soc Trans *36*, 653-657.

Agirrezabala, X., and Frank, J. (2009). Elongation in translation as a dynamic interaction among the ribosome, tRNA, and elongation factors EF-G and EF-Tu. Q Rev Biophys *42*, 159-200.

Agirrezabala, X., Lei, J., Brunelle, J.L., Ortiz-Meoz, R.F., Green, R., and Frank, J. (2008). Visualization of the hybrid state of tRNA binding promoted by spontaneous ratcheting of the ribosome. Mol Cell *32*, 190-197.

Agrawal, R.K., Penczek, P., Grassucci, R.A., and Frank, J. (1998). Visualization of elongation factor G on the Escherichia coli 70S ribosome: the mechanism of translocation. Proc Natl Acad Sci U S A *95*, 6134-6138.

al-Karadaghi, S., Aevarsson, A., Garber, M., Zheltonosova, J., and Liljas, A. (1996). The structure of elongation factor G in complex with GDP: conformational flexibility and nucleotide exchange. Structure *4*, 555-565.

Algire, M.A., Maag, D., Savio, P., Acker, M.G., Tarun, S.Z., Jr., Sachs, A.B., Asano, K., Nielsen, K.H., Olsen, D.S., Phan, L., *et al.* (2002). Development and characterization of a reconstituted yeast translation initiation system. RNA *8*, 382-397.

Alkalaeva, E.Z., Pisarev, A.V., Frolova, L.Y., Kisselev, L.L., and Pestova, T.V. (2006). In vitro reconstitution of eukaryotic translation reveals cooperativity between release factors eRF1 and eRF3. Cell *125*, 1125-1136.

Allmang, C., Mitchell, P., Petfalski, E., and Tollervey, D. (2000). Degradation of ribosomal RNA precursors by the exosome. Nucleic Acids Res *28*, 1684-1691.

Andersen, K.R., Jensen, T.H., and Brodersen, D.E. (2008). Take the "A" tail--quality control of ribosomal and transfer RNA. Biochim Biophys Acta *1779*, 532-537.

Angermayr, M., and Bandlow, W. (2002). RIO1, an extraordinary novel protein kinase. FEBS Lett *524*, 31-36.

Aravind, L., and Koonin, E.V. (2000). Eukaryote-specific domains in translation initiation factors: implications for translation regulation and evolution of the translation system. Genome Res *10*, 1172-1184.

Armache, J.P., Jarasch, A., Anger, A.M., Villa, E., Becker, T., Bhushan, S., Jossinet, F., Habeck, M., Dindar, G., Franckenberg, S., *et al.* (2010a). Cryo-EM structure and rRNA model of a translating eukaryotic 80S ribosome at 5.5-A resolution. Proc Natl Acad Sci U S A *107*, 19748-19753.

Armache, J.P., Jarasch, A., Anger, A.M., Villa, E., Becker, T., Bhushan, S., Jossinet, F., Habeck, M., Dindar, G., Franckenberg, S., *et al.* (2010b). Localization of eukaryote-specific ribosomal proteins in a 5.5-A cryo-EM map of the 80S eukaryotic ribosome. Proc Natl Acad Sci U S A *107*, 19754-19759.
Ashe, M.P., De Long, S.K., and Sachs, A.B. (2000). Glucose depletion rapidly inhibits translation initiation in yeast. Mol Biol Cell *11*, 833-848.
Baim, S.B., Pietras, D.F., Eustice, D.C., and Sherman, F. (1985). A mutation allowing an mRNA secondary structure diminishes translation of Saccharomyces cerevisiae iso-1-cytochrome c. Mol Cell Biol *5*, 1839-1846.
Balagopal, V., and Parker, R. (2009). Polysomes, P bodies and stress granules: states and fates of eukaryotic mRNAs. Curr Opin Cell Biol *21*, 403-408.
Ballesta, J.P., and Remacha, M. (1996). The large ribosomal subunit stalk as a regulatory element of the eukaryotic translational machinery. Prog Nucleic Acid Res Mol Biol *55*, 157-193.
Ban, N., Nissen, P., Hansen, J., Moore, P.B., and Steitz, T.A. (2000). The complete atomic structure of the large ribosomal subunit at 2.4 A resolution. Science *289*, 905-920.
Bashan, A., and Yonath, A. (2008). Correlating ribosome function with high-resolution structures. Trends Microbiol *16*, 326-335.
Bassler, J., Grandi, P., Gadal, O., Lessmann, T., Petfalski, E., Tollervey, D., Lechner, J., and Hurt, E. (2001). Identification of a 60S preribosomal particle that is closely linked to nuclear export. Mol Cell *8*, 517-529.
Basu, U., Si, K., Warner, J.R., and Maitra, U. (2001). The Saccharomyces cerevisiae TIF6 gene encoding translation initiation factor 6 is required for 60S ribosomal subunit biogenesis. Mol Cell Biol *21*, 1453-1462.
Beau, I., Esclatine, A., and Codogno, P. (2008). Lost to translation: when autophagy targets mature ribosomes. Trends Cell Biol *18*, 311-314.
Becam, A.M., Nasr, F., Racki, W.J., Zagulski, M., and Herbert, C.J. (2001). Ria1p (Ynl163c), a protein similar to elongation factors 2, is involved in the biogenesis of the 60S subunit of the ribosome in Saccharomyces cerevisiae. Mol Genet Genomics *266*, 454-462.
Becker, T., Bhushan, S., Jarasch, A., Armache, J.P., Funes, S., Jossinet, F., Gumbart, J., Mielke, T., Berninghausen, O., Schulten, K., *et al.* (2009). Structure of monomeric yeast and mammalian Sec61 complexes interacting with the translating ribosome. Science *326*, 1369-1373.
Ben-Shem, A., Jenner, L., Yusupova, G., and Yusupov, M. (2010). Crystal structure of the eukaryotic ribosome. Science *330*, 1203-1209.
Benne, R., Edman, J., Traut, R.R., and Hershey, J.W. (1978). Phosphorylation of eukaryotic protein synthesis initiation factors. Proc Natl Acad Sci U S A *75*, 108-112.
Berk, V., and Cate, J.H. (2007). Insights into protein biosynthesis from structures of bacterial ribosomes. Curr Opin Struct Biol *17*, 302-309.

Bernstein, K.A., Bleichert, F., Bean, J.M., Cross, F.R., and Baserga, S.J. (2007). Ribosome biogenesis is sensed at the Start cell cycle checkpoint. Mol Biol Cell *18*, 953-964.
Blaha, G., Stanley, R.E., and Steitz, T.A. (2009). Formation of the first peptide bond: the structure of EF-P bound to the 70S ribosome. Science *325*, 966-970.
Blanchard, S.C., Kim, H.D., Gonzalez, R.L., Jr., Puglisi, J.D., and Chu, S. (2004). tRNA dynamics on the ribosome during translation. Proc Natl Acad Sci U S A *101*, 12893-12898.
Bodian, M., Sheldon, W., and Lightwood, R. (1964). CONGENITAL HYPOPLASIA OF THE EXOCRINE PANCREAS. Acta Paediatr *53*, 282-293.
Boisvert, F.M., van Koningsbruggen, S., Navascues, J., and Lamond, A.I. (2007). The multifunctional nucleolus. Nat Rev Mol Cell Biol *8*, 574-585.
Bradatsch, B., Katahira, J., Kowalinski, E., Bange, G., Yao, W., Sekimoto, T., Baumgartel, V., Boese, G., Bassler, J., Wild, K., *et al.* (2007). Arx1 functions as an unorthodox nuclear export receptor for the 60S preribosomal subunit. Mol Cell *27*, 767-779.
Briceno, V., Camargo, H., Remacha, M., Santos, C., and Ballesta, J.P. (2009). Structural and functional characterization of the amino terminal domain of the yeast ribosomal stalk P1 and P2 proteins. Int J Biochem Cell Biol *41*, 1315-1322.
Britton, R.A. (2009). Role of GTPases in bacterial ribosome assembly. Annu Rev Microbiol *63*, 155-176.
Cavaille, J., Nicoloso, M., and Bachellerie, J.P. (1996). Targeted ribose methylation of RNA in vivo directed by tailored antisense RNA guides. Nature *383*, 732-735.
Cole, S.E., LaRiviere, F.J., Merrikh, C.N., and Moore, M.J. (2009). A convergence of rRNA and mRNA quality control pathways revealed by mechanistic analysis of nonfunctional rRNA decay. Mol Cell *34*, 440-450.
Collins, S.R., Kemmeren, P., Zhao, X.C., Greenblatt, J.F., Spencer, F., Holstege, F.C., Weissman, J.S., and Krogan, N.J. (2007). Toward a comprehensive atlas of the physical interactome of Saccharomyces cerevisiae. Mol Cell Proteomics *6*, 439-450.
Connolly, K., and Culver, G. (2009). Deconstructing ribosome construction. Trends Biochem Sci *34*, 256-263.
Cornish, P.V., Ermolenko, D.N., Noller, H.F., and Ha, T. (2008). Spontaneous intersubunit rotation in single ribosomes. Mol Cell *30*, 578-588.
Cornish, P.V., Ermolenko, D.N., Staple, D.W., Hoang, L., Hickerson, R.P., Noller, H.F., and Ha, T. (2009). Following movement of the L1 stalk between three functional states in single ribosomes. Proc Natl Acad Sci U S A *106*, 2571-2576.
Czworkowski, J., Wang, J., Steitz, T.A., and Moore, P.B. (1994). The crystal structure of elongation factor G complexed with GDP, at 2.7 A resolution. EMBO J *13*, 3661-3668.
de Oliveira, J.F., Sforca, M.L., Blumenschein, T.M., Goldfeder, M.B., Guimaraes, B.G., Oliveira, C.C., Zanchin, N.I., and Zeri, A.C. (2010). Structure, dynamics, and RNA interaction analysis of the human SBDS protein. J Mol Biol *396*, 1053-1069.

Decatur, W.A., Liang, X.H., Piekna-Przybylska, D., and Fournier, M.J. (2007). Identifying effects of snoRNA-guided modifications on the synthesis and function of the yeast ribosome. Methods Enzymol *425*, 283-316.
Demoinet, E., Jacquier, A., Lutfalla, G., and Fromont-Racine, M. (2007). The Hsp40 chaperone Jjj1 is required for the nucleo-cytoplasmic recycling of preribosomal factors in Saccharomyces cerevisiae. RNA *13*, 1570-1581.
Derek J Taylor, J.N., A Rod Merrill, Gregers Rom Andersen, Poul Nissen and Joachim Frank (2007). EMBO J *26*, 2421-2431.
Dez, C., Dlakic, M., and Tollervey, D. (2007). Roles of the HEAT repeat proteins Utp10 and Utp20 in 40S ribosome maturation. RNA *13*, 1516-1527.
Dez, C., Houseley, J., and Tollervey, D. (2006). Surveillance of nuclear-restricted pre-ribosomes within a subnucleolar region of Saccharomyces cerevisiae. Embo J *25*, 1534-1546.
Diaconu, M., Kothe, U., Schlunzen, F., Fischer, N., Harms, J.M., Tonevitsky, A.G., Stark, H., Rodnina, M.V., and Wahl, M.C. (2005). Structural basis for the function of the ribosomal L7/12 stalk in factor binding and GTPase activation. Cell *121*, 991-1004.
Doma, M.K., and Parker, R. (2006). Endonucleolytic cleavage of eukaryotic mRNAs with stalls in translation elongation. Nature *440*, 561-564.
Dong, X., Biswas, A., Suel, K.E., Jackson, L.K., Martinez, R., Gu, H., and Chook, Y.M. (2009). Structural basis for leucine-rich nuclear export signal recognition by CRM1. Nature *458*, 1136-1141.
Du, Y.C., and Stillman, B. (2002). Yph1p, an ORC-interacting protein: potential links between cell proliferation control, DNA replication, and ribosome biogenesis. Cell *109*, 835-848.
Ermolenko, D.N., Majumdar, Z.K., Hickerson, R.P., Spiegel, P.C., Clegg, R.M., and Noller, H.F. (2007). Observation of intersubunit movement of the ribosome in solution using FRET. J Mol Biol *370*, 530-540.
Fan-Minogue, H., Du, M., Pisarev, A.V., Kallmeyer, A.K., Salas-Marco, J., Keeling, K.M., Thompson, S.R., Pestova, T.V., and Bedwell, D.M. (2008). Distinct eRF3 requirements suggest alternate eRF1 conformations mediate peptide release during eukaryotic translation termination. Mol Cell *30*, 599-609.
Fei, J., Kosuri, P., MacDougall, D.D., and Gonzalez, R.L., Jr. (2008). Coupling of ribosomal L1 stalk and tRNA dynamics during translation elongation. Mol Cell *30*, 348-359.
Fornerod, M., and Ohno, M. (2002). Exportin-mediated nuclear export of proteins and ribonucleoproteins. Results Probl Cell Differ *35*, 67-91.
Frank, J., and Agrawal, R.K. (2000). A ratchet-like inter-subunit reorganization of the ribosome during translocation. Nature *406*, 318-322.
Frank, J., and Agrawal, R.K. (2001). Ratchet-like movements between the two ribosomal subunits: their implications in elongation factor recognition and tRNA translocation. Cold Spring Harb Symp Quant Biol *66*, 67-75.

Fried, H., and Kutay, U. (2003). Nucleocytoplasmic transport: taking an inventory. Cell Mol Life Sci *60*, 1659-1688.
Frolova, L.Y., Tsivkovskii, R.Y., Sivolobova, G.F., Oparina, N.Y., Serpinsky, O.I., Blinov, V.M., Tatkov, S.I., and Kisselev, L.L. (1999). Mutations in the highly conserved GGQ motif of class 1 polypeptide release factors abolish ability of human eRF1 to trigger peptidyl-tRNA hydrolysis. RNA *5*, 1014-1020.
Fromont-Racine, M., Senger, B., Saveanu, C., and Fasiolo, F. (2003). Ribosome assembly in eukaryotes. Gene *313*, 17-42.
Fujii, K., Kitabatake, M., Sakata, T., Miyata, A., and Ohno, M. (2009). A role for ubiquitin in the clearance of nonfunctional rRNAs. Genes Dev *23*, 963-974.
Gabashvili, I.S., Agrawal, R.K., Spahn, C.M., Grassucci, R.A., Svergun, D.I., Frank, J., and Penczek, P. (2000). Solution structure of the E. coli 70S ribosome at 11.5 A resolution. Cell *100*, 537-549.
Gadal, O., Strauss, D., Kessl, J., Trumpower, B., Tollervey, D., and Hurt, E. (2001). Nuclear export of 60s ribosomal subunits depends on Xpo1p and requires a nuclear export sequence-containing factor, Nmd3p, that associates with the large subunit protein Rpl10p. Mol Cell Biol *21*, 3405-3415.
Ganot, P., Bortolin, M.L., and Kiss, T. (1997). Site-specific pseudouridine formation in preribosomal RNA is guided by small nucleolar RNAs. Cell *89*, 799-809.
Gao, H., Sengupta, J., Valle, M., Korostelev, A., Eswar, N., Stagg, S.M., Van Roey, P., Agrawal, R.K., Harvey, S.C., Sali, A., *et al.* (2003). Study of the structural dynamics of the E coli 70S ribosome using real-space refinement. Cell *113*, 789-801.
Gao, Y.G., Selmer, M., Dunham, C.M., Weixlbaumer, A., Kelley, A.C., and Ramakrishnan, V. (2009). The structure of the ribosome with elongation factor G trapped in the posttranslocational state. Science *326*, 694-699.
Gartmann, M., Blau, M., Armache, J.P., Mielke, T., Topf, M., and Beckmann, R. (2010). Mechanism of eIF6-mediated inhibition of ribosomal subunit joining. J Biol Chem *285*, 14848-14851.
Gavin, A.C., Aloy, P., Grandi, P., Krause, R., Boesche, M., Marzioch, M., Rau, C., Jensen, L.J., Bastuck, S., Dumpelfeld, B., *et al.* (2006). Proteome survey reveals modularity of the yeast cell machinery. Nature *440*, 631-636.
Gavin, A.C., Bosche, M., Krause, R., Grandi, P., Marzioch, M., Bauer, A., Schultz, J., Rick, J.M., Michon, A.M., Cruciat, C.M., *et al.* (2002). Functional organization of the yeast proteome by systematic analysis of protein complexes. Nature *415*, 141-147.
Gomez-Lorenzo, M.G., Spahn, C.M., Agrawal, R.K., Grassucci, R.A., Penczek, P., Chakraburtty, K., Ballesta, J.P., Lavandera, J.L., Garcia-Bustos, J.F., and Frank, J. (2000). Three-dimensional cryo-electron microscopy localization of EF2 in the Saccharomyces cerevisiae 80S ribosome at 17.5 A resolution. EMBO J *19*, 2710-2718.
Gonzalo, P., and Reboud, J.P. (2003). The puzzling lateral flexible stalk of the ribosome. Biol Cell *95*, 179-193.

Gorlich, D., and Kutay, U. (1999). Transport between the cell nucleus and the cytoplasm. Annu Rev Cell Dev Biol *15*, 607-660.
Graindorge, J.S., Rousselle, J.C., Senger, B., Lenormand, P., Namane, A., Lacroute, F., and Fasiolo, F. (2005). Deletion of EFL1 results in heterogeneity of the 60 S GTPase-associated rRNA conformation. J Mol Biol *352*, 355-369.
Green, R., and Noller, H.F. (1996). In vitro complementation analysis localizes 23S rRNA posttranscriptional modifications that are required for Escherichia coli 50S ribosomal subunit assembly and function. RNA *2*, 1011-1021.
Green, R., and Noller, H.F. (1997). Ribosomes and translation. Annu Rev Biochem *66*, 679-716.
Gutell, R.R., Weiser, B., Woese, C.R., and Noller, H.F. (1985). Comparative anatomy of 16-S-like ribosomal RNA. Prog Nucleic Acid Res Mol Biol *32*, 155-216.
Guttler, T., Madl, T., Neumann, P., Deichsel, D., Corsini, L., Monecke, T., Ficner, R., Sattler, M., and Gorlich, D. (2010). NES consensus redefined by structures of PKI-type and Rev-type nuclear export signals bound to CRM1. Nat Struct Mol Biol *17*, 1367-1376.
Hage, A.E., and Tollervey, D. (2004). A surfeit of factors: why is ribosome assembly so much more complicated in eukaryotes than bacteria? RNA Biol *1*, 10-15.
Hansson, S., Singh, R., Gudkov, A.T., Liljas, A., and Logan, D.T. (2005). Structural insights into fusidic acid resistance and sensitivity in EF-G. J Mol Biol *348*, 939-949.
Harms, J., Schluenzen, F., Zarivach, R., Bashan, A., Gat, S., Agmon, I., Bartels, H., Franceschi, F., and Yonath, A. (2001). High resolution structure of the large ribosomal subunit from a mesophilic eubacterium. Cell *107*, 679-688.
Hedges, J., Chen, Y.I., West, M., Bussiere, C., and Johnson, A.W. (2006). Mapping the functional domains of yeast NMD3, the nuclear export adapter for the 60 S ribosomal subunit. J Biol Chem *281*, 36579-36587.
Hedges, J., West, M., and Johnson, A.W. (2005). Release of the export adapter, Nmd3p, from the 60S ribosomal subunit requires Rpl10p and the cytoplasmic GTPase Lsg1p. EMBO J *24*, 567-579.
Henras, A.K., Soudet, J., Gerus, M., Lebaron, S., Caizergues-Ferrer, M., Mougin, A., and Henry, Y. (2008). The post-transcriptional steps of eukaryotic ribosome biogenesis. Cell Mol Life Sci *65*, 2334-2359.
Hinnebusch, A.G., and Natarajan, K. (2002). Gcn4p, a master regulator of gene expression, is controlled at multiple levels by diverse signals of starvation and stress. Eukaryot Cell *1*, 22-32.
Hirashima, A., and Kaji, A. (1973). Role of elongation factor G and a protein factor on the release of ribosomes from messenger ribonucleic acid. J Biol Chem *248*, 7580-7587.
Ho, J.H., and Johnson, A.W. (1999). NMD3 encodes an essential cytoplasmic protein required for stable 60S ribosomal subunits in Saccharomyces cerevisiae. Mol Cell Biol *19*, 2389-2399.
Ho, J.H., Kallstrom, G., and Johnson, A.W. (2000a). Nascent 60S ribosomal subunits enter the free pool bound by Nmd3p. RNA *6*, 1625-1634.

Ho, J.H., Kallstrom, G., and Johnson, A.W. (2000b). Nmd3p is a Crm1p-dependent adapter protein for nuclear export of the large ribosomal subunit. J Cell Biol *151*, 1057-1066.
Hofer, A., Bussiere, C., and Johnson, A.W. (2007). Mutational analysis of the ribosomal protein Rpl10 from yeast. J Biol Chem *282*, 32630-32639.
Horan, L.H., and Noller, H.F. (2007). Intersubunit movement is required for ribosomal translocation. Proc Natl Acad Sci U S A *104*, 4881-4885.
Houseley, J., LaCava, J., and Tollervey, D. (2006). RNA-quality control by the exosome. Nat Rev Mol Cell Biol *7*, 529-539.
Huh, W.K., Falvo, J.V., Gerke, L.C., Carroll, A.S., Howson, R.W., Weissman, J.S., and O'Shea, E.K. (2003). Global analysis of protein localization in budding yeast. Nature *425*, 686-691.
Hung, N.J., and Johnson, A.W. (2006). Nuclear recycling of the pre-60S ribosomal subunit-associated factor Arx1 depends on Rei1 in Saccharomyces cerevisiae. Mol Cell Biol *26*, 3718-3727.
Hung, N.J., Lo, K.Y., Patel, S.S., Helmke, K., and Johnson, A.W. (2008). Arx1 is a nuclear export receptor for the 60S ribosomal subunit in yeast. Mol Biol Cell *19*, 735-744.
Hurt, E., Hannus, S., Schmelzl, B., Lau, D., Tollervey, D., and Simos, G. (1999). A novel in vivo assay reveals inhibition of ribosomal nuclear export in ran-cycle and nucleoporin mutants. J Cell Biol *144*, 389-401.
Iost, I., and Dreyfus, M. (2006). DEAD-box RNA helicases in Escherichia coli. Nucleic Acids Res *34*, 4189-4197.
Jackson, R.J., Hellen, C.U., and Pestova, T.V. (2010). The mechanism of eukaryotic translation initiation and principles of its regulation. Nat Rev Mol Cell Biol *11*, 113-127.
Jenner, L., Demeshkina, N., Yusupova, G., and Yusupov, M. (2010a). Structural rearrangements of the ribosome at the tRNA proofreading step. Nat Struct Mol Biol *17*, 1072-1078.
Jenner, L.B., Demeshkina, N., Yusupova, G., and Yusupov, M. (2010b). Structural aspects of messenger RNA reading frame maintenance by the ribosome. Nat Struct Mol Biol *17*, 555-560.
Jiang, M., Sullivan, S.M., Walker, A.K., Strahler, J.R., Andrews, P.C., and Maddock, J.R. (2007). Identification of novel Escherichia coli ribosome-associated proteins using isobaric tags and multidimensional protein identification techniques. J Bacteriol *189*, 3434-3444.
Johnson, A.E. (2009). The structural and functional coupling of two molecular machines, the ribosome and the translocon. J Cell Biol *185*, 765-767.
Johnson, A.W., Ho, J.H., Kallstrom, G., Trotta, C., Lund, E., Kahan, L., Dahlberg, J., and Hedges, J. (2001). Nuclear export of the large ribosomal subunit. Cold Spring Harb Symp Quant Biol *66*, 599-605.
Johnson, A.W., Lund, E., and Dahlberg, J. (2002). Nuclear export of ribosomal subunits. Trends Biochem Sci *27*, 580-585.

Jorgensen, R., Carr-Schmid, A., Ortiz, P.A., Kinzy, T.G., and Andersen, G.R. (2002). Purification and crystallization of the yeast elongation factor eEF2. Acta Crystallogr D Biol Crystallogr *58*, 712-715.
Jorgensen, R., Ortiz, P.A., Carr-Schmid, A., Nissen, P., Kinzy, T.G., and Andersen, G.R. (2003). Two crystal structures demonstrate large conformational changes in the eukaryotic ribosomal translocase. Nat Struct Biol *10*, 379-385.
Julian, P., Konevega, A.L., Scheres, S.H., Lazaro, M., Gil, D., Wintermeyer, W., Rodnina, M.V., and Valle, M. (2008). Structure of ratcheted ribosomes with tRNAs in hybrid states. Proc Natl Acad Sci U S A *105*, 16924-16927.
Kaczanowska, M., and Ryden-Aulin, M. (2007). Ribosome biogenesis and the translation process in Escherichia coli. Microbiol Mol Biol Rev *71*, 477-494.
Kallstrom, G., Hedges, J., and Johnson, A. (2003). The putative GTPases Nog1p and Lsg1p are required for 60S ribosomal subunit biogenesis and are localized to the nucleus and cytoplasm, respectively. Mol Cell Biol *23*, 4344-4355.
Kapp, L.D., and Lorsch, J.R. (2004). The molecular mechanics of eukaryotic translation. Annu Rev Biochem *73*, 657-704.
Karbstein, K. (2007). Role of GTPases in ribosome assembly. Biopolymers *87*, 1-11.
Karl, T., Onder, K., Kodzius, R., Pichova, A., Wimmer, H., Th r, A., Hundsberger, H., Loffler, M., Klade, T., Beyer, A., *et al.* (1999). GRC5 and NMD3 function in translational control of gene expression and interact genetically. Curr Genet *34*, 419-429.
Katahira, J., Strasser, K., Podtelejnikov, A., Mann, M., Jung, J.U., and Hurt, E. (1999). The Mex67p-mediated nuclear mRNA export pathway is conserved from yeast to human. EMBO J *18*, 2593-2609.
Kazemie, M. (1975). The importance of Escherichia coli ribosomal proteins L1, L11 and L16 for the association of ribosomal subunits and the formation of the 70-S initiation complex. Eur J Biochem *58*, 501-510.
Kemmler, S., Occhipinti, L., Veisu, M., and Panse, V.G. (2009). Yvh1 is required for a late maturation step in the 60S biogenesis pathway. J Cell Biol *186*, 863-880.
Killian, A., Le Meur, N., Sesboue, R., Bourguignon, J., Bougeard, G., Gautherot, J., Bastard, C., Frebourg, T., and Flaman, J.M. (2004). Inactivation of the RRB1-Pescadillo pathway involved in ribosome biogenesis induces chromosomal instability. Oncogene *23*, 8597-8602.
Kirillov, S.V., Wower, J., Hixson, S.S., and Zimmermann, R.A. (2002). Transit of tRNA through the Escherichia coli ribosome: cross-linking of the 3' end of tRNA to ribosomal proteins at the P and E sites. FEBS Lett *514*, 60-66.
Kiss-Laszlo, Z., Henry, Y., Bachellerie, J.P., Caizergues-Ferrer, M., and Kiss, T. (1996). Site-specific ribose methylation of preribosomal RNA: a novel function for small nucleolar RNAs. Cell *85*, 1077-1088.
Kohler, A., and Hurt, E. (2007). Exporting RNA from the nucleus to the cytoplasm. Nat Rev Mol Cell Biol *8*, 761-773.
Kozak, M. (2002). Pushing the limits of the scanning mechanism for initiation of translation. Gene *299*, 1-34.

Kressler, D., Hurt, E., and Bassler, J. (2010). Driving ribosome assembly. Biochim Biophys Acta *1803*, 673-683.
Kressler, D., Linder, P., and de La Cruz, J. (1999). Protein trans-acting factors involved in ribosome biogenesis in Saccharomyces cerevisiae. Mol Cell Biol *19*, 7897-7912.
Krokowski, D., Boguszewska, A., Abramczyk, D., Liljas, A., Tchorzewski, M., and Grankowski, N. (2006). Yeast ribosomal P0 protein has two separate binding sites for P1/P2 proteins. Mol Microbiol *60*, 386-400.
Kudo, N., Matsumori, N., Taoka, H., Fujiwara, D., Schreiner, E.P., Wolff, B., Yoshida, M., and Horinouchi, S. (1999). Leptomycin B inactivates CRM1/exportin 1 by covalent modification at a cysteine residue in the central conserved region. Proc Natl Acad Sci U S A *96*, 9112-9117.
Kutay, U., and Guttinger, S. (2005). Leucine-rich nuclear-export signals: born to be weak. Trends Cell Biol *15*, 121-124.
la Cour, T., Kiemer, L., Molgaard, A., Gupta, R., Skriver, K., and Brunak, S. (2004). Analysis and prediction of leucine-rich nuclear export signals. Protein Eng Des Sel *17*, 527-536.
Lafontaine, D.L. (2010). A 'garbage can' for ribosomes: how eukaryotes degrade their ribosomes. Trends Biochem Sci *35*, 267-277.
Lafontaine, D.L., Preiss, T., and Tollervey, D. (1998). Yeast 18S rRNA dimethylase Dim1p: a quality control mechanism in ribosome synthesis? Mol Cell Biol *18*, 2360-2370.
Lamanna, A.C., and Karbstein, K. (2009). Nob1 binds the single-stranded cleavage site D at the 3'-end of 18S rRNA with its PIN domain. Proc Natl Acad Sci U S A *106*, 14259-14264.
Lancaster, L., Lambert, N.J., Maklan, E.J., Horan, L.H., and Noller, H.F. (2008). The sarcin-ricin loop of 23S rRNA is essential for assembly of the functional core of the 50S ribosomal subunit. RNA *14*, 1999-2012.
LaRiviere, F.J., Cole, S.E., Ferullo, D.J., and Moore, M.J. (2006). A late-acting quality control process for mature eukaryotic rRNAs. Mol Cell *24*, 619-626.
Lebreton, A., Saveanu, C., Decourty, L., Jacquier, A., and Fromont-Racine, M. (2006a). Nsa2 is an unstable, conserved factor required for the maturation of 27 SB pre-rRNAs. J Biol Chem *281*, 27099-27108.
Lebreton, A., Saveanu, C., Decourty, L., Rain, J.C., Jacquier, A., and Fromont-Racine, M. (2006b). A functional network involved in the recycling of nucleocytoplasmic pre-60S factors. J Cell Biol *173*, 349-360.
Lo, K.Y., and Johnson, A.W. (2009). Reengineering ribosome export. Mol Biol Cell *20*, 1545-1554.
Lo, K.Y., Li, Z., Bussiere, C., Bresson, S., Marcotte, E.M., and Johnson, A.W. (2010). Defining the pathway of cytoplasmic maturation of the 60S ribosomal subunit. Mol Cell *39*, 196-208.

Lo, K.Y., Li, Z., Wang, F., Marcotte, E.M., and Johnson, A.W. (2009). Ribosome stalk assembly requires the dual-specificity phosphatase Yvh1 for the exchange of Mrt4 with P0. J Cell Biol *186*, 849-862.
Lorsch, J.R., and Dever, T.E. (2010). Molecular view of 43 S complex formation and start site selection in eukaryotic translation initiation. J Biol Chem *285*, 21203-21207.
Lorsch, J.R., and Herschlag, D. (1999). Kinetic dissection of fundamental processes of eukaryotic translation initiation in vitro. EMBO J *18*, 6705-6717.
Lowe, T.M., and Eddy, S.R. (1999). A computational screen for methylation guide snoRNAs in yeast. Science *283*, 1168-1171.
Luz, J.S., Georg, R.C., Gomes, C.H., Machado-Santelli, G.M., and Oliveira, C.C. (2009). Sdo1p, the yeast orthologue of Shwachman-Bodian-Diamond syndrome protein, binds RNA and interacts with nuclear rRNA-processing factors. In Yeast, pp. 287-298.
Maguire, B.A., Beniaminov, A.D., Ramu, H., Mankin, A.S., and Zimmermann, R.A. (2005). A protein component at the heart of an RNA machine: the importance of protein l27 for the function of the bacterial ribosome. Mol Cell *20*, 427-435.
Maki, J.A., Schnobrich, D.J., and Culver, G.M. (2002). The DnaK chaperone system facilitates 30S ribosomal subunit assembly. Mol Cell *10*, 129-138.
Menacho-Marquez, M., Perez-Valle, J., Arino, J., Gadea, J., and Murguia, J.R. (2007). Gcn2p regulates a G1/S cell cycle checkpoint in response to DNA damage. Cell Cycle *6*, 2302-2305.
Menne, T.F., Goyenechea, B., Sanchez-Puig, N., Wong, C.C., Tonkin, L.M., Ancliff, P.J., Brost, R.L., Costanzo, M., Boone, C., and Warren, A.J. (2007). The Shwachman-Bodian-Diamond syndrome protein mediates translational activation of ribosomes in yeast. Nat Genet *39*, 486-495.
Meyer, A.E., Hung, N.J., Yang, P., Johnson, A.W., and Craig, E.A. (2007). The specialized cytosolic J-protein, Jjj1, functions in 60S ribosomal subunit biogenesis. Proc Natl Acad Sci U S A *104*, 1558-1563.
Miluzio, A., Beugnet, A., Volta, V., and Biffo, S. (2009). Eukaryotic initiation factor 6 mediates a continuum between 60S ribosome biogenesis and translation. EMBO Rep *10*, 459-465.
Moazed, D., and Noller, H.F. (1989). Intermediate states in the movement of transfer RNA in the ribosome. Nature *342*, 142-148.
Mohr, D., Wintermeyer, W., and Rodnina, M.V. (2002). GTPase activation of elongation factors Tu and G on the ribosome. Biochemistry *41*, 12520-12528.
Moore, J.B.t., Farrar, J.E., Arceci, R.J., Liu, J.M., and Ellis, S.R. (2010). Distinct ribosome maturation defects in yeast models of Diamond-Blackfan anemia and Shwachman-Diamond syndrome. Haematologica *95*, 57-64.
Moore, V.G., Atchison, R.E., Thomas, G., Moran, M., and Noller, H.F. (1975). Identification of a ribosomal protein essential for peptidyl transferase activity. Proc Natl Acad Sci U S A *72*, 844-848.

Moran, S.J., Flanagan, J.F.t., Namy, O., Stuart, D.I., Brierley, I., and Gilbert, R.J. (2008). The mechanics of translocation: a molecular "spring-and-ratchet" system. Structure *16*, 664-672.
Morgan, D.G., Menetret, J.F., Radermacher, M., Neuhof, A., Akey, I.V., Rapoport, T.A., and Akey, C.W. (2000). A comparison of the yeast and rabbit 80 S ribosome reveals the topology of the nascent chain exit tunnel, inter-subunit bridges and mammalian rRNA expansion segments. J Mol Biol *301*, 301-321.
Moy, T.I., and Silver, P.A. (1999). Nuclear export of the small ribosomal subunit requires the ran-GTPase cycle and certain nucleoporins. Genes Dev *13*, 2118-2133.
Mulder, A.M., Yoshioka, C., Beck, A.H., Bunner, A.E., Milligan, R.A., Potter, C.S., Carragher, B., and Williamson, J.R. (2010). Visualizing ribosome biogenesis: parallel assembly pathways for the 30S subunit. Science *330*, 673-677.
Nechifor, R., Murataliev, M., and Wilson, K.S. (2007). Functional interactions between the G' subdomain of bacterial translation factor EF-G and ribosomal protein L7/L12. J Biol Chem *282*, 36998-37005.
Neville, M., and Rosbash, M. (1999). The NES-Crm1p export pathway is not a major mRNA export route in Saccharomyces cerevisiae. EMBO J *18*, 3746-3756.
Ng, C.L., Waterman, D.G., Koonin, E.V., Walters, A.D., Chong, J.P., Isupov, M.N., Lebedev, A.A., Bunka, D.H., Stockley, P.G., Ortiz-Lombardia, M., and Antson, A.A. (2009). Conformational flexibility and molecular interactions of an archaeal homologue of the Shwachman-Bodian-Diamond syndrome protein. BMC Struct Biol *9*, 32.
Ni, J., Tien, A.L., and Fournier, M.J. (1997). Small nucleolar RNAs direct site-specific synthesis of pseudouridine in ribosomal RNA. Cell *89*, 565-573.
Nikulin, A., Eliseikina, I., Tishchenko, S., Nevskaya, N., Davydova, N., Platonova, O., Piendl, W., Selmer, M., Liljas, A., Drygin, D., *et al.* (2003). Structure of the L1 protuberance in the ribosome. Nat Struct Biol *10*, 104-108.
Nishimura, M., Yoshida, T., Shirouzu, M., Terada, T., Kuramitsu, S., Yokoyama, S., Ohkubo, T., and Kobayashi, Y. (2004). Solution structure of ribosomal protein L16 from Thermus thermophilus HB8. J Mol Biol *344*, 1369-1383.
Nissen, P., Hansen, J., Ban, N., Moore, P.B., and Steitz, T.A. (2000). The structural basis of ribosome activity in peptide bond synthesis. Science *289*, 920-930.
Noller, H.F. (1991). Ribosomal RNA and translation. Annu Rev Biochem *60*, 191-227.
Panse, V.G., and Johnson, A.W. (2010). Maturation of eukaryotic ribosomes: acquisition of functionality. Trends Biochem Sci *35*, 260-266.
Pemberton, L.F., and Paschal, B.M. (2005). Mechanisms of receptor-mediated nuclear import and nuclear export. Traffic *6*, 187-198.
Pertschy, B., Saveanu, C., Zisser, G., Lebreton, A., Tengg, M., Jacquier, A., Liebminger, E., Nobis, B., Kappel, L., van der Klei, I., *et al.* (2007). Cytoplasmic recycling of 60S preribosomal factors depends on the AAA protein Drg1. Mol Cell Biol *27*, 6581-6592.

Pertschy, B., Schneider, C., Gnadig, M., Schafer, T., Tollervey, D., and Hurt, E. (2009). RNA helicase Prp43 and its co-factor Pfa1 promote 20 to 18 S rRNA processing catalyzed by the endonuclease Nob1. J Biol Chem *284*, 35079-35091.
Petes, T.D. (1979). Yeast ribosomal DNA genes are located on chromosome XII. Proc Natl Acad Sci U S A *76*, 410-414.
Pisarev, A.V., Hellen, C.U., and Pestova, T.V. (2007). Recycling of eukaryotic posttermination ribosomal complexes. Cell *131*, 286-299.
Pisarev, A.V., Skabkin, M.A., Pisareva, V.P., Skabkina, O.V., Rakotondrafara, A.M., Hentze, M.W., Hellen, C.U., and Pestova, T.V. (2010). The role of ABCE1 in eukaryotic posttermination ribosomal recycling. Mol Cell *37*, 196-210.
Pisareva, V.P., Pisarev, A.V., Hellen, C.U., Rodnina, M.V., and Pestova, T.V. (2006). Kinetic analysis of interaction of eukaryotic release factor 3 with guanine nucleotides. J Biol Chem *281*, 40224-40235.
Planta, R.J., and Mager, W.H. (1998). The list of cytoplasmic ribosomal proteins of Saccharomyces cerevisiae. Yeast *14*, 471-477.
Ramakrishnan, V. (2002). Ribosome structure and the mechanism of translation. Cell *108*, 557-572.
Raychaudhuri, P., Stringer, E.A., Valenzuela, D.M., and Maitra, U. (1984). Ribosomal subunit antiassociation activity in rabbit reticulocyte lysates. Evidence for a low molecular weight ribosomal subunit antiassociation protein factor (Mr = 25,000). J Biol Chem *259*, 11930-11935.
Ribbeck, K., and Gorlich, D. (2001). Kinetic analysis of translocation through nuclear pore complexes. EMBO J *20*, 1320-1330.
Rodnina, M.V., Savelsbergh, A., Katunin, V.I., and Wintermeyer, W. (1997). Hydrolysis of GTP by elongation factor G drives tRNA movement on the ribosome. Nature *385*, 37-41.
Rodnina, M.V., and Wintermeyer, W. (2009). Recent mechanistic insights into eukaryotic ribosomes. Curr Opin Cell Biol *21*, 435-443.
Rodriguez-Mateos, M., Garcia-Gomez, J.J., Francisco-Velilla, R., Remacha, M., de la Cruz, J., and Ballesta, J.P. (2009). Role and dynamics of the ribosomal protein P0 and its related trans-acting factor Mrt4 during ribosome assembly in Saccharomyces cerevisiae. Nucleic Acids Res *37*, 7519-7532.
Rohl, R., and Nierhaus, K.H. (1982). Assembly map of the large subunit (50S) of Escherichia coli ribosomes. Proc Natl Acad Sci U S A *79*, 729-733.
Rout, M.P., Aitchison, J.D., Suprapto, A., Hjertaas, K., Zhao, Y., and Chait, B.T. (2000). The yeast nuclear pore complex: composition, architecture, and transport mechanism. J Cell Biol *148*, 635-651.
Russell, D.W., and Spremulli, L.L. (1979). Purification and characterization of a ribosome dissociation factor (eukaryotic initiation factor 6) from wheat germ. J Biol Chem *254*, 8796-8800.
Saini, P., Eyler, D.E., Green, R., and Dever, T.E. (2009). Hypusine-containing protein eIF5A promotes translation elongation. Nature *459*, 118-121.

Samarsky, D.A., and Fournier, M.J. (1999). A comprehensive database for the small nucleolar RNAs from Saccharomyces cerevisiae. Nucleic Acids Res *27*, 161-164.
Sanchez, M.E., Urena, D., Amils, R., and Londei, P. (1990). In vitro reassembly of active large ribosomal subunits of the halophilic archaebacterium Haloferax mediterranei. Biochemistry *29*, 9256-9261.
Santos-Rosa, H., Moreno, H., Simos, G., Segref, A., Fahrenkrog, B., Pante, N., and Hurt, E. (1998). Nuclear mRNA export requires complex formation between Mex67p and Mtr2p at the nuclear pores. Mol Cell Biol *18*, 6826-6838.
Saraste, M., Sibbald, P.R., and Wittinghofer, A. (1990). The P-loop--a common motif in ATP- and GTP-binding proteins. Trends Biochem Sci *15*, 430-434.
Savchenko, A., Krogan, N., Cort, J.R., Evdokimova, E., Lew, J.M., Yee, A.A., Sanchez-Pulido, L., Andrade, M.A., Bochkarev, A., Watson, J.D., *et al.* (2005). The Shwachman-Bodian-Diamond syndrome protein family is involved in RNA metabolism. J Biol Chem *280*, 19213-19220.
Schafer, T., Strauss, D., Petfalski, E., Tollervey, D., and Hurt, E. (2003). The path from nucleolar 90S to cytoplasmic 40S pre-ribosomes. EMBO J *22*, 1370-1380.
Schmeing, T.M., and Ramakrishnan, V. (2009). What recent ribosome structures have revealed about the mechanism of translation. Nature *461*, 1234-1242.
Schmeing, T.M., Voorhees, R.M., Kelley, A.C., Gao, Y.G., Murphy, F.V.t., Weir, J.R., and Ramakrishnan, V. (2009). The crystal structure of the ribosome bound to EF-Tu and aminoacyl-tRNA. Science *326*, 688-694.
Schmid, M., and Jensen, T.H. (2008). The exosome: a multipurpose RNA-decay machine. Trends Biochem Sci *33*, 501-510.
Schuwirth, B.S., Borovinskaya, M.A., Hau, C.W., Zhang, W., Vila-Sanjurjo, A., Holton, J.M., and Cate, J.H. (2005). Structures of the bacterial ribosome at 3.5 A resolution. Science *310*, 827-834.
Selmer, M., Dunham, C.M., Murphy, F.V.t., Weixlbaumer, A., Petry, S., Kelley, A.C., Weir, J.R., and Ramakrishnan, V. (2006). Structure of the 70S ribosome complexed with mRNA and tRNA. Science *313*, 1935-1942.
Senger, B., Lafontaine, D.L., Graindorge, J.S., Gadal, O., Camasses, A., Sanni, A., Garnier, J.M., Breitenbach, M., Hurt, E., and Fasiolo, F. (2001). The nucle(ol)ar Tif6p and Efl1p are required for a late cytoplasmic step of ribosome synthesis. Mol Cell *8*, 1363-1373.
Sengupta, J., Bussiere, C., Pallesen, J., West, M., Johnson, A.W., and Frank, J. (2010). Characterization of the nuclear export adaptor protein Nmd3 in association with the 60S ribosomal subunit. J Cell Biol *189*, 1079-1086.
Sengupta, J., Nilsson, J., Gursky, R., Spahn, C.M., Nissen, P., and Frank, J. (2004). Identification of the versatile scaffold protein RACK1 on the eukaryotic ribosome by cryo-EM. Nat Struct Mol Biol *11*, 957-962.
Shammas, C., Menne, T.F., Hilcenko, C., Michell, S.R., Goyenechea, B., Boocock, G.R., Durie, P.R., Rommens, J.M., and Warren, A.J. (2005). Structural and mutational analysis of the SBDS protein family. Insight into the leukemia-associated Shwachman-Diamond Syndrome. J Biol Chem *280*, 19221-19229.

Shoemaker, C.J., Eyler, D.E., and Green, R. (2010). Dom34:Hbs1 promotes subunit dissociation and peptidyl-tRNA drop-off to initiate no-go decay. Science *330*, 369-372.
Shwachman, H., Diamond, L.K., Oski, F.A., and Khaw, K.T. (1964). THE SYNDROME OF PANCREATIC INSUFFICIENCY AND BONE MARROW DYSFUNCTION. J Pediatr *65*, 645-663.
Si, K., and Maitra, U. (1999). The Saccharomyces cerevisiae homologue of mammalian translation initiation factor 6 does not function as a translation initiation factor. Mol Cell Biol *19*, 1416-1426.
Song, H., Mugnier, P., Das, A.K., Webb, H.M., Evans, D.R., Tuite, M.F., Hemmings, B.A., and Barford, D. (2000). The crystal structure of human eukaryotic release factor eRF1--mechanism of stop codon recognition and peptidyl-tRNA hydrolysis. Cell *100*, 311-321.
Spahn, C.M., Beckmann, R., Eswar, N., Penczek, P.A., Sali, A., Blobel, G., and Frank, J. (2001). Structure of the 80S ribosome from Saccharomyces cerevisiae--tRNA-ribosome and subunit-subunit interactions. Cell *107*, 373-386.
Spahn, C.M., Gomez-Lorenzo, M.G., Grassucci, R.A., Jorgensen, R., Andersen, G.R., Beckmann, R., Penczek, P.A., Ballesta, J.P., and Frank, J. (2004). Domain movements of elongation factor eEF2 and the eukaryotic 80S ribosome facilitate tRNA translocation. EMBO J *23*, 1008-1019.
Spiegel, P.C., Ermolenko, D.N., and Noller, H.F. (2007). Elongation factor G stabilizes the hybrid-state conformation of the 70S ribosome. RNA *13*, 1473-1482.
Staley, J.P., and Woolford, J.L., Jr. (2009). Assembly of ribosomes and spliceosomes: complex ribonucleoprotein machines. Curr Opin Cell Biol *21*, 109-118.
Stark, H., Rodnina, M.V., Wieden, H.J., van Heel, M., and Wintermeyer, W. (2000). Large-scale movement of elongation factor G and extensive conformational change of the ribosome during translocation. Cell *100*, 301-309.
Steiner-Mosonyi, M., Leslie, D.M., Dehghani, H., Aitchison, J.D., and Mangroo, D. (2003). Utp8p is an essential intranuclear component of the nuclear tRNA export machinery of Saccharomyces cerevisiae. J Biol Chem *278*, 32236-32245.
Steitz, T.A. (2008). A structural understanding of the dynamic ribosome machine. Nat Rev Mol Cell Biol *9*, 242-253.
Strunk, B.S., and Karbstein, K. (2009). Powering through ribosome assembly. RNA *15*, 2083-2104.
Sung, M.K., Ha, C.W., and Huh, W.K. (2008). A vector system for efficient and economical switching of C-terminal epitope tags in Saccharomyces cerevisiae. Yeast *25*, 301-311.
Takyar, S., Hickerson, R.P., and Noller, H.F. (2005). mRNA helicase activity of the ribosome. Cell *120*, 49-58.
Taylor, D.J., Nilsson, J., Merrill, A.R., Andersen, G.R., Nissen, P., and Frank, J. (2007). Structures of modified eEF2 80S ribosome complexes reveal the role of GTP hydrolysis in translocation. EMBO J *26*, 2421-2431.

Teraoka, H., and Nierhaus, K.H. (1978). Protein L16 induces a conformational change when incorporated into a L16-deficient core derived from Escherichia coli ribosomes. FEBS Lett *88*, 223-226.
Thomas, F., and Kutay, U. (2003). Biogenesis and nuclear export of ribosomal subunits in higher eukaryotes depend on the CRM1 export pathway. J Cell Sci *116*, 2409-2419.
Thomson, E., and Tollervey, D. (2010). The final step in 5.8S rRNA processing is cytoplasmic in Saccharomyces cerevisiae. Mol Cell Biol *30*, 976-984.
Tollervey, D., Lehtonen, H., Jansen, R., Kern, H., and Hurt, E.C. (1993). Temperature-sensitive mutations demonstrate roles for yeast fibrillarin in pre-rRNA processing, pre-rRNA methylation, and ribosome assembly. Cell *72*, 443-457.
Trabuco, L.G., Schreiner, E., Eargle, J., Cornish, P., Ha, T., Luthey-Schulten, Z., and Schulten, K. (2010). The role of L1 stalk-tRNA interaction in the ribosome elongation cycle. J Mol Biol *402*, 741-760.
Tran, E.J., Bolger, T.A., and Wente, S.R. (2007). SnapShot: nuclear transport. Cell *131*, 420.
Trotta, C.R., Lund, E., Kahan, L., Johnson, A.W., and Dahlberg, J.E. (2003). Coordinated nuclear export of 60S ribosomal subunits and NMD3 in vertebrates. EMBO J *22*, 2841-2851.
Tschochner, H., and Hurt, E. (2003). Pre-ribosomes on the road from the nucleolus to the cytoplasm. Trends Cell Biol *13*, 255-263.
Tycowski, K.T., Smith, C.M., Shu, M.D., and Steitz, J.A. (1996). A small nucleolar RNA requirement for site-specific ribose methylation of rRNA in Xenopus. Proc Natl Acad Sci U S A *93*, 14480-14485.
Uchiumi, T., Hori, K., Nomura, T., and Hachimori, A. (1999). Replacement of L7/L12.L10 protein complex in Escherichia coli ribosomes with the eukaryotic counterpart changes the specificity of elongation factor binding. J Biol Chem *274*, 27578-27582.
Valenzuela, D.M., Chaudhuri, A., and Maitra, U. (1982). Eukaryotic ribosomal subunit anti-association activity of calf liver is contained in a single polypeptide chain protein of Mr = 25,500 (eukaryotic initiation factor 6). J Biol Chem *257*, 7712-7719.
Valle, M., Zavialov, A., Sengupta, J., Rawat, U., Ehrenberg, M., and Frank, J. (2003). Locking and unlocking of ribosomal motions. Cell *114*, 123-134.
VanLoock, M.S., Agrawal, R.K., Gabashvili, I.S., Qi, L., Frank, J., and Harvey, S.C. (2000). Movement of the decoding region of the 16 S ribosomal RNA accompanies tRNA translocation. J Mol Biol *304*, 507-515.
Venema, J., and Tollervey, D. (1999). Ribosome synthesis in Saccharomyces cerevisiae. Annu Rev Genet *33*, 261-311.
Voorhees, R.M., Weixlbaumer, A., Loakes, D., Kelley, A.C., and Ramakrishnan, V. (2009). Insights into substrate stabilization from snapshots of the peptidyl transferase center of the intact 70S ribosome. Nat Struct Mol Biol *16*, 528-533.

Wang, Y., Liu, C.L., Storey, J.D., Tibshirani, R.J., Herschlag, D., and Brown, P.O. (2002). Precision and functional specificity in mRNA decay. Proc Natl Acad Sci U S A *99*, 5860-5865.
Weixlbaumer, A., Jin, H., Neubauer, C., Voorhees, R.M., Petry, S., Kelley, A.C., and Ramakrishnan, V. (2008). Insights into translational termination from the structure of RF2 bound to the ribosome. Science *322*, 953-956.
Weixlbaumer, A., Petry, S., Dunham, C.M., Selmer, M., Kelley, A.C., and Ramakrishnan, V. (2007). Crystal structure of the ribosome recycling factor bound to the ribosome. Nat Struct Mol Biol *14*, 733-737.
Wente, S.R., and Rout, M.P. (2010). The nuclear pore complex and nuclear transport. Cold Spring Harb Perspect Biol *2*, a000562.
Wery, M., Ruidant, S., Schillewaert, S., Lepore, N., and Lafontaine, D.L. (2009). The nuclear poly(A) polymerase and Exosome cofactor Trf5 is recruited cotranscriptionally to nucleolar surveillance. RNA *15*, 406-419.
West, M., Hedges, J.B., Chen, A., and Johnson, A.W. (2005). Defining the order in which Nmd3p and Rpl10p load onto nascent 60S ribosomal subunits. Mol Cell Biol *25*, 3802-3813.
Wilmes, G.M., Bergkessel, M., Bandyopadhyay, S., Shales, M., Braberg, H., Cagney, G., Collins, S.R., Whitworth, G.B., Kress, T.L., Weissman, J.S., *et al.* (2008). A genetic interaction map of RNA-processing factors reveals links between Sem1/Dss1-containing complexes and mRNA export and splicing. Mol Cell *32*, 735-746.
Wilson, D.N., Schluenzen, F., Harms, J.M., Yoshida, T., Ohkubo, T., Albrecht, R., Buerger, J., Kobayashi, Y., and Fucini, P. (2005). X-ray crystallography study on ribosome recycling: the mechanism of binding and action of RRF on the 50S ribosomal subunit. EMBO J *24*, 251-260.
Wimberly, B.T., Brodersen, D.E., Clemons, W.M., Jr., Morgan-Warren, R.J., Carter, A.P., Vonrhein, C., Hartsch, T., and Ramakrishnan, V. (2000). Structure of the 30S ribosomal subunit. Nature *407*, 327-339.
Wower, I.K., Wower, J., and Zimmermann, R.A. (1998). Ribosomal protein L27 participates in both 50 S subunit assembly and the peptidyl transferase reaction. J Biol Chem *273*, 19847-19852.
Yao, W., Roser, D., Kohler, A., Bradatsch, B., Bassler, J., and Hurt, E. (2007). Nuclear export of ribosomal 60S subunits by the general mRNA export receptor Mex67-Mtr2. Mol Cell *26*, 51-62.
Yao, Y., Demoinet, E., Saveanu, C., Lenormand, P., Jacquier, A., and Fromont-Racine, M. (2010). Ecm1 is a new pre-ribosomal factor involved in pre-60S particle export. RNA *16*, 1007-1017.
Yusupov, M.M., Yusupova, G.Z., Baucom, A., Lieberman, K., Earnest, T.N., Cate, J.H., and Noller, H.F. (2001). Crystal structure of the ribosome at 5.5 A resolution. Science *292*, 883-896.
Zakalskiy, A., Hogenauer, G., Ishikawa, T., Wehrschutz-Sigl, E., Wendler, F., Teis, D., Zisser, G., Steven, A.C., and Bergler, H. (2002). Structural and enzymatic

properties of the AAA protein Drg1p from Saccharomyces cerevisiae. Decoupling of intracellular function from ATPase activity and hexamerization. J Biol Chem *277*, 26788-26795.
Zanchin, N.I., and Goldfarb, D.S. (1999). The exosome subunit Rrp43p is required for the efficient maturation of 5.8S, 18S and 25S rRNA. Nucleic Acids Res *27*, 1283-1288.
Zebarjadian, Y., King, T., Fournier, M.J., Clarke, L., and Carbon, J. (1999). Point mutations in yeast CBF5 can abolish in vivo pseudouridylation of rRNA. Mol Cell Biol *19*, 7461-7472.
Zemp, I., and Kutay, U. (2007). Nuclear export and cytoplasmic maturation of ribosomal subunits. FEBS Lett *581*, 2783-2793.
Zuk, D., Belk, J.P., and Jacobson, A. (1999). Temperature-sensitive mutations in the Saccharomyces cerevisiae MRT4, GRC5, SLA2 and THS1 genes result in defects in mRNA turnover. Genetics *153*, 35-47.

VITA

Cyril Luc Cassien Bussiere attended Lacordaire High School, Marseille, France. In 2002 he graduated from the University of Utah with a Bachelor of Science in Biology. After one year working as a research assistant in Dr Roth Laboratory at the University of California at Davis he entered the program of Molecular Genetics and Microbiology at the University of Texas at Austin in August 2004.

Permanent address: 56 rue Edmond Rostand 13006 Marseille FRANCE.

This manuscript was typed by the author.